HEAT AND MASS TRANSFER STUDY OF A PACKED BED ABSORBER/REGENERATOR FOR SOLAR DESICCANT COOLING

By

VIKTORIA ÖBERG

A DISSERTATION PRESENTED TO THE GRADUATE SCHOOL
OF THE UNIVERSITY OF FLORIDA IN PARTIAL FULFILLMENT
OF THE REQUIREMENTS FOR THE DEGREE OF
DOCTOR OF PHILOSOPHY

UNIVERSITY OF FLORIDA

1998

ACKNOWLEDGMENTS

Completing this dissertation would not have been possible without the help and encouragement from so many people. My sincerest gratitude goes to all of those who have been directly and indirectly involved. Dr. Yogi Goswami, who served as the chair in my Ph.D. committee, is to be thanked for his patient guidance and support. Professors C. K. Hsieh, S. A. Sherif, J. F. Klausner, and D. O. Shah, who constitute the remainder of my committee, are also to be thanked for their advice and guidance. Thanks are due to Mr. Charles Garretson whose marvelous skills played a vital part in the construction of the experimental facility. Mrs. Lovely Goswami is to be thanked for her helpful advice in analytical chemistry, and for lending the equipment necessary to carry out the analyses. Also, I feel honored to have worked close to so many brilliant graduate students whose friendship and support will be remembered a lifetime.

Finally, it is not possible to describe the thankfulness I feel towards my family. Without their abundant love and support, this dissertation would not have been completed. Especially I would like to acknowledge my husband, Andrew, who with warm humor and constant positivism has provided me with the ideal environment for obtaining this Ph.D.

TABLE OF CONTENTS

NOMENCLATURE

A	area (m^2)
a	area for heat and mass transfer (m^2/m^3)
a_t	specific surface area of packing (m^2/m^3)
a_w	wetted surface area of packing (m^2/m^3)
b	gap height between collector surface and glazing (m)
C	capacitance rate (mc_p)
CELD	50/50 mixture of lithium chloride and calcium chloride
COP	coefficient of performance
c_p	specific heat (kJ/kg-°C)
D	diffusivity (m^2/s)
d	plate spacing in a plate heat exchanger
d_p	equivalent sphere diameter of packing particle (m)
EER	energy efficiency ratio (ratio of cooling in Btu/h to the electrical power input in W)
F_G	gas phase mass transfer coefficient ($kmol/m^2$-s)
F_L	liquid phase mass transfer coefficient ($kmol/m^2$-s)
f	wetting factor
G	superficial air (gas) flow rate (kg dry air / m^2-s)
g	acceleration of gravity (m/s^2)

H	enthalpy (kJ/kg)
HE	heat exchanger
h_G	gas side heat transfer coefficient (kJ/m^2-s-°C)
I	solar radiation incident on solar collector (W/m^2 or kW/m^2)
j_h	dimensionless heat transfer group (Equation (3.26))
j_m	dimensionless mass transfer group (Equation (3.26))
K_G	overall gas side mass transfer coefficient (kmol/m^2-s)
k_G	gas phase mass transfer coefficient (kmol/m^2-s-Pa)
k_L	liquid phase mass transfer coefficient (m/s)
L	superficial desiccant flow rate (kg/m^2-s)
Le	Lewis number
l	length (m)
M	molar mass (kg/kmol)
m	flow rate (kg/s) or mass (kg)
N_v	molar vapor mass transfer flux (kmol/m^2-s)
NTU	number of transfer units
P	total pressure (Pa)
Pr	Prandtl number
p	vapor pressure (Pa)
Q	rate of heat transfer (kW or kJ/hr)
q	heat transfer flux (kW/m^2)
R	universal gas constant (J/kmol-K)
Re	Reynolds number

RH	relative humidity (%)
Sc	Schmidt number
SHR	sensible heat ratio
T	temperature (°C)
TEG	triethylene glycol
t	time (s or hr)
U	heat loss coefficient (kW/m^2-s)
V	volume (m^3) or volumetric flow rate (l/s)
v	velocity (m/s)
W	power (kW or kJ/hr)
w	width (m)
X	desiccant concentration (kg desiccant / kg solution or % desiccant by weight)
x	desiccant mole fraction (kmol desiccant / kmol solution)
Y	air humidity ratio (kg water/kg dry air or g water/kg dry air)
y	water mole fraction (kmol water / kmol air)
Z	tower height (m)

Greek:

α	absorptance
Γ	flow rate per unit coil width (kg/m-s)
γ	surface tension (N/m)
ϵ	effectiveness
η	efficiency

λ	latent heat of condensation/vaporization (kJ/kg)
μ	viscosity (Ns/m^2)
ξ	absolute error
π	dimensionless vapor pressure difference (Equation 2.2)
ρ	density (kg/m^3)

Subscripts:

a	air
amb	ambient
avg	average
boil	boiler
c	critical
cond	water condensation
conv	conventional
cool	cooling
cs	cross sectional
DE	dehumidifier
DP	dew point
DS	desiccant storage
E	energy
equ	equilibrium
evap	water evaporation
G	gas phase
g	glazed

H	enthalpy
HE	heat exchanger
heat	heat or heating
IN	inlet
i	interface
L	desiccant or liquid phase
l	latent
min	minimum
OA	outside air
OUT	outlet
o	open
R	regenerator
r	refrigerant
s	sensible
sat	saturation
T	tilted surface
tot	total
v	vapor
WB	wet bulb
w	water
Y	humidity
0	reference state

Abstract of Dissertation Presented to the Graduate School
of the University of Florida in Partial Fulfillment of the
Requirements for the Degree of Doctor of Philosophy

HEAT AND MASS TRANSFER STUDY OF A PACKED BED ABSORBER/REGENERATOR FOR SOLAR DESICCANT COOLING

By

Viktoria Öberg

May 1998

Chairperson: Dr. D. Yogi Goswami
Major Department: Mechanical Engineering

The main objective of this investigation is to explore liquid desiccant cooling as a solar alternative to conventional air conditioning techniques, with additional objectives of reducing the electrical energy requirement and improving the humidity control in buildings. Since the desiccant air dehumidification and regeneration processes greatly influence the overall system performance, a detailed study of the simultaneous heat and mass transfer between air and a desiccant in a packed bed absorption tower is conducted. Triethylene glycol is selected as the desiccant since it is noncorrosive and has good wetting characteristics. Finite difference modeling, as well as an experimental investigation of the packed bed absorber/regenerator performance, is carried out. In addition, a hybrid desiccant cooling system expected to provide reliable and efficient air conditioning is proposed, and a performance simulation of this system is carried out to provide insight into the design of solar desiccant cooling systems.

Through the study of the absorber/regenerator, important design variables are defined as the air flow rate and humidity, the desiccant temperature and concentration, and the packed bed height. The liquid flow rate and the air temperature do not have a significant effect on the performance; however, the liquid flow rate must be sufficiently high to ensure wetting of the packing. The performance predictions from the finite difference model compare well with the experimental findings. To facilitate the integration of a packed bed absorber/regenerator in a desiccant cooling system simulation, two performance correlations are derived based on experimental data from the present investigation and the literature: one for the humidity effectiveness and one for the enthalpy effectiveness of the absorption/regeneration. These correlations predict the performance within 15 % of all the experimental data, and they give good predictions of the influence of design variables.

Results from the performance simulation of the proposed solar hybrid liquid desiccant cooling system show that in applications with a large latent cooling load, as much as 80 % of the electrical energy can be saved as compared to conventional cooling techniques when care is taken to minimize the amount of electrical energy used for auxiliary regeneration heat.

CHAPTER 1
INTRODUCTION

Growing concerns for the environmental risks associated with the use of fossil fuels and nuclear power make energy conservation and use of renewable energy sources increasingly important. Air conditioning is an energy intensive process, especially in hot and humid climates. Therefore, increased research and development of solar alternatives to conventional space conditioning techniques are desirable both in terms of overall cost savings and minimizing the environmental impact. While solar heating systems are well developed, a more challenging task is to design cost-competitive and energy efficient solar cooling systems. Clearly, solar cooling has the advantage of having the largest amount of solar energy available when the cooling demand is the highest.

Air conditioning requires efficient control of both temperature and humidity. Conventional vapor compression air conditioning systems cool the air below its dew point to condense moisture from the air. Thus, the evaporator in a vapor compression system may operate at a lower temperature than what is required to meet the sensible cooling load, which lowers the coefficient of performance (COP). Furthermore, it is sometimes necessary to reheat the air in order to avoid excessive sensible cooling of the conditioned space. With energy savings in mind, conventional vapor compression systems have been designed to operate at higher evaporator temperatures, but those

systems have been found incapable of maintaining indoor relative humidity within a comfortable range in hot and humid climates [56]. Decoupling the latent cooling (air dehumidification) and sensible cooling processes may yield not only energy savings but may also improve indoor air quality by more efficient humidity control.

One way of handling the control of humidity and temperature independently is to bring the air in contact with a desiccant material that absorbs moisture before the air is sensibly cooled in a vapor compression system, absorption chiller, or an evaporative cooling unit. The main energy requirement for desiccant cooling is low temperature heat for regeneration of the desiccant. Hence, when using desiccant cooling it is possible to shift part of the cooling energy demand from high quality electrical energy to low temperature heat which can be obtained from solar flat-plate collectors or other low grade energy sources. Although the overall COP of desiccant systems has been found to be low as compared to conventional vapor compression systems, the electrical energy consumption can be reduced [59, 102]. Thus, there is a potential for cost savings by using desiccant cooling, especially in applications where the latent cooling load comprises a large part of the total cooling load. For example, Burns et al. [8] found that utilizing desiccant cooling in a supermarket reduced the cost of air conditioning by 60% as compared to conventional cooling. These findings show desiccant cooling as a promising alternative to conventional cooling techniques. Therefore, research leading to reliable, energy efficient, and cost-competitive desiccant systems is warranted.

In this chapter, a general description of the desiccant cooling concept is given, along with an outline of the major contributions of the current investigation.

1.1 Desiccant Cooling Concept

In a desiccant air conditioning system the moisture content is first reduced by bringing the air in contact with a desiccant material that absorbs water from the air. The sensible cooling load can then be handled by a conventional vapor compression system, an absorption chiller, and/or evaporative cooling. Two basic types of desiccants can be used: solids (e.g., silica gel and solid lithium chloride) or liquids (e.g., salt solutions and glycols). The driving force for the absorption process is the difference in vapor pressure between the air and the desiccant. As depicted in Figure 1.1, when the water vapor pressure on the desiccant surface is lower than in the air, water is absorbed by the desiccant. When water is absorbed, the vapor pressure in the desiccant increases. Eventually, equilibrium is reached when the vapor pressure in the

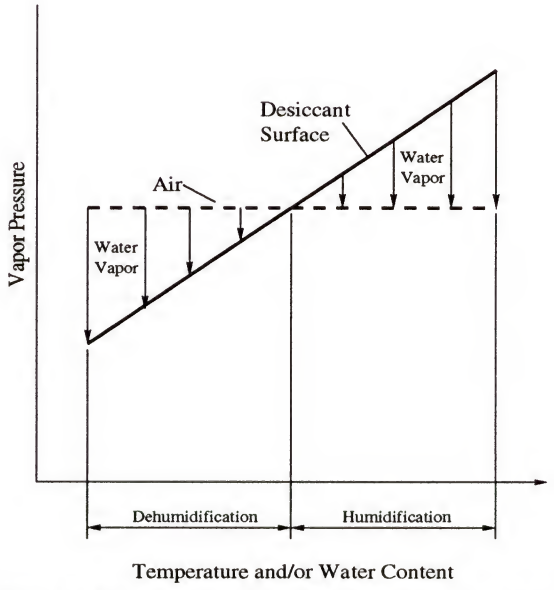

Figure 1.1: Vapor pressure versus temperature and water content for desiccant and air (based on Agarwal et al. [1]).

desiccant is equal to that in the air. To allow for repeated use of the desiccant, regeneration is required. This can be accomplished by heating the desiccant to increase its vapor pressure, followed by contact with an air stream with lower vapor pressure. The heat required for regeneration can be supplied at a low temperature (60-100 °C) so that flat-plate solar thermal collectors may be utilized.

In a solid desiccant cooling system, the desiccant bed is typically configured as a rotary wheel (Figure 1.2). The air to be dehumidified is passed through one part of the wheel, while a hot air stream passes through the other part for simultaneous desiccant regeneration and dehumidification. After the air is dehumidified, its temperature must be lowered before it enters the conditioned space. This may be done by evaporative cooling as shown in Figure 1.2. A schematic of a conceptual liquid desiccant system is

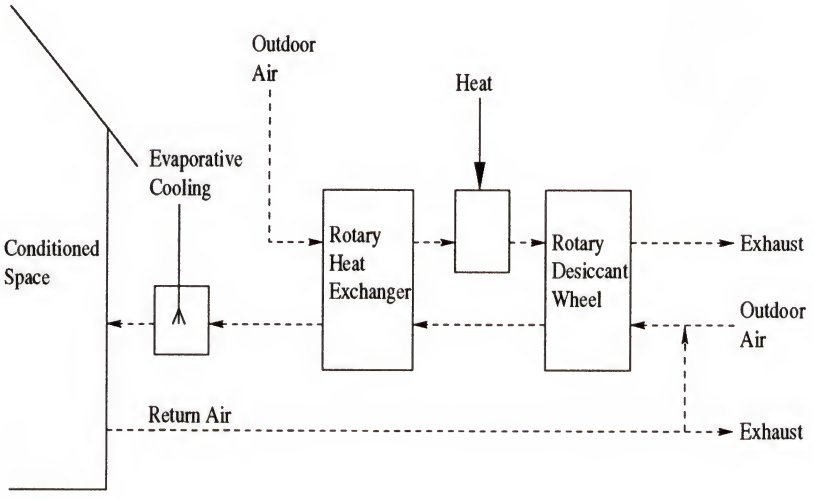

Figure 1.2: Solid desiccant cooling cycle.

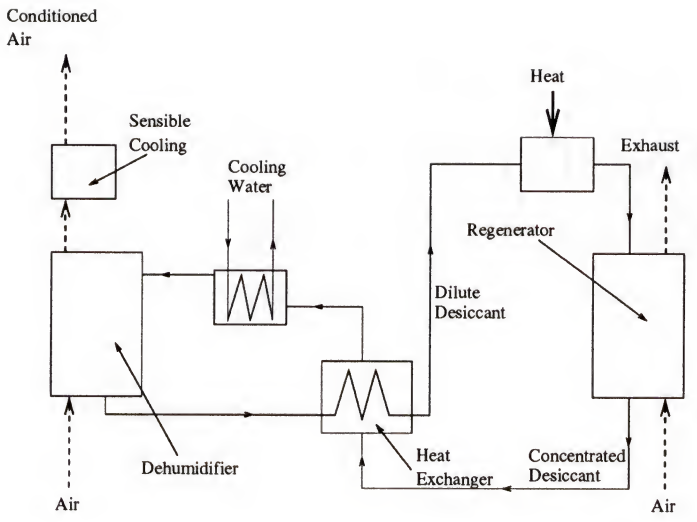

Figure 1.3: A conceptual liquid desiccant cooling system.

shown in Figure 1.3. Concentrated desiccant is brought in contact with the air in the dehumidifier. An extended contact surface is commonly utilized to enhance the heat and mass transfer between the air and the desiccant. Water is absorbed from the air into the desiccant, removing the latent load. After leaving the dehumidifier, the air is sensibly cooled before entering the conditioned space. As mentioned before, the desiccant must be regenerated to allow for repeated use. For this reason, the desiccant is heated to release water and is then brought in contact with a moisture scavenging air stream in the regenerator. Before the concentrated desiccant returns to the dehumidifier, it is cooled to minimize the heat addition to the air to be conditioned, and to lower the desiccant's vapor pressure.

Overall, the use of liquid desiccants may be advantageous compared to solid desiccants. Some advantages of the liquid desiccant systems include a smaller air pressure drop and the fact that a liquid can be transported directly to the source of regeneration heat [36]. The ability to pump the liquid desiccant makes it possible to connect several small desiccant dehumidifiers to a larger regeneration unit [32], which would be especially beneficial in large buildings. Using a liquid desiccant also enables more efficient heat transfer since highly efficient liquid-liquid heat exchangers may be employed [31]. Finally, since a liquid desiccant system does not require simultaneous air dehumidification and desiccant regeneration, it is possible to store the dilute liquid until regeneration heat is available. For these reasons, further investigation of liquid desiccant systems is of great interest.

1.2 Contributions of Present Study

The main objective of this investigation is to explore liquid desiccant cooling as a solar alternative to conventional air conditioning techniques with additional objectives of reducing the electrical energy requirement and improving the humidity control in buildings. Since the desiccant air dehumidification and regeneration processes greatly influence the overall performance of a desiccant system, the main part of this investigation consists of a detailed study of the heat and mass transfer between air and desiccant in a packed bed absorption tower. The following topics are covered in this investigation:

- A detailed literature review of liquid desiccant cooling is presented. Physical properties for commonly used liquid desiccants are compared, and findings from studies of desiccant-air contact equipment and various system configurations are discussed.

- A finite difference model is employed for the adiabatic gas absorption in a packed bed serving as the air dehumidifier and desiccant regenerator. This model is used to carry out a theoretical parametric study of the simultaneous heat and mass transfer between the air and the desiccant.

- An experimental investigation of the packed bed absorption tower is also conducted to verify the theoretical model and to explore the influence of design parameters on the desiccant-air absorption processes. Since gas absorption in a randomly packed tower involves complex fluid flow patterns and simultaneous heat and mass transfer, theoretical modeling relies heavily upon experimental studies.

- To aid in performance estimates and the design of liquid desiccant systems, correlations for the effectiveness of the absorption process as a function of design variables are presented. These correlations are based on a careful evaluation of experimental data from the literature and from the present study.

- A system configuration expected to provide reliable and energy efficient air conditioning is proposed. Insight into the design of solar desiccant cooling systems is provided through a performance simulation of this system for ventilation air preconditioning; an application where the latent part of the total cooling load is large. Electrical energy requirements for the desiccant system are compared to those of a conventional vapor compression system.

CHAPTER 2
REVIEW OF LIQUID DESICCANT COOLING

Desiccant cooling systems have been studied for many years by numerous researchers [75]. Nevertheless, widespread utilization of this technology for air conditioning of buildings has not yet been realized. In this chapter, a detailed review of publications related to liquid desiccant cooling is given. Physical properties are compared for commonly used liquid desiccants (salt solutions and triethylene glycol). Findings from studies of desiccant-air contact equipment, such as packed towers, finned coils, and solar collector regenerators, have been summarized in tables for easy comparison. Key features of these tables include the desiccant material, the influence of design variables on the dehumidifier/regenerator performance, and whether experiments were performed. System configurations are presented schematically, with additional information listed in tabular form.

2.1 Liquid Desiccants

Hygroscopic liquids used as desiccants are characterized by their low vapor pressure. The driving force for mass transfer is the difference between the vapor pressure in the air and in the desiccant. In addition to low vapor pressure, desiccants should have low viscosity and good heat transfer characteristics. Also, it is preferred that they are noncorrosive, odorless, nontoxic, nonflammable, stable, readily available,

and inexpensive [29]. Furthermore, the surface tension of a liquid desiccant is important since it directly influences the static hold up and surface wetting in the desiccant-air contact equipment.

Desiccants commonly used are aqueous solutions of lithium bromide, lithium chloride, calcium chloride, mixtures of these solutions, and triethylene glycol (TEG). The vapor pressures of these common liquid desiccants as a function of temperature and concentration are shown in Figure 2.1, as compiled from Dow Chemical Company [17, 18], Cyprus Foote Mineral Company [16], Ertas et al. [20], and Zaytsev and Aseyev [104]. Other physical properties of desiccants that are important for evaluating the heat and mass transfer processes, along with the pumping requirements, are listed in Table 2.1.

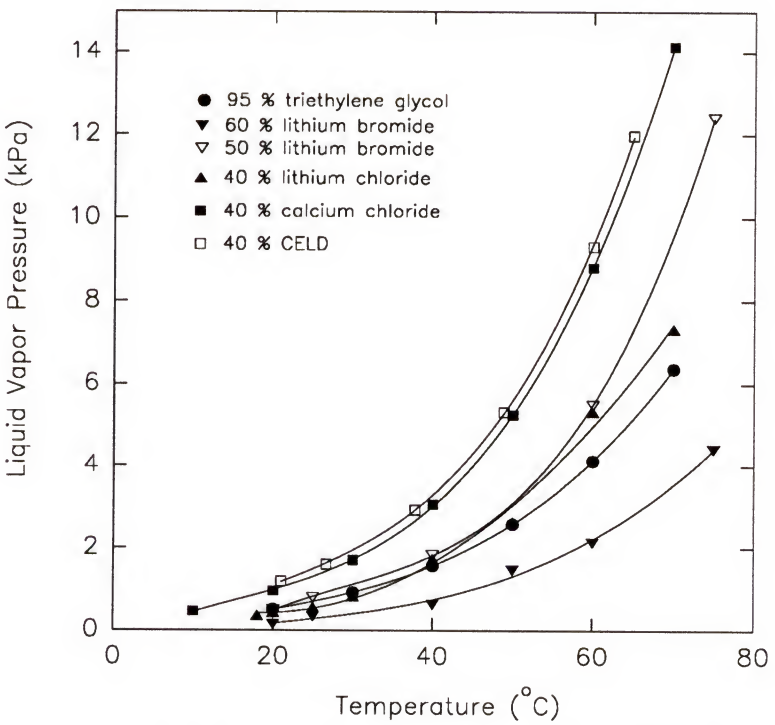

Figure 2.1: Vapor pressures of liquid desiccants.

Table 2.1: Physical properties of liquid desiccants at 25 °C.

Desiccant	$\rho \cdot 10^{-3}$ (kg/m^3)	$\mu \cdot 10^{3}$ (Ns/m^2)	$\gamma \cdot 10^{3}$ (N/m)	c_p (kJ/kg-°C)	Reference
95 % by weight triethylene glycol	1.1	28	46	2.3	[18]
55 % by weight lithium bromide	1.6	6	89	2.1	[16, 100, 104]
40 % calcium chloride	1.4	7	93	2.5	[7, 17, 104]
40 % by weight lithium chloride	1.2	9	96	2.5	[100, 103, 104]
40 % by weight CELD	1.3	5	-	-	[20]

As shown in Figure 2.1, the salt solutions and triethylene glycol have comparable vapor pressures. However, salt solutions are corrosive, and their use may increase the equipment cost since corrosion resistant materials are required. Also, salt solutions have higher surface tension than the glycols (Table 2.1). Hence, adequate wetting of the extended mass transfer surfaces would be more difficult using salt solutions, although surfactants can be added to salt solutions to lower their surface tension [103]. While triethylene glycol has low vapor pressure and low surface tension, the vapor pressure of pure triethylene glycol is not zero, resulting in some evaporation of the glycol into the air. Triethylene glycol is not particularly toxic but inhaling vapors may cause respiratory irritation [23], making it necessary to prevent glycol vapor from entering into the air. By adding 10 % by weight of polystyrene sulfonic acid salts to triethylene glycol, Meckler et al. [61] obtained a 15 % higher moisture absorption capacity compared to using the glycol without the salt added. They also suggested that

these TEG-polymer mixtures may have lower vapor pressure than TEG, which would reduce the glycol losses via evaporation. Finally, the high viscosity of triethylene glycol will increase the pumping power in a system as compared to the less viscous salt solutions.

Desiccant mixtures have been proposed in order to combine the advantages of the individual components and to improve the overall characteristics of the desiccant. For example, in an attempt to obtain a liquid desiccant with lower cost than aqueous lithium chloride, but more stable than calcium chloride, aqueous solutions containing a mixture of these two salts have been investigated [20, 21]. Ertas et al. [21] calculated the heat and mass transfer coefficients for the desiccant-air system in a packed bed absorption tower using empirical correlations from the literature. Three desiccants were compared: calcium chloride, lithium chloride, and CELD. The mixture solution was found to greatly improve the mass transfer compared to the calcium chloride solution, while the liquid side heat transfer coefficients were similar for the three salt solutions.

In addition to dehumidification, an added benefit of the desiccants is that they are capable of absorbing inorganic and organic contaminants in the air, thus improving indoor air quality. Findings from experiments where moist air was simultaneously dehumidified and purified in a packed bed absorber were reported by Chung et al. [13, 15]. The pollutants were formaldehyde (0.02 ppm), toluene (3 ppm), 1,1,1-trichloroethane (24 ppm), and carbon dioxide (1000 ppm). It was found that all of toluene and 1,1,1-trichloroethane, 56 % of the carbon dioxide, and 30 % of the formaldehyde were removed by a 95 % by weight triethylene glycol solution [13]. The removal of micro-organisms by a desiccant system has also been reported [63].

2.2 Desiccant-Air Contact Equipment

Liquid desiccant cooling systems require two desiccant-air contact devices: a dehumidifier and a regenerator. In the dehumidifier, air is brought in contact with the liquid desiccant, and water is absorbed from the air into the desiccant. As water is absorbed, the latent heat of condensation of the water, as well as the heat of mixing, is evolved. In the desiccant regenerator, the temperature of the desiccant is raised so that water can be evaporated into a moisture scavenging air stream. Both the air dehumidification and the desiccant regeneration involve simultaneous heat and mass transfer with large heat effects.

Many contact devices have been utilized to bring the air in contact with the desiccant. For instance, packed bed absorption towers have been commonly used as air dehumidifiers and desiccant regenerators. Simple boilers and trickle solar collectors are also used to regenerate the desiccants. Some of the less common desiccant-air contact devices proposed in the literature include a mesh covered rotating cylindrical frame dehumidifier [4], and a passively controlled simultaneous dehumidifier and regenerator [87]. The importance of the choice of a dehumidifier and regenerator is brought forward by the investigations summarized below.

Lowenstein and Gabruk [53] studied the effect of absorber design on the performance of a liquid desiccant air conditioning system. An adiabatic packed bed absorber was compared to an internally cooled absorber consisting of a flat plate air-to-air heat exchanger, with each absorber configured both in counter and cross flows. The highest system coefficient of performance was achieved with the adiabatic packed bed

absorber (COP=0.79). However, it was also pointed out that this configuration was the most capital-intensive of all the systems studied. Also, compared to an adiabatic absorber, an internally cooled dehumidifier could operate at an order of magnitude lower ratio of desiccant to air flow rates. Both the adiabatic and internally cooled absorbers produced similar COPs when operating in cross and counter flow arrangements.

Lowenstein and Dean [52] analyzed the performance of a liquid desiccant air conditioner comparing four types of regenerators: an air-dried packed bed unit, a simple boiler, a multiple-effect boiler, and an engine driven vapor compression distillation unit. For all the cases considered, a counter flow packed bed dehumidifier with indirect evaporative cooling following the dehumidifier was used. A system COP of 0.71 was obtained with the packed bed operating at 121 °C, and the replacement of the packed bed with a simple boiler resulted in a slightly lower COP due to higher regeneration temperatures. Operating the boiler at a sub-atmospheric pressure reduced the required regeneration temperature, resulting in a higher COP (0.79-0.82). Significant improvements were obtained by recovering the latent heat in the water evaporated. A double-effect boiler achieved a system COP between 1.36 and 1.43. The highest system COP (2.4) was obtained by using an engine driven vapor compression distillation unit where the evaporated water was compressed so that its saturation temperature was increased. Latent heat was then recovered as this vapor was condensed in a coil passing through the regenerator.

Peng and Howell [71] modeled the performance of desiccant regenerators suitable for solar desiccant cooling and dehumidification systems. An open surface trickle solar

collector regenerator, a glazed trickle solar collector regenerator, and a regeneration chamber containing a finned tube heating coil were analyzed and compared. It was concluded that an open regenerator design was not practical for hot and humid climates. As opposed to a glazed trickle solar collector regenerator, the authors concluded that a regeneration chamber design would be compact, allow for steady operation, and it could be powered by low-grade heat from sources other than solar.

Additional details on frequently utilized packed towers, coil and plate heat exchangers, and trickle solar collectors are given below.

2.2.1 Packed Towers

The performance of a packed bed absorption tower operating as an air dehumidifier or a desiccant regenerator is influenced by many operating parameters and conditions: desiccant fluid characteristics (viscosity, density, and surface tension), packing type (shape, size, and material), desiccant distribution over the packing, flow configuration (counter or co-current flow), tower height, fluid flow rates, and the inlet conditions of the desiccant (temperature and concentration) and the air (temperature and humidity). Below, the performance of packed towers with respect to a number of design variables is summarized. In addition, theoretical models are also reviewed.

2.2.1.1 Tower performance

One way of representing the performance of a packed bed air dehumidifier is to consider the humidity effectiveness, ϵ_Y, defined as the ratio of the actual change in humidity of the air flowing through the tower to the maximum possible change for a given set of operating conditions [12, 43, 94].

$$\epsilon_Y = \frac{Y_{IN} - Y_{OUT}}{Y_{IN} - Y_{equ}} \qquad (2.1)$$

Here, Y_{IN} and Y_{OUT}, are the humidity ratios at the air inlet and outlet, respectively, and Y_{equ} is the humidity ratio in equilibrium with the desiccant solution at the local solution temperature and concentration. For a counter flow arrangement, Y_{equ} would be the humidity ratio of the air in equilibrium with the desiccant at the desiccant inlet. Ullah et al. [94] presented a curve fit for the humidity effectiveness based on theoretical heat and mass transfer calculations for an adiabatic packed bed tower. This curve fit gave the effectiveness as a function of the inlet desiccant and air temperatures, and the desiccant inlet concentration for a given tower height, liquid flow rate, air flow rate, geometry, and desiccant. A more general correlation of the humidity effectiveness of a packed bed tower as a function of air and liquid flow rates, column and packing dimensions, and equilibrium properties of the desiccant solution was suggested by Chung [12]. To obtain this correlation, experimental dehumidification performance data already available in the literature were employed. The packings considered were glass Raschig rings, polypropylene pall rings, polypropylene flexi rings, and ceramic Berl saddles. Two desiccants were represented: lithium chloride, and triethylene glycol. A parameter, π, representing the desiccant was defined as the ratio of vapor pressure depression to the vapor pressure of pure water (Equation (2.2)). The correlation by Chung [12] is given in Equation (2.3).

$$\pi = \frac{p_w - p_L}{p_w} \tag{2.2}$$

$$\epsilon_Y = \frac{1 - \left\{ \dfrac{0.205\left(\dfrac{G_{IN}}{L_{IN}}\right)^{0.174} \exp\left[0.985\left(\dfrac{T_{a,IN}}{T_{L,IN}}\right)\right]}{(aZ)^{0.184}\pi^{1.680}} \right\}}{1 - \left\{ \dfrac{0.152\exp\left[-0.686\left(\dfrac{T_{a,IN}}{T_{L,IN}}\right)\right]}{\pi^{3.388}} \right\}} \tag{2.3}$$

A 7 % average error between predicted and experimental results was obtained. In addition to ϵ_Y, an enthalpy effectiveness, ϵ_H (Equation (2.4)), was used as a performance parameter by Khan [42, 43].

$$\epsilon_H = \frac{H_{a,IN} - H_{a,OUT}}{H_{a,IN} - H_{a,equ.}} \tag{2.4}$$

Here, $H_{a,IN}$, $H_{a,OUT}$, and $H_{a,equ.}$ are the enthalpies of the air at the tower inlet and outlet, and the enthalpy in equilibrium with the desiccant at the local desiccant conditions, respectively.

Numerous parametric performance evaluations have been conducted on packed bed absorption towers operating as dehumidifiers or regenerators. The influence of design variables on the performance of a packed bed dehumidifier and a packed bed regenerator is shown in Tables 2.2 and 2.3, respectively. These tables show the desiccant employed, the parameters used to describe the performance, the independent

Table 2.2: Packed bed dehumidifier performance.

Reference	Desiccant	Performance Parameter	Independent Variables							Experiments	Additional Comments
Chen et al. [11]	LiCl		L (kg/m^2-s)	X_{IN} (%)	$T_{L,IN}$ (°C)	G (kg/m^2-s)	$T_{a,IN}$ (°C)	Y_{IN} (g/kg)	Z (m)	yes	crown-type and mesh-type polypropylene packing, and polystyrene foam balls
			0.1-1.0	30-40	26-39	0.2-1.2	25-35	17-22	0.1-0.6		
		m_{cond}	↑	↑	↓	↑	↑	↑	↑		
Chung et al. [13]	TEG		L (kg/m^2-s)		X_{IN} (%)		G (kg/m^2-s)			yes	⅝ inch polypropylene flexi rings, ½ inch ceramic Intalox saddles, 0.28 inch structured cellulose and PVC packing
			6-11		90-95		0.8-1.2				
		ϵ_Y	↑		↑		↓				
		K_Ga	↑		↑		↑				
Chung et al. [14]	LiCl		L (kg/m^2-s)		X_{IN} (%)		G (kg/m^2-s)			yes	⅝ inch polypropylene flexi rings
			9-15		30-40		0.8-1.7				
		ϵ_Y	↑		↑		↓				
		K_Ga	↑		↑		↑				
Gandhidasan et al. [28]	$CaCl_2$		L (kg/m^2-s)	X_{IN} (%)	$T_{L,IN}$ (°C)	G (kg/m^2-s)	$T_{a,IN}$ (°C)	Y_{IN} (g/kg)	Y_{OUT} (g/kg)	no	2 inch Raschig rings
			0.5-3.8	40-45	25-32	0.1-1.8	25-33	22-27	9-13		
		required Z	↓	↓	↑	↑	↕	↑	↓		
Khan [42, 43]	LiCl		NTU	L/G		X_{IN} (%)	$T_{L,IN}$ (°C)		Le	no	Performance correlation given.
			0.5-5.0	0.25-2.0		25-45	15-35		0.8-1.2		
		ϵ_Y	↑	↑		↕	↕		↕		
		ϵ_H	↑	↑		↕	↕		↑		

Table 2.2--continued.

Reference	Desiccant	Performance Parameter	Independent Variables						Experiments	Additional Comments
McDonald et al. [57]	CELD		L (kg/m^2-s)	X_{IN} (%)	$T_{L,IN}$ (°C)	$T_{a,IN}$ (°C)	Y_{IN} (g/kg)	Z (m)	yes	Intalox Snowflake packing. $G = 3.6$ kg/m^2-s. Performance correlation given.
			1.5-3.9	40-45	28-43	31-36	21-41	0.5-1.4		
		$T_{a,OUT}$	↓	↕	↑	↕	↑	↕		
		Y_{OUT}	↓	↕	↑	↕	↑	↕		
Patnaik et al. [69, 70]	LiBr		L (kg/m^2-s)	G (kg/m^2-s)	X_{IN} (%)	$T_{L,IN}$ (°C)	$T_{a,IN}$ (°C)	Y_{IN} (g/kg)	yes	Polypropylene Tripack no.½ packing. Z=0.28 m Performance correlation given.
			0.6-1.7	1.3-1.9	45-58	24-32	24-36	9-22		
		m_{cond}	↑	↕	↑	↕	↓	↑		
Potnis and Lenz [77]	LiBr		L (kg/m^2-s)						yes	Z=0.3 m (0.3-0.55 m for structured packing) X_{IN}=51 % Random polypropylene Tripack and structured Munter's CELDEK packing.
			1.0-2.3							
		m_{cond}	↑							
Ullah et al. [94]	$CaCl_2$		X_{IN} (%)	$T_{L,IN}$ (°C)	G (kg/m^2-s)	$T_{a,IN}$ (°C)	Z (m)		no	2 inch Raschig rings Performance correlation given.
			40-45	27-30	1.0-2.0	25-45	0.4-1.0			
		ϵ_Y	↑	↓	↓	↑	↑			

↑ performance parameter increases with increasing variable
↓ performance parameter decreases with increasing variable
↕ variable has no significant effect on the performance parameter

Table 2.3: Packed bed regenerator performance.

Reference	Desiccant	Performance Parameter	Independent Variables					Experiments	Additional Comments
Ertas et al. [19]	CELD		L (kg/m^2-s)	X_{IN} (%)	$T_{L,IN}$ (°C)	Y_{IN} (g/kg)		yes	Intalox Snowflake Packing (9.4 cm). G=3.5 kg/m^2-s $T_{a,IN}$ = 32 °C.
			0.8-3.1	32-46	60-90	18-25			
		X_{OUT}	↓	↑	↑	↓			
		T_{OUT}	↑	↑	↑	↑			
Gandhidasan, [26]	$CaCl_2$		L (kg/m^2-s)	$T_{L,IN}$ (°C)	G (kg/m^2-s)	$T_{a,IN}$ (°C)	Y_{IN} (g/kg)	no	X_{IN}= 45-47 % 1 inch Raschig rings.
			0.003-0.03	25-45	0.006-0.06	50-90	6-18		
		m_{evap}	↑	↑	↑	↑	↓		
Khan [43]	LiCl		NTU	L/G	X (%)	$T_{L,IN}$ (°C)		no	-
			0.5-5.0	1.5-5.0	25-44	50-80			
		ϵ_Y	↑	↑	↑	↓			
		ϵ_H	↑	↑	↑	↓			
Löf et al. [51]	LiCl		G (kg/m^2-s)					yes	1 inch Raschig rings. Z=0.229 m $T_{L,IN}$=37-48 °C $T_{a,IN}$=83-102 °C X_{avg}=26-35 %
			0.7-0.74						
		h_Ga	↑						
Patnaik et al. [69]	LiBr		L (kg/m^2-s)	X (%)	$T_{L,IN}$ (°C)	$T_{a,IN}$ (°C)	Y_{IN} (g/kg)	yes	Tripack no.½ polyethylene packing. Z=0.28 m Performance correlation given. Spray nozzles vs. tray distributor.
			1.1-1.5	57-60	40-56	55-75	5-9		
		m_{evap}	↑	↑	↑	↑	↓		
Potnis and Lenz [77]	LiBr		L (kg/m^2-s)					yes	Z=0.3 m (0.3-0.55 m for structured packing) X_{IN}=51 % Random polypropylene Tripack and structured Munter's CELDEK packing.
			0.8-2.3						
		m_{evap}	↑						

↑ performance parameter increases with increasing variable
↓ performance parameter decreases with increasing variable
↕ variable has no significant effect on the performance parameter

variables and their ranges that were examined, whether experiments were conducted, and other details such as packing type. Under each independent variable, the effect of the variable on the performance parameter is also indicated.

Table 2.2 shows that for dehumidification, the effectiveness of the absorption process increases with the liquid flow rate and concentration, whereas it decreases with increasing air flow rate [13, 14, 42, 94]. Indeed, increasing the air flow rate will result in a lesser reduction in the humidity of the air through the tower, thus decreasing the effectiveness. However, the condensation rate may increase [11], as will the overall mass transfer coefficient [13, 14]. Increasing the inlet desiccant temperature has been found to decrease the condensation rate [11], and the humidity effectiveness [94]. On the other hand, Patnaik et al. [69, 70] found that the inlet liquid temperature had no effect on the condensation rate. This was explained by the fact that a lower liquid temperature results in more dehumidification which means a larger liquid temperature increase through the tower due to the latent heat of condensation released during dehumidification. Thus, a lower inlet desiccant temperature does not necessarily mean a lower average temperature in the tower. A more humid air entering the dehumidifier will result in a more humid air leaving the tower [57]. However, the condensation rate has been found to increase with the air inlet humidity [11, 69]. Finally, the condensation rate and the moisture removal effectiveness increase with the packed bed height [11, 94], although a limiting height beyond which no additional increase occurred was found by Chen et al. [11]. At this limiting value, the conditions of the air leaving the tower would be very close to the conditions in equilibrium with the desiccant entering the tower (counter flow arrangement).

With respect to the regenerator performance, Table 2.3 shows that the rate of water evaporation in the regenerator increases with increasing liquid flow rate [26, 69], and air flow rate [26]. However, the concentration of the desiccant leaving the regenerator decreases with increasing liquid flow rate [19]. Löf et al. [51] suggested that the highest possible air flow rate consistent with pressure drop and flooding constraints should be used. Increasing the humidity of the air used in the regeneration process has a negative effect on the regeneration, decreasing both the rate of evaporation and the concentration of the desiccant leaving the regenerator. The rate of evaporation increases with increasing temperature of the desiccant and air entering the tower [19, 26, 69].

As seen from Tables 2.2 and 2.3, a variety of tower packings have been used, and the choice of tower packing will influence the performance of the dehumidifier/regenerator. Chen et al. [11] found a mesh type polypropylene packing to give the best performance, presumably due to its ability to aid in the uniform distribution of the desiccant over the packing. Random polypropylene tripack and structured Munter's CELDEK were tested by Potnis and Lenz [77]. Experiments showed that the evaporation rate in the regenerator was 130-300 % greater in the randomly packed bed than in the bed using structured packing, and the condensation rate in the dehumidifier was 45-60 % greater in the randomly packed bed. Chung et al. [13] also found the random packings to give higher effectiveness than the structured packings. In addition to the choice of packing, the distribution of the liquid over the packing is important to the absorber performance. Patnaik et al. [69] compared two liquid distributors in a packed bed regenerator; a gravity tray and spray nozzle

distributor. Using the spray nozzle liquid distributor resulted in 40-50 % higher capacity of the tower, and 30-40 % lower pressure drop.

2.2.1.2 Modeling considerations

Many theoretical models for packed bed absorption dehumidifiers/regenerators have been developed, and some of them are summarized in Table 2.4. A finite difference model was developed by Factor and Grossman [22]. In this model, it was assumed that the resistances to heat and mass transfer in the liquid phase are negligible. However, some experimental findings suggest that the resistance to mass transfer in the liquid phase may be dominating [77]. Gandhidasan et al. [28] included resistance to mass transfer in the liquid phase in a finite difference model.

Table 2.4: Theoretical models for packed bed absorbers.

Reference	Model	Verifying Experiments	Additional Comments
Factor and Grossman [22]	finite difference	yes	Assumptions: slug flow, temperature and concentration gradient in flow direction only, adiabatic process, negligible heat and mass transfer resistances in the liquid phase, the surface area for heat and mass transfer is the same.
Gandhidasan et al. [28]	finite difference	no	Assumptions: in addition to the assumptions by Factor and Grossman [22], the resistance to mass transfer in the liquid phase was considered.
Khan and Ball [45] and Khan [43]	based on algebraic correlations	no	The correlations were obtained from data obtained using a finite difference model.
Sadasivam and Balakrishnan [82]	effectiveness-NTU	yes	Assumptions: negligible change in the liquid flow rate throughout the tower, unit Lewis number, and linear saturated air enthalpy versus temperature curve.
Stevens et al. [89]	effectiveness-NTU	yes	Assumptions: same as those by Sadasivam and Balakrishnan [82].

Stevens et al. [89] developed an effectiveness-NTU model analogous to an effectiveness-NTU model used in heat exchanger analysis. However, the number of

transfer units (NTU) was based on the air flow rate rather than the minimum fluid capacity rate. Sadasivam and Balakrishnan [82] improved this effectiveness-NTU model by considering the minimum fluid capacity rate when calculating the number of transfer units. Compared to a finite difference model, one additional assumption of a linear relationship between saturated air enthalpy and temperature is introduced in the effectiveness-NTU model. The main advantage of an effectiveness-NTU model is that the packed bed does not have to be divided in as many segments for each iteration, thus decreasing the computational time. However, iteration is still needed. Good agreements between the effectiveness-NTU model and the finite difference model, as well as experiments, have been shown in the above studies.

Aside from the above theoretical models, Khan [43] and Khan and Ball [45] presented formulations based on fitted algebraic equations. Because of their simplicity, such models are useful for long term performance simulations of desiccant cooling systems. However, they are not very general since the algebraic equations depend on system-dependent variables such as the ratio of liquid to air flow rate, the number of transfer units in the tower, and the desiccant used.

When water is absorbed into the desiccant, the latent heat of condensation of water and the heat of mixing are evolved. For dilute solutions (i.e., low concentration of the transferred solute which is water in this case), it is often assumed that the heat evolved during the absorption process is taken up by the liquid, neglecting the temperature rise in the gas stream [92]. This gives a higher liquid temperature increase through the tower than what actually occurs, and the tower height required to obtain a certain dehumidification may be overpredicted [92]. Sadasivam and Balakrishnan [81,

83] carried out theoretical and experimental studies to determine the fraction of the heat evolved that goes into the air stream. The experimental outlet conditions were compared to those obtained from theoretical modeling, and the fraction was adjusted until a match between the theoretical and experimental results was found. Introducing a fraction of the heat evolved into a model may result in a better agreement between theoretical and experimental data but will not account for the discrepancies due to the various parameters specific to a given system, such as liquid distribution, wetting characteristics between the packing and the desiccant, the use of correlations in a model to estimate the heat and mass transfer coefficients, and the uncertainty of the experimental measurements.

2.2.2 Finned Coil and Plate Heat Exchangers

Packed bed absorption towers offer a large area for heat and mass transfer per unit volume. However, as water is absorbed by the desiccant, heat is evolved so that the desiccant temperature increases, reducing the potential for mass transfer. Although not at all uncommon in air conditioning systems, parallel-plate heat exchangers have been only infrequently used in desiccant systems. Zografos and Petroff [105] analyzed a desiccant counterflow parallel-plate dehumidifier, where the latent load is removed from the indoor air and the heat of absorption is rejected to an evaporatively cooled outdoor air stream. Utilizing a cooling coil for contact between the desiccant and the air is an alternative to a packed tower. In this configuration, air is dehumidified as it is brought in contact with a desiccant film flowing over the coil. Cooling water or refrigerant flowing through the coil removes the heat evolved during the absorption,

allowing for an isothermal process. Some studies on the use of near isothermal dehumidifiers and regenerators are summarized in tables 2.5 (dehumidifiers) and 2.6 (regenerators).

An air dehumidifier where the air is brought in contact with a desiccant (TEG) film falling over a finned tube heat exchanger was analyzed by Peng and Howell [72]. In this dehumidifier, water was circulated through the tubes for cooling the desiccant and the air. Through theoretical modeling the authors found that the ratio of air flow to water flow rate and the ratio of air flow rate to desiccant flow rate should be as small as possible for best dehumidifier performance. In a different investigation, Peng and Howell [71] modeled a regeneration chamber containing a finned heating coil, where hot water flowing through the coil provides the heat for regeneration. Increasing the ratio of the air flow rate to desiccant flow rate, and increasing the hot water flow rate were found to give a stronger desiccant leaving the chamber.

Chebba [10] presented results from performance modeling of a finned tube coil desiccant-air contactor operating at nearly isothermal conditions. In the dehumidifier, for a given desiccant flow rate, a larger number of coil rows decreased the outlet air humidity ratio and temperature. Increasing the desiccant flow rate also decreased the outlet air humidity ratio. However, the outlet temperature increased. Hence, for a specific number of rows, the leaving air enthalpy as a function of liquid flow rate was found to have a minimum. Increasing the cooling water flow rate and lowering the cooling water temperature resulted in cooler and dryer air leaving the dehumidifier. Both temperature and humidity of the air leaving the dehumidifier increased with increasing inlet desiccant temperature. A larger inlet desiccant concentration resulted in

Table 2.5: Coil and plate heat exchanger dehumidifiers.

Reference	Desiccant	Performance Parameter	Independent Variables							Experiments	Additional Comments
Chebbah [10]	TEG		# of coil rows	L (kg/m^2-s)	$T_{L,IN}$ (°C)	X_{IN} (%)	m_w/A_{cs} (kg/m^2-s)		T_w (°C)	yes, for an optimized design	Coil. Simplified model using logarithmic mean differences in fluid properties.
			5-50	0.1-1.1	32-38	92-98	2.2-4.3		16-21		
		$T_{a,OUT}$	↓	↑	↑	↑	↓		↑		
		Y_{OUT}	↓	↓	↑	↓	↓		↑		
Khan and Ball [46]	LiCl		# of coil rows			$T_{a,IN}$-$T_{w,IN}$ (°C)		m_w (kg/s)		no	Coil.
			8-16			3-12		0.25-0.5			
		ϵ_Y	↑			-		-			
		Q_{cool}	↑			↑		↑			
Khan and Ball [44]	LiCl		m_a (kg/s)			Y_{IN} (g/kg)				yes	Coil. Comparison of experimental results to dehumidifier manufacturer's data.
			0.5-0.7			11-19					
		ϵ_Y	↑			-					
		Y_{OUT}	-			↑					
Park et al. [66, 67]	TEG		X_{IN} (%)	$T_{L,IN}$ (°C)	Γ_L (kg/m-s)	G (kg/m^2-s)	$T_{a,IN}$ (°C)	Y_{IN} (g/kg)	T_r (°C)	no	Evaporator coil. Performance correlations provided. The influence of fin geometry was investigated.
			74-86	20-32	0.0012-0.015	0.9-3.0	29-37	12-25	7-17		
		ϵ_Y	↑	↕	↕	↓	↕	↑	↕		
		m_{cond}	↑	↓	↕	↑	↕	↑	↓		

Table 2.5--continued.

Reference	Desiccant	Performance Parameter	Independent Variables			Experiments	Additional Comments
Park et al. [68]	TEG		X_{IN} (%)	m_a (kg/s)		yes	Evaporator coil. Finite difference model.
			75-84	0.2-0.5			
		m_{cond}	↕	↑			
		Y_{OUT}	↕	↑			
Peng and Howell [72]	TEG		$K_G a M_a A_{cs} Z/m_a$	m_a/m_w	m_a/m_L	no	Coil. Finite difference model.
			2-6	0.5-2.5	1-15		
		$H_{a,OUT}$	↑	↑	↑		
		Y_{OUT}	↑: low m_a/m_L ↓: high m_a/m_L	↑	↑		
Zografos and Petroff [105]	LiCl		l/d	Re		no	Plate heat exchanger. Finite difference model.
			25-250	200-6000			
		ϵ_Y	↑	↓			
		EER (system)	↓	↓ (optimum in laminar region)			

↑ performance parameter increases with increasing variable

↓ performance parameter decreases with increasing variable

↕ variable has no significant effect on the performance parameter

Table 2.6: Coil regenerators.

Author	Desiccant	Performance Parameter	Independent Variables							Experiments	Additional Comments
Chebbah [10]	TEG		# of coil rows			m_w/A_{cs} (kg/m^2-s)			T_w (°C)	yes, for an optimized design	Simplified model using logarithmic mean differences in fluid properties.
			4-20			2.2-4.3			54-71		
		X_{OUT}	↑			↑			↑		
Park et al. [66, 67]	TEG		X_{IN} (%)	$T_{L,IN}$ (°C)	Γ_L (kg/m-s)	G (kg/m^2-s)	$T_{a,IN}$ (°C)	Y_{IN} (g/kg)	T_r (°C)	no	Condenser coil. Performance correlation provided. The influence of fin geometry also investigated.
			72-84	27-40	0.0012-0.015	0.9-3.0	29-37	12-25	40-50		
		$\eta_R = \frac{m_{evap}\lambda}{Q_{heat}}$	↓	↑	↓	↕	↑	↓	↓		
		m_{evap}	↓	↑	↕	↑	↑	↓	↑		
Park et al. [68]	TEG		X_{IN} (%)			m_a (kg/s)				yes	Condenser coil. Finite difference model.
			75-84			0.2-0.5					
		m_{evap}	↓			↓					
Peng and Howell [71]	TEG		$K_G a M_a A_{cs} Z/m_a$			m_a/m_w			m_a/m_L	no	Finite difference model.
			1-4			0.5-2.5			3-12		
		X_{OUT}	↑			↑			↑		

↑ performance parameter increases with increasing variable

↓ performance parameter decreases with increasing variable

↕ variable has no significant effect on the performance parameter

a lower humidity of the air leaving the dehumidifier. For the regenerator, a higher hot water temperature and larger number of rows resulted in a more concentrated desiccant leaving the regenerator. The same was seen for higher hot water flow rates.

Heat and mass transfer between air and a uniformly distributed falling liquid desiccant film in a cross-flow plate-fin tube heat exchanger was considered by Park et al. [68]. In this study, the dehumidifier was considered to be the evaporator of a vapor compression system with the refrigerant flowing through the heat exchanger tubes removing the heat of absorption. The desiccant regenerator was the condenser of the vapor compression unit, and the heat for regeneration was thus provided by the condensing refrigerant. A theoretical analysis as well as an experimental investigation were performed, using triethylene glycol as the desiccant. A numerical method was utilized to solve the finite difference equations governing the problem. The model was found to compare well with the experimental data, and trends similar to those seen from the experiments were predicted by the model. For this system configuration, correlations based on results from the numerical model were given for the rate of dehumidification, the rate of sensible air cooling, the ratio of sensible to total cooling, the regeneration rate, and the regeneration efficiency as a function of design parameters [66, 67]. The rate of dehumidification was found to increase with decreasing desiccant temperature, increasing desiccant concentration, decreasing refrigerant temperature, increasing inlet air humidity ratio, and increasing air flow rate. The humidity effectiveness (previously defined in Equation (2.1)), increased with increasing desiccant concentration, increasing inlet air humidity ratio, and decreasing air flow rate. The rate of regeneration increased with increasing desiccant temperature, decreasing

concentration, increasing refrigerant temperature, decreasing inlet air humidity ratio, increasing inlet air temperature, and increasing air flow rate. Finally, the regeneration efficiency (defined as the ratio of the latent heat transfer to the total heat supplied for regeneration) increased with decreasing desiccant flow rate, increasing desiccant temperature, decreasing desiccant concentration, decreasing inlet air humidity ratio, and increasing inlet air temperature.

2.2.3 Trickle Solar Collector Regenerators

Since only low temperature heat is needed for regeneration of a dilute desiccant, flat-plate solar collectors are suitable for providing this heat. Instead of bringing the desiccant in contact with air in a spray tower, the collector itself can function as a regenerator if the desiccant is allowed to trickle down the collector. As the desiccant is heated, water evaporates into the air flowing over the falling desiccant film. The efficiency, η_R of this regeneration process is defined as the energy required to evaporate the water from the desiccant divided by the solar radiation incident on the solar collector.

$$\eta_R = \frac{m_{evap}\lambda}{IA_{collector}} \tag{2.6}$$

Investigations of this concept are discussed below, and a summary is given in Table 2.7.

A theoretical and experimental study of regeneration of a lithium chloride solution in a solar still was carried out by Hollands [35]. The solar still consisted of a blackened tray, a glass cover, and condensation troughs along each side of the still. In

Table 2.7: Trickle solar collector regenerators.

Author	Desiccant	Performance Parameter	Independent Variable				Experiments	Additional Comments
Gandhidasan and Al-Farayedhi [27]	$CaCl_2$		A_g/A_c	I (W/m^2)	Y_{amb} (g/kg)	T_{amb} (°C)	no	A partly glazed solar collector.
			0-3	470-920	8-17	25-40		
		η_R	optimum	↑	↓	↑		
Hollands [35]	LiCl		Daily Insolation (MJ/m^2-day)				yes	Studied the performance of a solar still regenerator.
			11-31					
		$\eta_{R,daily}$	↑					
Ji and Wood [37]	LiCl		b (m)	$m_L/A_{collector}$ (kg/m^2-hr)	Y_{IN} (g/kg)	Re	yes	Glass covered roofing shingles was used as the collector.
			0.01-0.25	5-35	6-43	2000-8000		
		η_R	optimum	↓	↓	↑		
Mullick and Gupta [62]	$CaCl_2$		I (W/m^2)				yes	Glazed solar collector regenerator. The air flows through the channel between the collector and the glazing by thermosiphon action.
			200-1000					
		η_R	↑					
Peng and Howell [71]	TEG		$M_aK_Glf/(m_L/w_c)$	$I\alpha l/[c_pT_{L,in}(m_L/w_c)]$	$Ul/[c_p(m_L/w_c)]$	l (m)	no	Open solar collector.
			0.1-0.7	0.2-0.4	0.1-0.5	to 25		
		m_{evap}/l	↑	↑	↓	optimum		
Peng and Howell [71]	TEG		M_aK_Gl/m_a	m_v/m_L	l (m)	$UT_{amb}l/[H_{amb}m_L]$	$I\alpha l/[m_LH_{amb}]$	Glazed solar collector.
			0.03-0.08	5-10	0.5-4	0-0.1	0.2-0.3	
		m_{evap}/l	↑	↑↓†	opt.	↓	↑	
Thornbloom and Nimmo [90]	$CaCl_2$		b (m)		$m_a/A_{collector}$ (kg/m^2-hr)		yes	Glass covered roofing shingles was used as the collector.
			0.041-0.157		8.15-16.11			
		$m_{evap}/A_{collector}$	optimum		↑			

† Depending on the heat loss parameter $UT_{amb}l/[H_{amb}m_L]$
↑ performance parameter increases with increasing variable
↓ performance parameter decreases with increasing variable
↕ variable has no significant effect on the performance parameter

this configuration, water evaporates from the solution, condenses on the glass cover, and is removed through the troughs. The analysis showed that lithium chloride brine could be regenerated in a solar still with a daily efficiency of 5-20 %.

To improve the regeneration efficiency compared to the solar still, Mullick and Gupta [62] proposed a glazed trickle solar collector desiccant regenerator where the air is allowed to flow through the channel between the glazing and the collector surface by thermosiphon action. Compared to a solar still, this system achieved higher efficiencies (30-40 %), could operate at lower irradiation, and had a quicker response to irradiation since the fluid flowed as a thin film over the surface.

Peng and Howell [71] compared an open and a glazed solar collector regenerator. Theoretical modeling showed that the glazed solar collector required a much shorter length because of a higher mass transfer coefficient due to the air circulation, and smaller heat loss. A partly glazed and partly open solar collector regenerator was studied by Gandhidasan and Al-Farayedhi [27]. In this configuration, the upper part of the collector is covered with a single glazing, and the desiccant is heated without any evaporation taking place. Evaporation starts as the liquid enters the open lower part of the collector. A theoretical analysis revealed that as the glazed section was enlarged, the efficiency increased compared to a fully open collector for otherwise equal conditions. An optimum value of the ratio of glazed to unglazed collector area was found. This optimum value was found to decrease as the insolation increased. For hot and dry climates, the glazing decreased the efficiency, and it was found that for an ambient temperature of 40 °C, the collector worked well without glazing. For lower temperatures (25-30 °C) however, the glazing improved the regeneration efficiency.

Finally, the influence of the gap between the collector surface and glazing was investigated by Ji and Wood [37], and Thornbloom and Nimmo [90]. Both studies showed that an optimum gap height exists.

2.3 Liquid Desiccant Cooling Systems

Many system configurations using liquid desiccant cooling have been studied over the years. Although the concept is the same, the means of providing a contact area for heat and mass transfer between the desiccant and the air, the method of sensible air cooling, and the source of regeneration heat differ. Figure 2.2 and Table 2.8 summarize a number of liquid desiccant cooling systems. It should be pointed out that the definition of coefficient of performance (COP) reported varies among the authors. For example, Johannsen [38] defined a daily coefficient of performance as the amount of cooling supplied by the system divided by the solar energy incident on the solar collectors, so that the COP includes the collector efficiency. However, Scalabrin and Scaltriti [85] defined their coefficient of performance as the amount of cooling divided by the amount of heat supplied to the regenerator; i.e., the COP is independent of the heat source.

As previously mentioned, liquid desiccant cooling systems are capable of providing adequate dehumidification and cooling, and these systems may save a significant amount of energy compared to conventional air conditioning. Albers et al. [2] (Figure 2.2 (b)) estimated a 5 % lower energy consumption and 50 % lower operating cost for the desiccant system as compared to a conventional air conditioning

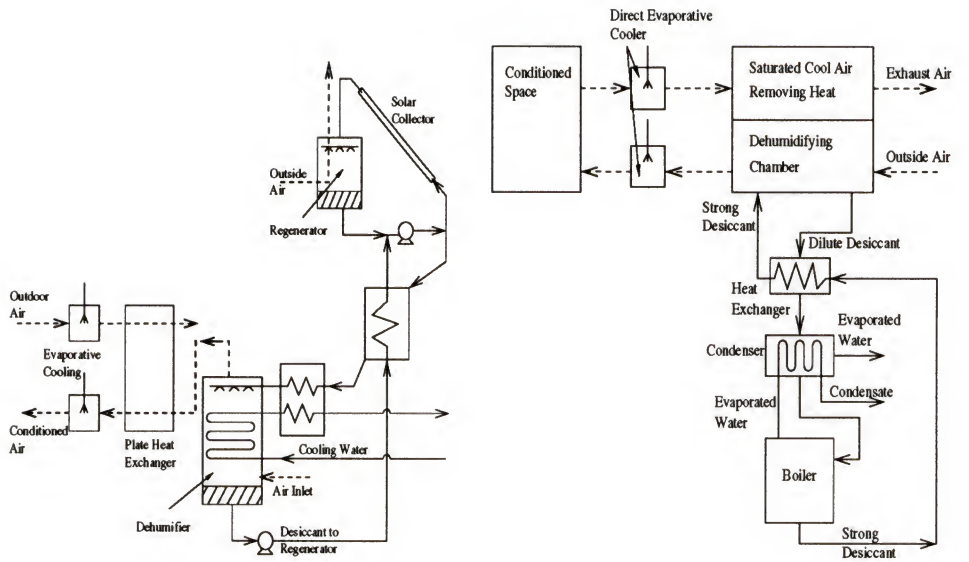

(a) (b)

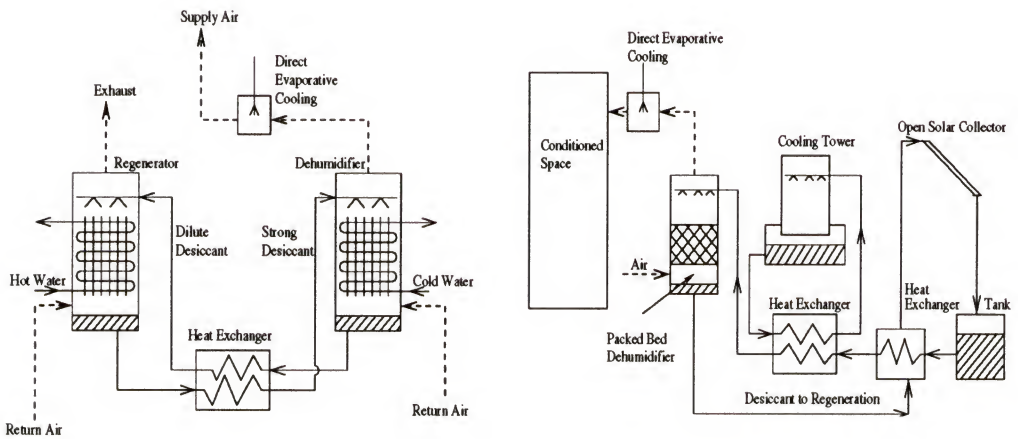

(c) (d)

Figure 2.2: Liquid desiccant systems - (a) Agarwal et al. [1]; (b) Albers et al. [2]; (c) Chebbah [10]; (d) Gandhidasan [24, 25]; (e) Griffiths [30]; (f) Johannsen [38, 39]; (g) Kettleborough and Waugaman [41]; (h) Khelifa et al. [47]; (i) Mahmoud and Ball [54]; (j) Marsala et al. [56] and Ryan et al. [80]; (k) Robison [79]; (l) Scalabrin and Scaltriti [85].

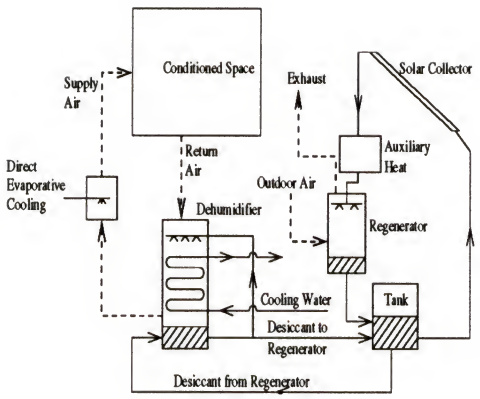

(e)

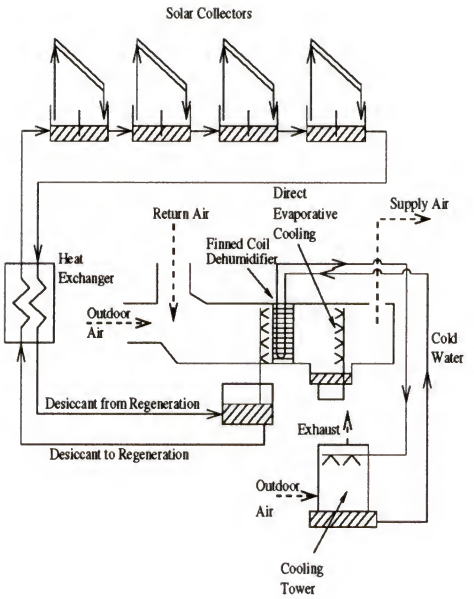

(f)

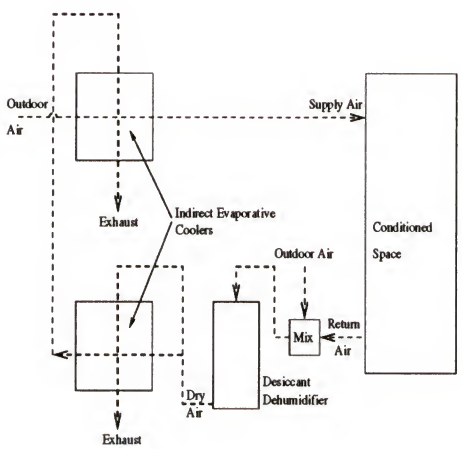

(g)

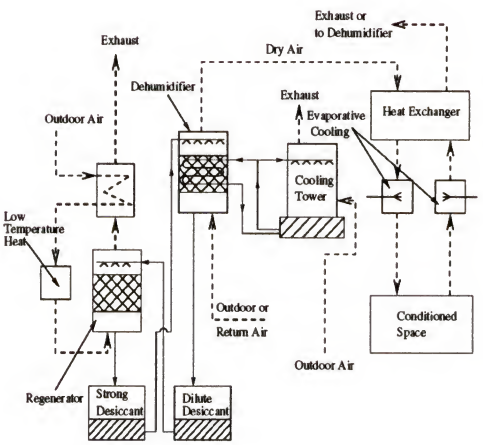

(h)

Figure 2.2--continued.

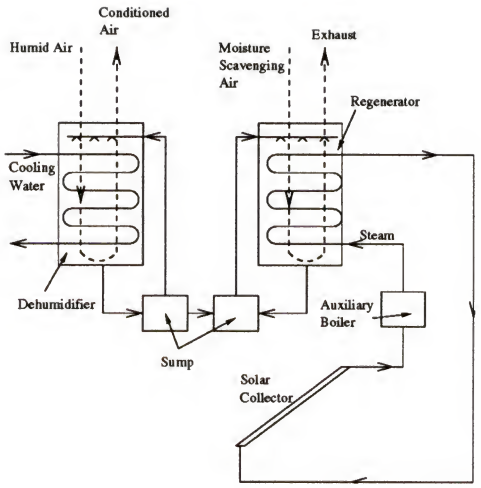

(i)

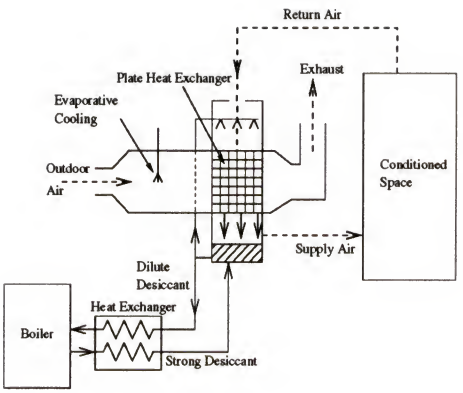

(j)

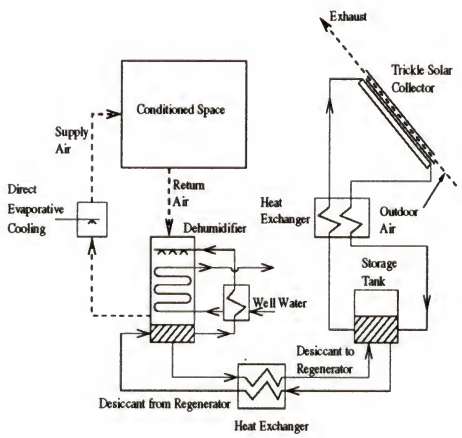

(k)

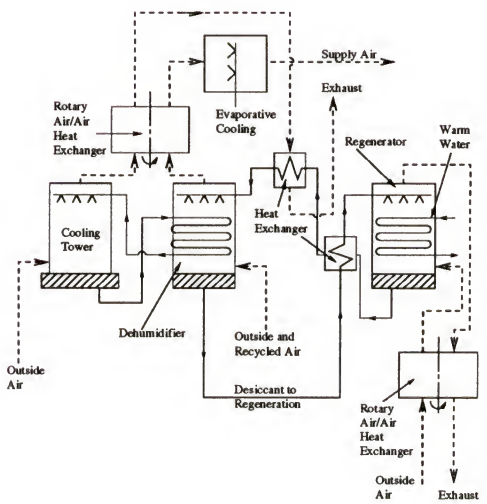

(l)

Figure 2.2--continued.

Table 2.8: Liquid desiccant cooling systems.

Author	Figure	Desiccant	COP	Experiments	Additional Comments
Agarwal et al. [1]	2.2 (a)	LiBr	N/A	no	Power consumption estimates for a conventional and a desiccant system for 12 locations in India.
Albers et al. [2]	2.2 (b)	LiBr	1.4 (Q_{cool}/Q_{boil})	yes	Heat and mass transfer technology employed patented by Albers and Beckman [3].
Chebbah [10]	2.2 (c)	TEG	0.31 ($Q_{cool}/IA_{collector}$)	yes	System optimization based on a cost analysis.
Gandhidasan [24, 25]	2.2 (d)	$CaCl_2$	N/A	no	Describe theoretical model for system analysis.
Griffiths [30]	2.2 (e)	-	-	-	U.S. Patent
Johannsen [38, 39]	2.2 (f)	TEG	0.23-0.36 (daily, $Q_{cool}/IA_{collector}$)	yes	Johannsen [38] presents theoretical models for the sprayed coil dehumidifier and the trickle solar collector. Experiments were conducted to verify the models. System performance simulation for five locations in South Africa.
Kettleborough et al. [41]	2.2 (g)	CELD	0.35 (Q_{cool}/Q_{heat})	no	Theoretical analysis of a desiccant cooling cycle where the building's supply air does not contact the desiccant.
Khelifa et al. [47]	2.2 (h)	$CaCl_2$	0.6 ($Q_{cool}/IA_{collector}$)	yes	Some typical experimental results based on long term testing listed.
Mahmoud and Ball [54]	2.2 (i)	LiCl	N/A	no	Condensing steam providing the regeneration heat. Thus the solar fraction obtained was very low.
Marsala et al. [56] and Ryan et al. [80]	2.2 (j)	LiCl	0.5-0.58 $(Q_{cool}/Q_{boil})_{avg}$	yes	System working as a free-standing residential dehumidifier. Economic projections for three U.S. locations show the cost benefits of the desiccant system compared to conventional dehumidification technology. Preliminary results from field testing.
Robison [79]	2.2 (k)	TEG	N/A	no	Detailed design description. Cycle shown on psychrometric chart.
Scalabrin and Scaltriti [83]	2.2 (l)	LiCl	0.7-0.9 (Q_{cool}/Q_{heat})	no	Theoretical performance modeling to examine ways of varying the refrigeration capacity, as well as the SHR.

system. In another study, field experiments demonstrated the ability of a residential packaged desiccant dehumidifier to maintain a test home at a desired dew point (Figure 2.2 (j)) [80]. An economic analysis of this system showed that using a combined desiccant dehumidifier and a vapor compression system met the latent cooling load and was more cost effective than using a standard vapor compression system together with a free-standing electric dehumidifier. A standard vapor compression unit by itself failed to meet the latent cooling load half of the time in the above case.

Liquid desiccant cooling systems using solar regenerators have been shown to be promising. Griffiths [30] patented a solar-assisted liquid desiccant cooling system. In this system, the dilute desiccant is first heated in solar collectors before it is brought in contact with a moisture scavenging air stream in a spray chamber (Figure 2.2 (e)). Strong desiccant is then brought to the air dehumidifier, where it is sprayed over a cooling coil in which cooling water flows, thereby removing the heat of absorption. The dried air is evaporatively cooled before it is brought to the conditioned space. Agarwal et al. [1] conducted a theoretical analysis of a liquid desiccant cooling system where heat from a solar collector was used for regeneration (Figure 2.2 (a)). It was found that this desiccant cooling system could reduce the power consumption by 24 to 48 % compared to a conventional vapor compression system. An experimental investigation as well as a theoretical simulation of a solar-assisted desiccant cooling system was conducted by Johannsen [38, 39] (Figure 2.2 (f)). It was concluded that the system was suitable for dry to moderate climates. Mahmoud and Ball [54] conducted the only study which found that using flat-plate solar collectors for regeneration of the desiccant is infeasible. However, in the system proposed, the desiccant was regenerated

by condensing steam in a coil in the regenerator (Figure 2.2 (i)), while solar collectors provided only preheat for steam generation.

Providing a storage for concentrated desiccant may improve the performance of solar liquid desiccant systems, since the system can continue to operate during times when there is little or no solar energy available [79]. This concept was also suggested by Johannsen [38] for elimination of the hourly imbalance between cooling load and capacity. In the system described by Khelifa et al. [47], one cubic meter of a concentrated calcium chloride solution (62 % by weight) was reported to provide 5 kW continuous cooling for about 5 days. Meckler [60] recommended employing chemical energy storage by regenerating desiccant during off-peak hours which could be stored for use during on-peak hours (latent cooling demand hours), thus increasing the overall performance of desiccant dehumidification systems.

In an alternative liquid desiccant cooling cycle described by Kettleborough and Waugaman [41], the cooled air supplied to the conditioned space does not contact the desiccant (Figure 2.2 (g)). In their system, a desiccant dehumidifier provides dry air which can then be evaporatively cooled to a very low temperature. This evaporatively cooled air is brought in contact with the ventilation air to be supplied to the building in an air-to-air heat exchanger. The supply air stream is then sufficiently cooled so that condensation occurs. This concept is interesting in that it would eliminate any health hazards resulting from exposing a building's supply air to the desiccant.

In hybrid systems, the desiccant dehumidifier handles the latent cooling load, and a conventional vapor compression or absorption refrigeration system handles the sensible cooling load. Waste heat from the condenser in a vapor compression system,

and from the absorber and condenser in an absorption system, may be used as part of the heat needed for the desiccant regeneration. Since the moisture is absorbed by the desiccant, the evaporator does not have to be maintained at the dew point of the air delivered. Hence, the evaporator temperature may be increased which will increase the COP of the vapor compression system. Figure 2.3 and Table 2.9 summarize hybrid liquid desiccant cooling systems.

A hybrid liquid desiccant vapor compression air conditioning system was patented in 1991 by Peterson and Howell [76] (Figure 2.3 (e)). In their system, the evaporator is used as the air dehumidifier, and the condenser is used as the desiccant regenerator. Desiccant is distributed over the fins in the evaporator and condenser coils. A thermodynamic analysis of such a hybrid system using lithium bromide as the desiccant was carried out by Yadav and Kaushik [102] and Yadav [101]. The overall COP of the hybrid system was found to decrease as the latent cooling load increased, and it was lower than for a conventional vapor compression system. However, the hybrid systems used 40-80 % less electrical energy compared to the conventional system, with the electrical energy savings increasing with increasing latent load.

Seasonal performance of a hybrid liquid desiccant cooling system operating in four modes was simulated by Sick et al. [86] (Figure 2.3 (f)). In mode one, a heat pump provided the regeneration heat and part of the cooling load. In mode two, a gas cogenerator produced both electricity and regeneration heat, and the sensible cooling load was met by a chiller. In mode three, solar energy was used as the regeneration heat source and the cooling load was met by the chiller. Mode four used a conventional air conditioning system. The total energy requirement was found to increase for the hybrid

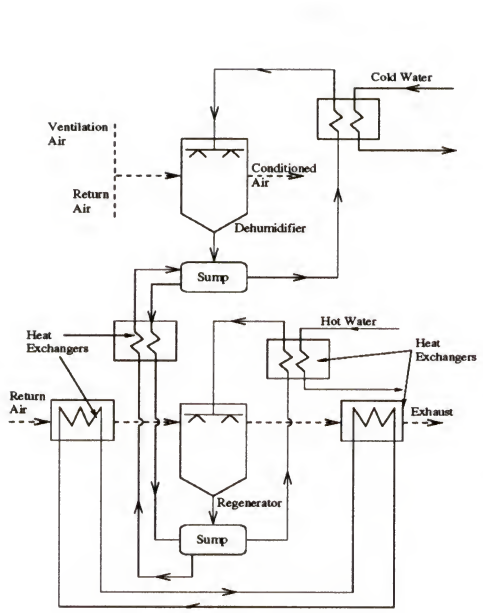

(a)

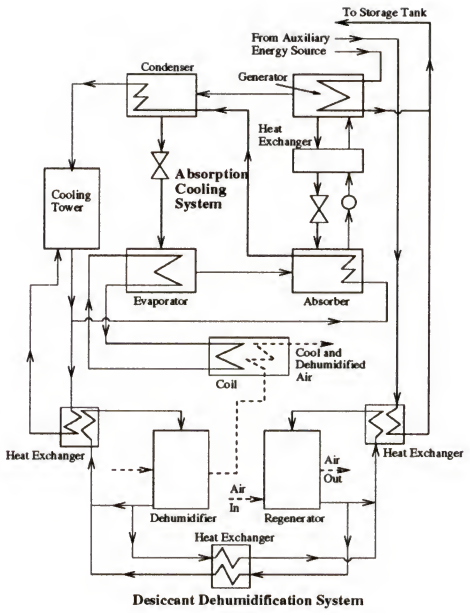

(b)

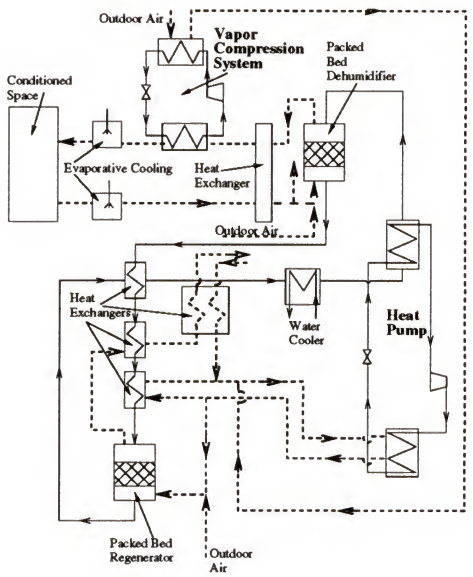

(c)

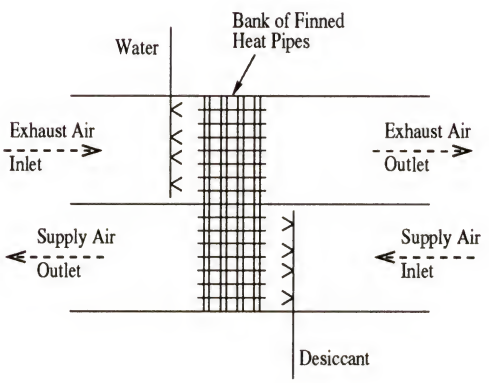

(d)

Figure 2.3: Hybrid liquid desiccant systems - (a) Buschulte and Klein [9]; (b) Hernandez et al. [33]; (c) Kinsara et al. [48]; (d) Pesaran et al. [74]; (e) Peterson and Howell [76]; (f) Sick et al. [86]; (g) Thornbloom and Nimmo [91]; (h) Wilkinson et al. [99].

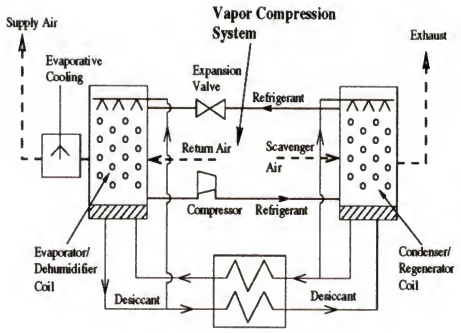

(e)

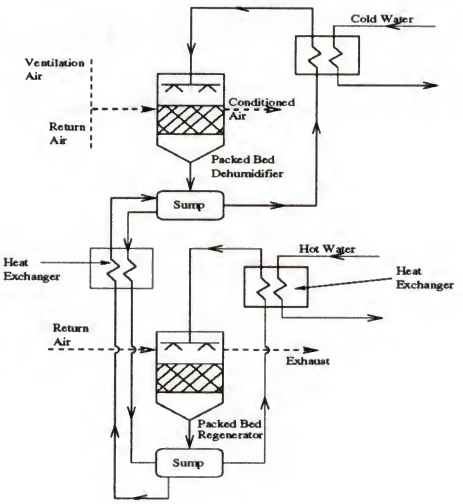

(f)

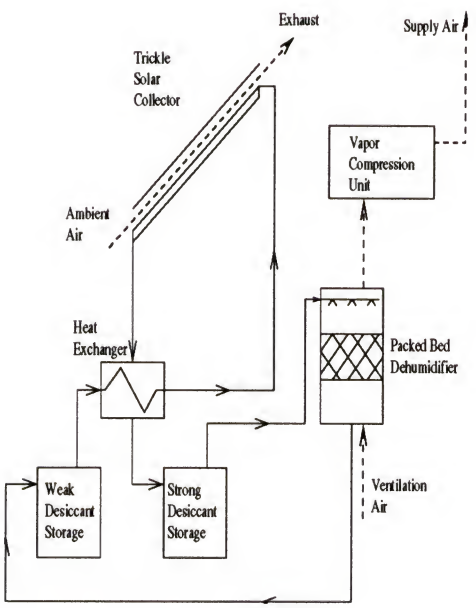

(g)

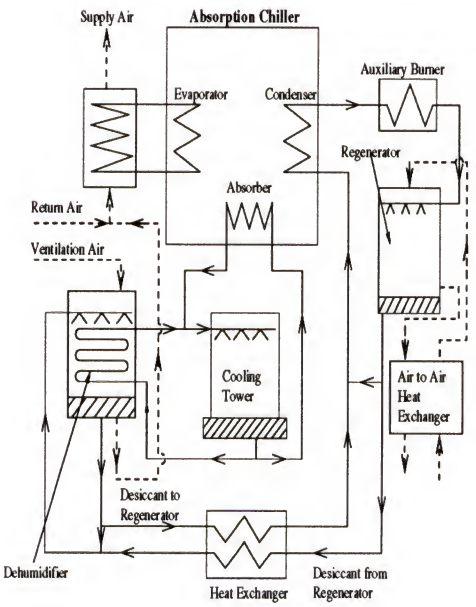

(h)

Figure 2.3--continued.

Table 2.9: Hybrid liquid desiccant cooling systems.

Author	Figure	Desiccant	COP	Experiments	Additional Comments
Buschulte and Klein [9]	2.3 (a)	LiCl	N/A	no	Compared three sources of regeneration heat: a heat pump, a gas cogenerator, and solar.
Hernández et al. [33]	2.3 (b)	LiBr	0.2-0.4 (Q_{cool}/Q_{heat})	no	Compared the performance of the hybrid desiccant system to the performance of a solar assisted absorption cooling system for tropical climates.
Kinsara et al. [48]	2.3 (c)	$CaCl_2$	See comments.	no	A ratio, $COP_{hybrid}/COP_{conventional}$= 0.5-3.0, was reported.
Pesaran et al. [74]	2.3 (d)	LiCl and TEG	-	yes	Desiccant enhanced heat pipe heat recovery unit.
Peterson and Howell [76]	2.3 (e)	-	-	-	U.S. Patent
Saunders et al. [84]	-	LiCl	1.0-1.4 ($Q_{cool}/Q_{E,tot}$)	no	Theoretical investigation of the influence of regeneration temperature, and fraction of ventilation air on the COP of a DUBSLORB system proposed by Wilkinson et al. [99].
Sick et al. [86]	2.3 (f)	LiCl	N/A	no	Compared three sources of regeneration heat: a heat pump, a gas cogenerator, and solar. Seasonal performance analysis.
Thornbloom and Nimmo [91]	2.3 (g)	$CaCl_2$	N/A	no	Cost comparison between the desiccant system and a conventional vapor compression system serving as a ventilation air pre-conditioner for a supermarket in Miami.
Wilkinson et al. [99]	2.3 (h)	-	1.0-1.3 ($Q_{cool}/Q_{E,tot}$)	no	Description of the DUBSLORB concept, i. e., a hybrid desiccant absorption chiller. Advanced concepts are described by Wilkinson [96, 97, 98]
Yadav and Kaushik [102], and Yadav [101]	-	LiBr	3.1-3.3 ($Q_{cool}/Q_{E,tot}$)	no	Thermodynamic analysis of a hybrid system similar to the system patented by Peterson and Howell [76].

liquid desiccant configuration compared to the conventional operation. However, not considering the first cost, the lowest operating cost was obtained by the solar hybrid system. Nevertheless, the operating cost was comparable to that for a conventional system. A lower regeneration temperature was found to lower the operating cost even if this required the regenerator to operate for longer periods of time. From this study it is evident that using 'free' solar energy is cost effective. However, the parasitic electrical energy requirement of the desiccant systems must be minimized to lower the operating cost.

Another economic analysis comparing a solar liquid desiccant system to a conventional vapor compression system for ventilation air preconditioning was carried out by Thornbloom and Nimmo [91] (Figure 2.3 (g)). In this study, it was found that a conventional system required more energy than the desiccant system. A six year payback time was estimated for the desiccant system. Kinsara et al. [48] showed via theoretical modeling that a hybrid system (Figure 2.3 (c)) is capable of reducing the electrical energy consumption for air conditioning compared to a conventional system by as much as two thirds. Pesaran et al. [74] studied the performance of a desiccant enhanced heat pipe heat recovery unit (Figure 2.3 (d)). The cooling capacity of the heat pipe system increased 20-40 % using the desiccant compared to a system using the heat pipe alone.

Hybrid air conditioning systems combining a conventional absorption chiller with a liquid desiccant system was described by Wilkinson et al. [99] (Figure 2.3 (h)). The cooling tower that is needed for the absorption chiller's absorber is enlarged to also handle the heat evolved in the dehumidifier. The heat rejected in the absorption chiller

is used for regeneration of the desiccant. Additional heat can be provided by an auxiliary burner, especially during times when the latent load is large compared to the sensible cooling load handled by the absorption chiller. The coefficient of performance of the hybrid system was predicted to be greater than for the desiccant and absorption chiller subsystems alone. Some advanced concepts combining an absorption chiller with a desiccant system have also been proposed [96, 97, 98]. For instance, the condenser and/or absorber in a primary absorption cycle can be operated at elevated temperatures so that the heat from these units may be used for desiccant regeneration and/or generation heat in a secondary absorption chiller. These advanced concepts make it possible to divert the heat rejected to the second absorption chiller or to the desiccant regeneration as needed. However, they also increase the complexity of the system, and the increase in working fluid temperatures in the absorption cycle limits the choice of materials used.

Hernández et al. [34] analyzed the performance of a solar-assisted absorption system alone, an absorption system coupled to a liquid desiccant dehumidifier, and an absorption system coupled to a solid desiccant system. A critical solar fraction was defined as the minimum solar fraction for which the solar-assisted air conditioning system would consume less auxiliary energy than the electrical energy required by a conventional vapor compression air conditioning system. The highest solar fraction (88.4 %) was obtained for the hybrid liquid desiccant system. However, this fraction was below the corresponding critical solar fraction calculated. The solar-assisted absorption system by itself had a solar fraction of 87.5 %, which was higher than the critical solar fraction for this system. Results from an annual performance simulation of

a solar-assisted absorption chiller system, as well as the performance of a hybrid liquid desiccant absorption chiller (Figure 2.3 (b)), has been presented as well [33]. This simulation showed that the solar-assisted absorption system averaged a higher coefficient of performance compared to the hybrid system. Also, larger solar collector areas were needed for the hybrid system, even at high latent loads.

2.4 Concluding Remarks

Although desiccant cooling systems offer certain benefits over other cooling techniques, the system COP reported in the literature are generally lower for desiccant systems than those obtained for conventional air conditioning systems. If COP is employed as the primary performance criterion, desiccant cooling would always appear to be the least attractive alternative. However, an overall COP by itself is not sufficient for making comparisons between desiccant and conventional systems, since the quality of the energy used for air conditioning is not taken into consideration. Conventional air conditioning requires a large amount of electrical energy to meet the latent cooling load in humid climates. This needs to be taken into account when a comparison among systems is made. Therefore, energy efficiency ratio, EER, is a more important performance parameter since it shows the consumption of high quality electrical energy for cooling.

Liquid desiccant cooling has the ability to provide an efficient control of indoor humidity and temperature, while at the same time reducing the electrical energy requirements for air conditioning. Nevertheless, widespread utilization of this technology for air conditioning of buildings has not yet been realized. It is believed that

hybrid liquid desiccant systems offer the greatest potential, since the sensible and latent cooling loads can be individually handled in an effective manner. Regardless of the system type, additional studies are warranted in order to further advance the energy savings and environmental benefits which may be achieved with liquid desiccant cooling technologies.

The effectiveness of the heat and mass transfer between the air and the desiccant in a system has a large impact on the overall system performance. As previously explained, coil-type heat exchangers allow for an isothermal dehumidification process, thus making them efficient in handling the latent heat released during dehumidification. Still, packed bed absorption towers offer a larger area for heat and mass transfer per unit volume, thus lending themselves to compact design. Therefore, packed towers are selected as the desiccant-air contact device for the present investigation. Triethylene glycol is chosen as the candidate desiccant because of its good characteristics as compared to salt solutions; it is noncorrosive and has lower surface tension.

Since vapor absorption and desorption in a randomly packed tower involves simultaneous heat and mass transfer between the gas and liquid phases, and complex fluid flow patterns, theoretical modeling relies heavily upon experimental studies. However, only a limited number of experimental data are reported in the literature, especially for the use of triethylene glycol as the desiccant. Also, the experimental investigations reviewed in this chapter only consider a few design variables, keeping the others constant. Thus, an experimental study of the effects of variables such as air and desiccant flow rates, air temperature and humidity, desiccant temperature and concentration, and the area available for heat and mass transfer are of great interest.

CHAPTER 3
HEAT AND MASS TRANSFER STUDY OF A PACKED BED ABSORBER/REGENERATOR

As concluded in the previous chapter, the simultaneous heat and mass transfer between the air and the desiccant have a large impact on the overall desiccant system performance. Because of its large area for heat and mass transfer per unit volume, a packed bed absorption tower was selected as the contact device. However, theoretical modeling of such an absorber/regenerator relies heavily on experimental results, while only a limited number of experimental studies are reported in the literature.

This chapter presents a thorough study of the heat and mass transfer in a packed bed absorber/regenerator. A finite difference model used in the theoretical analysis is described in detail. Experimental results along with theoretical predictions are discussed, and these findings are compared to results previously reported in the literature. From this investigation, the influence of a number of design variables on the performance of the absorber/regenerator, is revealed. Finally, based on an evaluation of the experimental data from the present study and from the literature, performance correlations are derived. These correlations will simplify performance estimates and the design of liquid desiccant systems.

3.1 Finite Difference Model for Adiabatic Gas Absorption

For dilute gas and liquid mixtures, it is commonly assumed that the gas absorption process is isothermal. However, when a large amount of solute is absorbed, the process is exothermic, and neglecting the temperature effects in a theoretical model would result in large errors. This is because an increase in the liquid temperature during the absorption will reduce the equilibrium solubility of the solute, decreasing the capacity of the absorber [92]. Therefore, for adiabatic operation a larger liquid to gas flow ratio and/or a larger area for heat and mass transfer must be used to obtain the same capacity as for an isothermal process [92]. The heat evolved during absorption consists of the heat of mixing, and if the solute is a liquid at the reference state, the latent heat of condensation [92]. For ideal solutions, the heat of mixing is zero [92].

A theoretical model for adiabatic gas absorption in a packed tower was developed by Treybal [93]. This model includes the resistance to heat and mass transfer in both the gas and liquid phases. Also, it allows for simultaneous absorption of a single solute and evaporation or condensation of the solvent. In this model, the interfacial area is assumed to be the same for heat and mass transfer which is true if the packing is completely wetted. Furthermore, axial dispersion is neglected so that there are concentration and temperature gradients in the flow direction, only.

For the present study, a finite difference model based on the model by Treybal [93] is employed. In addition to the assumptions made by Treybal [93], here it is assumed that: only water is transferred between the air and the desiccant; the interfacial area for heat and mass transfer is equal to the total surface area of the packing; the heat

of mixing is negligible compared to the latent heat of condensation; and the resistance to heat transfer is negligible in the liquid phase, resulting in the interfacial temperature being equal to the desiccant bulk temperature. However, Kelly et al. [41] pointed out that the heat often evolves at the gas-liquid interface, which may result in an interfacial temperature different from that of either the bulk gas or the bulk liquid. This model was adapted for the heat and mass transfer between a liquid desiccant and air as described below.

Figure 3.1 (a) gives an overview of the packed bed absorption tower. The governing equations are obtained by dividing the packed bed height Z into small segments, dZ (Figure 3.1 (b)). Mass and energy balances are then solved for each segment, from the bottom to the top of the tower. A mass balance over the differential element (control volume III, Figure 3.1 b) yields

$$L + dL + G(1 + Y) = L + G(1 + Y + dY) \tag{3.1}$$

Equation (3.1) can be simplified to give the change in liquid flow rate as a function of the change in air humidity across the segment.

$$dL = GdY \tag{3.2}$$

The mass flux of water vapor across the interface, taken positive from the gas to the liquid, is

$$N_v M_w a_t dZ = F_G M_w a_t dZ \ln\left(\frac{1 - y_i}{1 - y}\right) = -G\, dY \tag{3.3}$$

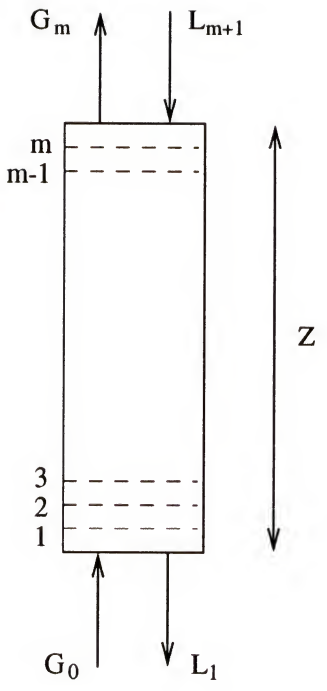

(a)

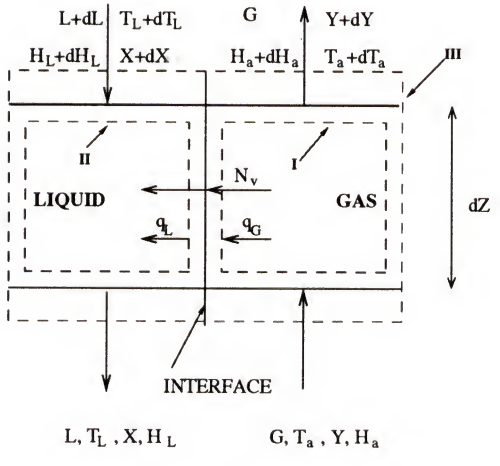

(b)

Figure 3.1: Packed bed absorption tower - (a) tower overview; (b) differential segment.

Equation (3.3) gives the change in air humidity across the segment as

$$\frac{dY}{dZ} = - \frac{M_w F_G a_t}{G} \ln\left(\frac{1 - y_i}{1 - y}\right) \tag{3.4}$$

Here the interfacial gas phase concentration is given by

$$y_i = 1 - (1 - y)\left(\frac{x}{x_i}\right)^{\frac{F_L}{F_G}} \tag{3.5}$$

Vapor-liquid equilibrium data for the triethylene glycol-water system [18] were used along with Equation (3.5) to solve for the interface concentrations in the gas and liquid phases.

The air temperature gradient across the segment is found from an energy balance across the gas phase (control volume I, Figure 3.1 (b)).

$$G H_a = G (H_a + dH_a) + N_v M_w a_t dZ H_v + q_G a_t dZ \tag{3.6}$$

Here H_v is the specific enthalpy of the water vapor.

$$H_v = c_{p,v} (T_a - T_0) + \lambda_0 \tag{3.7}$$

The heat transfer flux can also be written as

$$q_G a_t dZ = h_G' a_t (T_a - T_i) dZ \tag{3.8}$$

where $h_G' a_t$ is the heat transfer coefficient corrected for simultaneous heat and mass transfer as follows

$$h'_G a_t = \frac{-G\, c_{p,v} \frac{dY}{dZ}}{1 - \exp\left(\frac{G\, c_{p,v} \frac{dY}{dZ}}{h_G\, a_t} \right)} \tag{3.9}$$

The specific enthalpy of moist air is

$$H_a = c_{p,a} (T_a - T_0) + Y [c_{p,v} (T_a - T_0) + \lambda_0] \tag{3.10}$$

Since this enthalpy is a function of the air temperature and humidity (i.e., $H_a = H_a(T_a, Y)$), the differential change in air enthalpy is found from the partial derivatives of H_a:

$$dH_a = \frac{\partial H_a}{\partial T_a} dT_a + \frac{\partial H_a}{\partial Y} dY \tag{3.11}$$

so that

$$dH_a = (c_{p,a} + Y\, c_{p,v})\, dT_a + [c_{p,v} (T_a - T_0) + \lambda_0]\, dY \tag{3.12}$$

Applying equations (3.7) through (3.12) to Equation (3.6), and recognizing that $T_i = T_L$ when the resistance to heat transfer in the liquid phase is neglected, gives the air temperature gradient across the segment:

$$\frac{dT_a}{dZ} = \frac{- h'_G a_t (T_a - T_L)}{G (c_{p,a} + Y c_{p,v})} \tag{3.13}$$

An energy balance over the entire segment (control volume III, Figure 3.1 (b)) gives the change in desiccant temperature.

$$G\,H_a + (L + dL)(H_L + dH_L) = G(H_a + dH_a) + L\,H_L \qquad (3.14)$$

Simplifying Equation (3.14) and neglecting $dL dH_L$ gives

$$L\,dH_L + dL\,H_L = G\,dH_a \qquad (3.15)$$

Neglecting the heat of mixing, the enthalpy of the desiccant is given by Equation (3.16).

$$H_L = c_{p,L}(T_L - T_0) \qquad (3.16)$$

Assuming a constant desiccant specific heat gives

$$dH_L = c_{p,L}\,dT_L \qquad (3.17)$$

Combining equations (3.2), (3.12), (3.15), (3.16), and (3.17) gives the change in desiccant temperature across the segment.

$$\frac{dT_L}{dZ} = \frac{G}{c_{p,L}\,L}\left\{(c_{p,a} + Yc_{p,v})\frac{dT_a}{dZ} + \right.$$

$$\left. + [c_{p,v}\,(T_a - T_0) - c_{p,L}(T_L - T_0) + \lambda_0]\frac{dY}{dZ}\right\} \qquad (3.18)$$

A water mass balance across the segment (control volume III, Figure 3.1 (b)) gives the change in desiccant concentration across the segment.

$$(1 - [X + dX])(L + dL) + G\,Y = (1-X)L + G\,(Y + dY) \qquad (3.19)$$

Simplifying Equation (3.19) and applying Equation (3.2) gives the change in desiccant concentration as

$$\frac{dX}{dZ} = -\frac{G}{L}X\frac{dY}{dZ} \qquad (3.20)$$

Empirical correlations by Onda et al. [64] were used for the gas and liquid phase heat and mass transfer coefficients (equations (3.21), (3.22), and (3.23)).

$$k_L = 0.0051 \left(\frac{\mu_L g}{\rho_L}\right)^{1/3} \left(\frac{L}{a_w \mu_L}\right)^{2/3} \left(\frac{\rho_L D_L}{\mu_L}\right)^{1/2} (a_t d_p)^{0.4} \qquad (3.21)$$

$$\frac{a_w}{a_t} = 1 - \exp\left[-1.45 \left(\frac{\gamma_c}{\gamma_L}\right)^{0.75} \left(\frac{L}{a_t \mu_L}\right)^{0.1} \left(\frac{L^2 a_t}{\rho_L^2 g}\right)^{-0.05} \left(\frac{L^2}{\rho_L \gamma_L a_t}\right)^{0.2}\right] \qquad (3.22)$$

$$k_G = 5.23 \frac{a_t D_G}{RT_a} \left(\frac{G}{a_t\, \mu_g}\right)^{0.7} \left(\frac{\mu_G}{\rho_g\, D_G}\right)^{1/3} (a_t\, d_p)^{-2.0} \qquad (3.23)$$

These k-type mass transfer coefficients can be converted to F-type coefficients by equations (3.24) and (3.25) [93].

$$F_L = \frac{k_L\, \rho_L}{M_L} \qquad (3.24)$$

$$F_G = k_G P \tag{3.25}$$

The gas phase heat transfer coefficient is found by applying the heat and mass transfer analogy (Equation (3.26)).

$$j_h = \frac{h_G}{c_{p,a} G} Pr^{\frac{2}{3}} = j_m = \frac{F_G M_a}{G} Sc^{\frac{2}{3}} \tag{3.26}$$

Then,

$$h_G = F_G M_a c_{p,a} \frac{Sc^{\frac{2}{3}}}{Pr^{\frac{2}{3}}} \tag{3.27}$$

A FORTRAN computer program was written to carry out the finite difference analysis with the bed height Z divided into 1000 segments. The computation was carried out starting at the bottom of the packed bed (air inlet and desiccant outlet). The energy and mass balances described above were solved for each segment from the bottom to the top of the bed (air outlet and desiccant inlet). Since only the inlet conditions of the desiccant are known, the outlet conditions must initially be guessed, and iterations are required to find the desiccant outlet conditions that give the known inlet conditions at the top of the packed bed. An under-relaxation iterative procedure was utilized to promote convergence. The criteria for convergence was ± 0.05 °C for the inlet desiccant temperature, and ± 0.0001 kg TEG/kg solution for the inlet desiccant concentration.

3.2 Experimental Procedure

The rate of moisture removal from the air (water condensation rate) and the effectiveness of the dehumidification process, as well as the rate of water evaporation and the effectiveness of the regeneration process were studied experimentally as a function of the following variables: air and desiccant flow rates; air temperature and humidity ratio; desiccant temperature and concentration; and the height of the packed bed.

A schematic of the experimental facility is shown in Figure 3.2. The packed bed absorption tower was constructed from a 25.4 cm diameter acrylic tube to allow for flow visualization. The tower was made in sections so that the bed height could be varied without changing the distance from the liquid distribution to the top of the bed. The inner diameter of the tower was 0.24 m. The packing used was 2.54 cm polypropylene Rauschert Hiflow® rings with a specific surface area of 210 m^2/m^3. Fresh, unused triethylene glycol was stored in a tank, and its temperature was adjusted by circulating cold or warm water through a submerged copper coil. Before each experiment, the desiccant was allowed to recirculate to remove any temperature and concentration gradients. Air was blown past an air heater and through a humidifying chamber to adjust its temperature and relative humidity before it entered the packed tower. When the desired air and desiccant conditions were obtained, the desiccant was allowed to flow through the tower. The desiccant was distributed over the packing by three spray heads evenly spaced in an equilateral triangular configuration. Once steady state was obtained, measurements were taken for 10 to 20 minutes using a PC-based

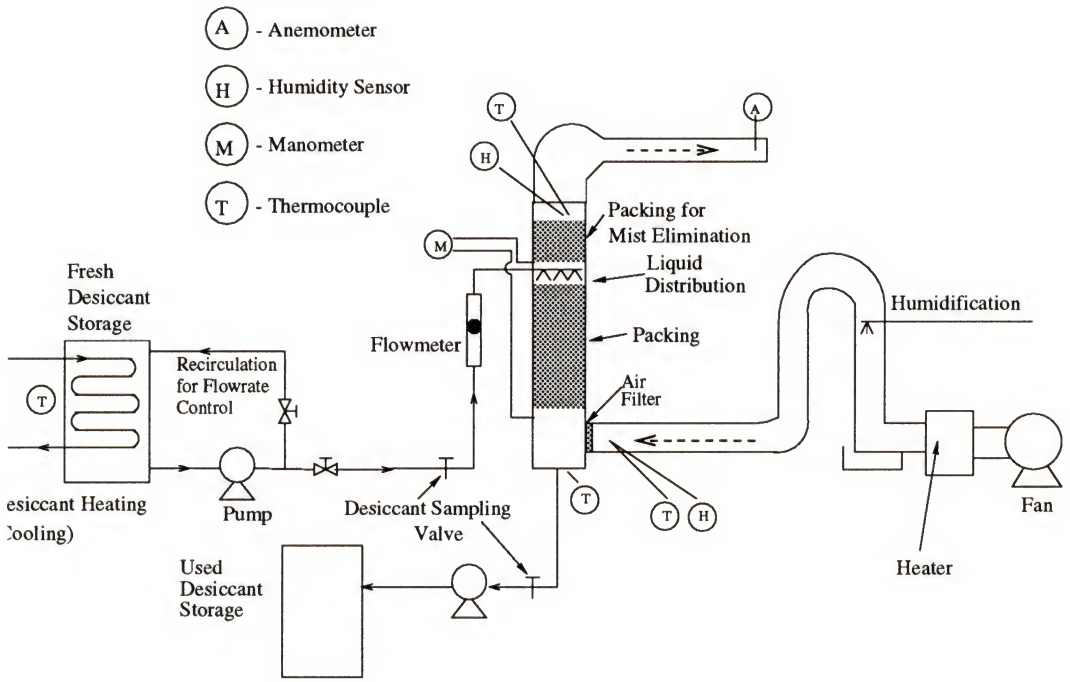

Figure 3.2: Experimental facility.

data acquisition system. These measurements included inlet and outlet temperatures of the desiccant and the air using copper-constantan thermocouples, as well as inlet and outlet air relative humidities using Mamac Hu-224-2-MA humidity probes. Samples of the desiccant entering and leaving the absorber/regenerator were taken during the experiment and analyzed for water content using Karl Fischer titration. The inlet desiccant concentration did not change during one experiment since the used desiccant was pumped to a separate storage tank. The liquid flow rate was set approximately using a Brooks Hi Pressure Thru-Flow Indicator and measured accurately by a catch-bucket method. Finally, the air velocity was measured using an anemometer at the air outlet and the air pressure drop over the packed bed was determined by an air-over-oil manometer. An uncertainty analysis is summarized in the APPENDIX.

Experiments were conducted for each variable at three levels (low, intermediate, and high value) while keeping the other variables constant at their intermediate value. Three experiments were conducted at each level.

3.3 Results of Desiccant Air Dehumidification

The results from the experimental study and theoretical modeling of the desiccant air dehumidification process are depicted graphically in figures 3.3 to 3.9. The figures show the water condensation rate, m_{cond} , the effectiveness, ϵ_Y (Equation (2.1)), and the enthalpy effectiveness, ϵ_H (Equation (2.4)), as a function of air and desiccant flow rates and inlet temperatures, desiccant concentration, inlet air humidity ratio, and packed bed height. As previously described, Chung [12] presented a correlation for the effectiveness as a function of design variables (Equation (2.3)). Results predicted from this correlation are also shown in figures 3.3 to 3.9. In each figure, error bars show the uncertainty of the experimental measurements. To cross-check the consistency of the data, a water mass balance across the dehumidifier was calculated, yielding ± 3 % deviation between the amount of water entering and leaving the dehumidifier. Similarly, an energy balance across the dehumidifier gave deviations of ± 6 %. Thus, the assumption of adiabatic absorption is satisfactory. The pressure drop across the packed bed varied between 30 and 210 Pa/m packing, depending on the air flow rate.

The experimental findings agree well with the predictions from the finite difference model described in this study. Only a slight discrepancy can be seen (approximately ± 15 %), and the difference is consistently within the error bars of the

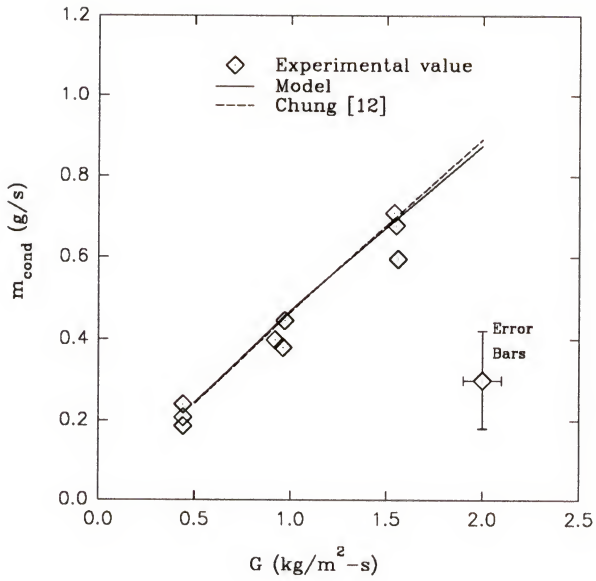

(a)

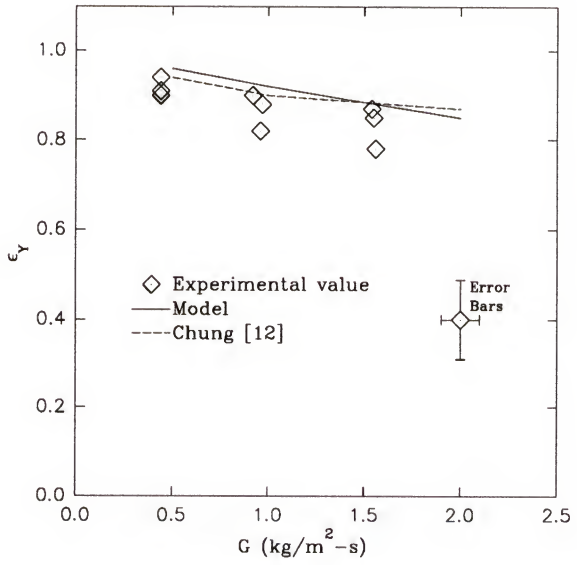

(b)

Figure 3.3: Influence of air flow rate on (a) condensation rate; (b) humidity effectiveness; (c) enthalpy effectiveness.

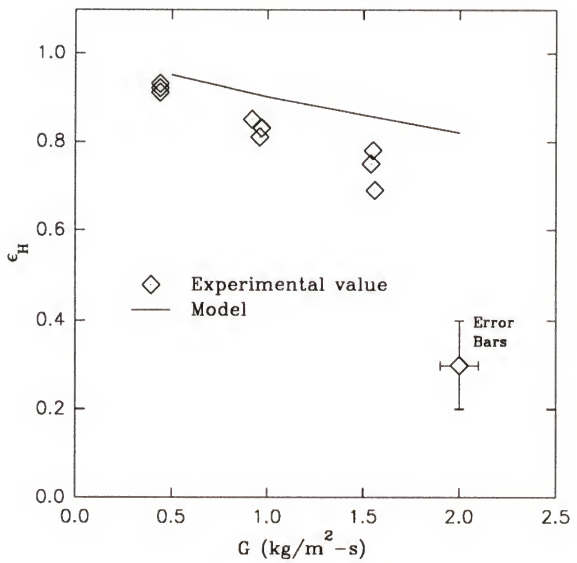

(c)

Figure 3.3 -- continued.

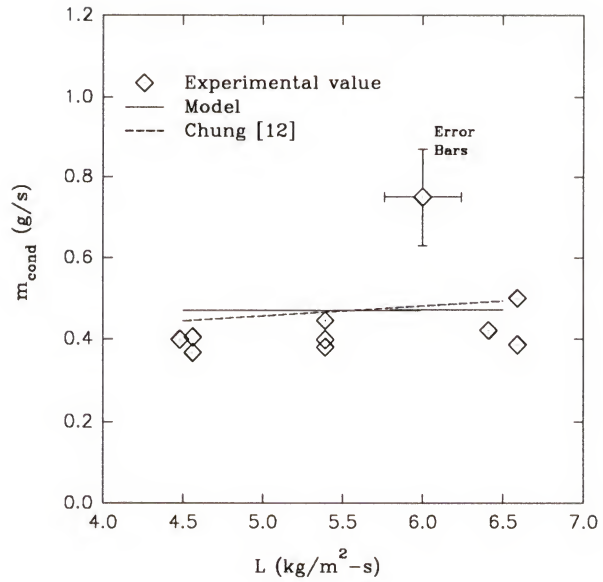

(a)

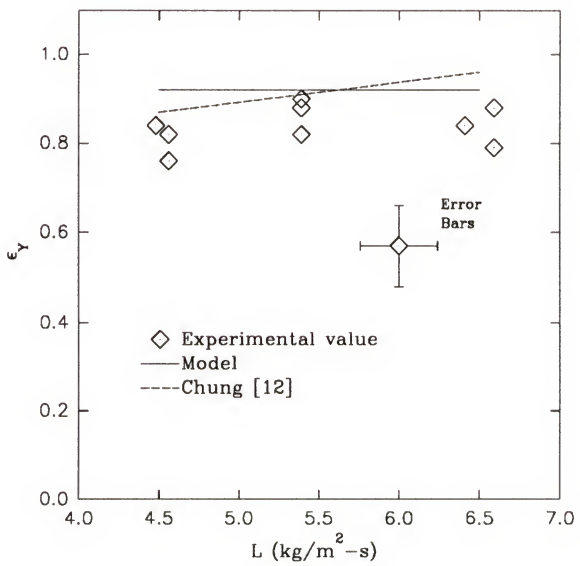

(b)

Figure 3.4: Influence of desiccant flow rate on (a) condensation rate; (b) humidity effectiveness; (c) enthalpy effectiveness.

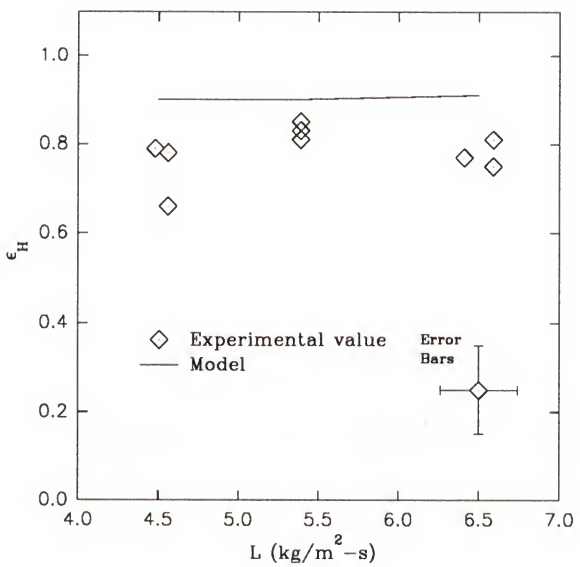

(c)

Figure 3.4 -- continued.

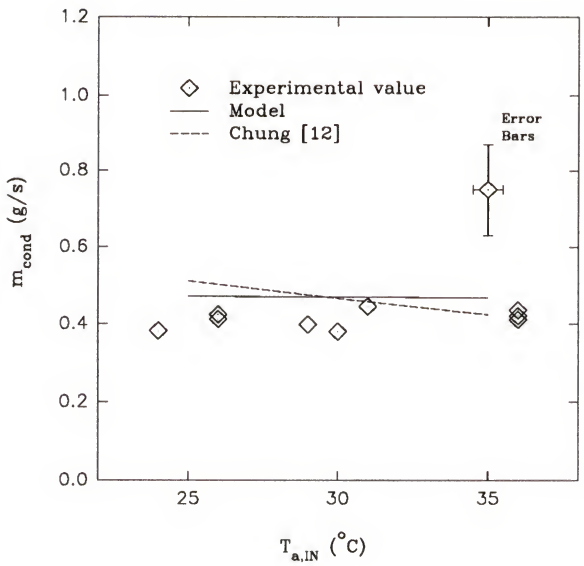

(a)

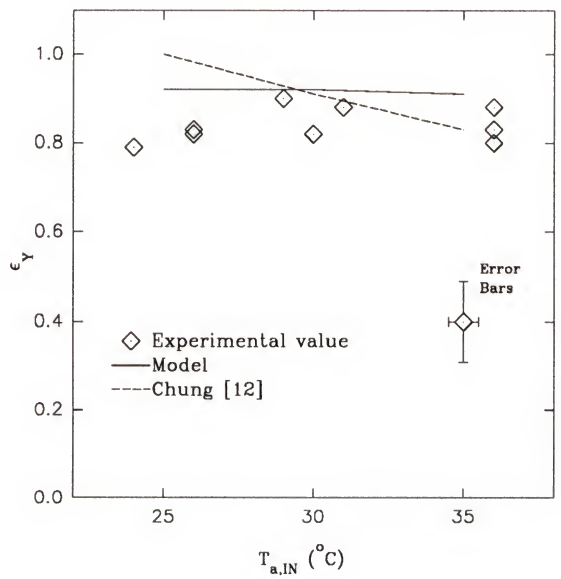

(b)

Figure 3.5: Influence of inlet air temperature on (a) condensation rate; (b) humidity effectiveness; (c) enthalpy effectiveness.

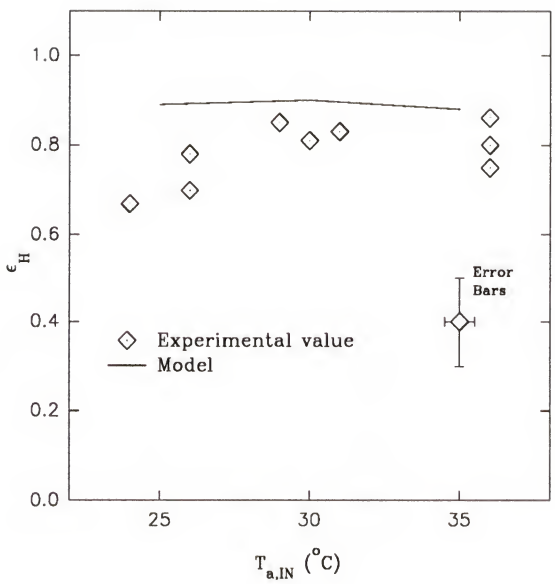

(c)

Figure 3.5 -- continued.

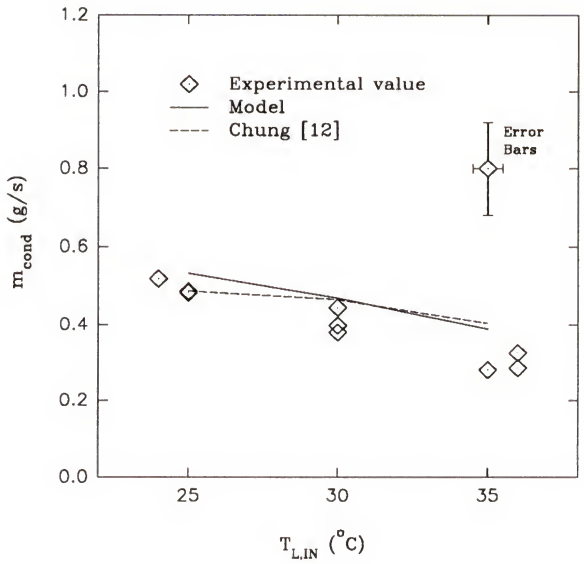

(a)

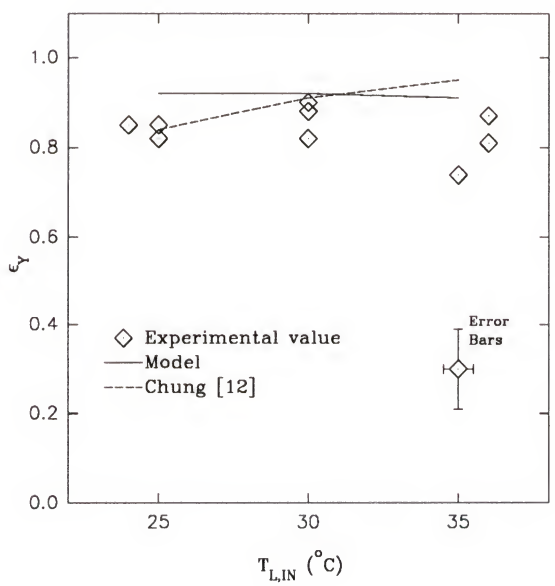

(b)

Figure 3.6: Influence of inlet desiccant temperature on (a) condensation rate; (b) humidity effectiveness; (c) enthalpy effectiveness.

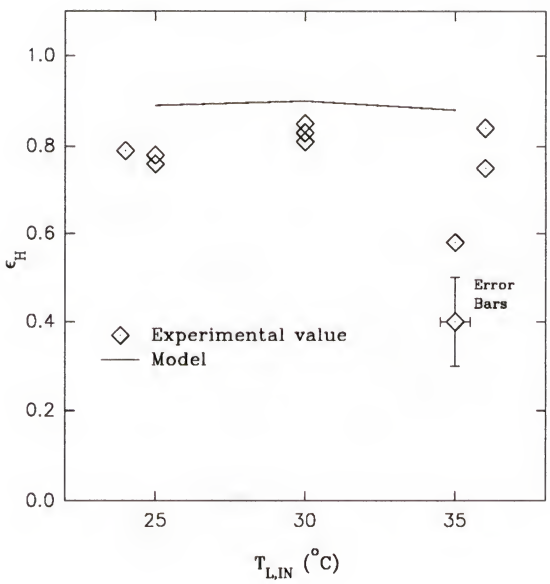

(c)

Figure 3.6 -- continued.

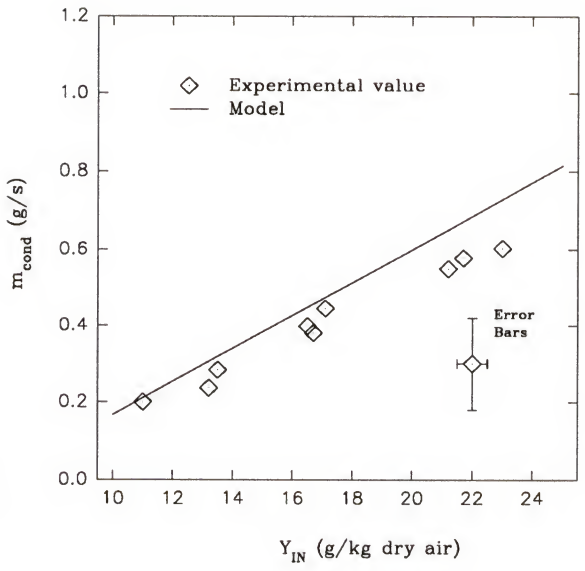

(a)

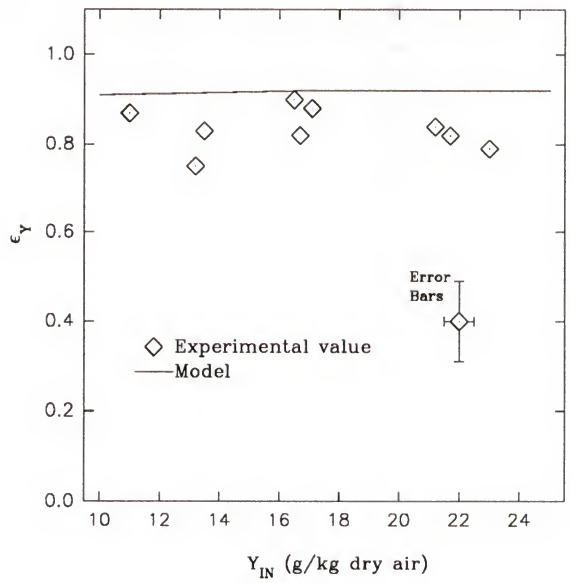

(b)

Figure 3.7: Influence of inlet air humidity ratio on (a) condensation rate; (b) humidity effectiveness; (c) enthalpy effectiveness.

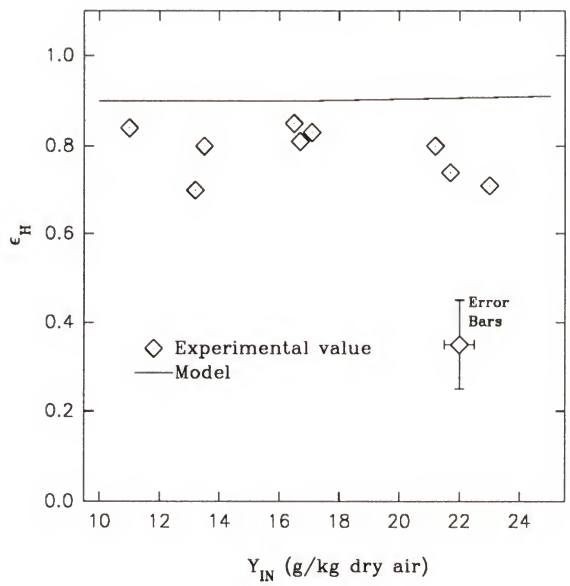

(c)

Figure 3.7 -- continued.

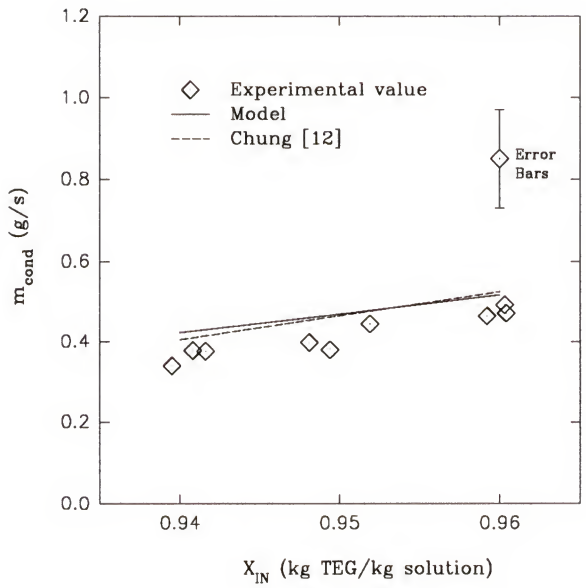

(a)

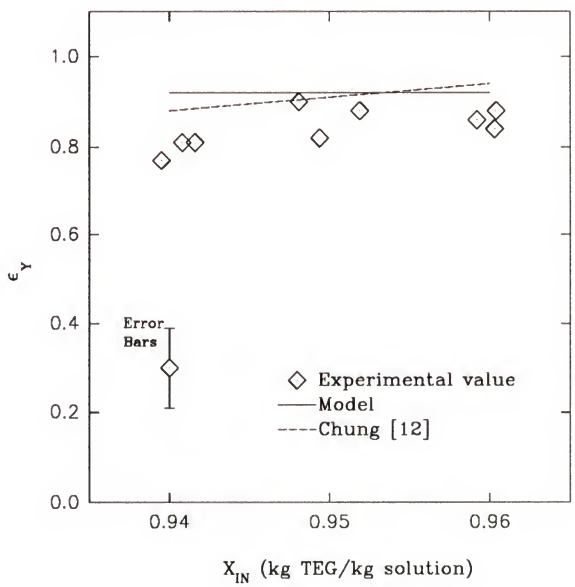

(b)

Figure 3.8: Influence of inlet desiccant concentration on (a) condensation rate; (b) humidity effectiveness; (c) enthalpy effectiveness.

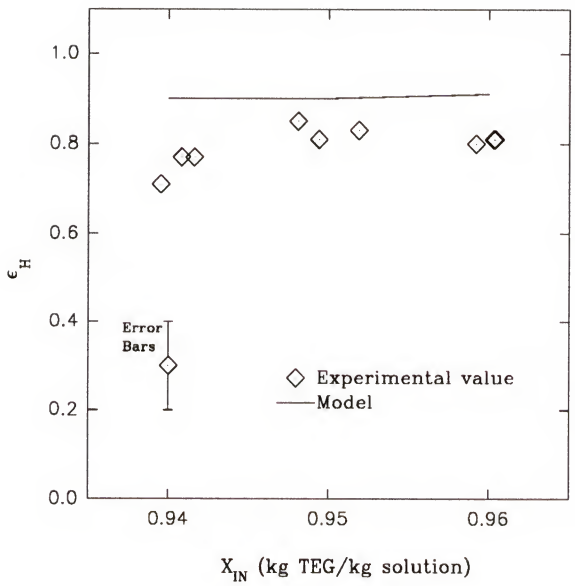

(c)

Figure 3.8 -- continued.

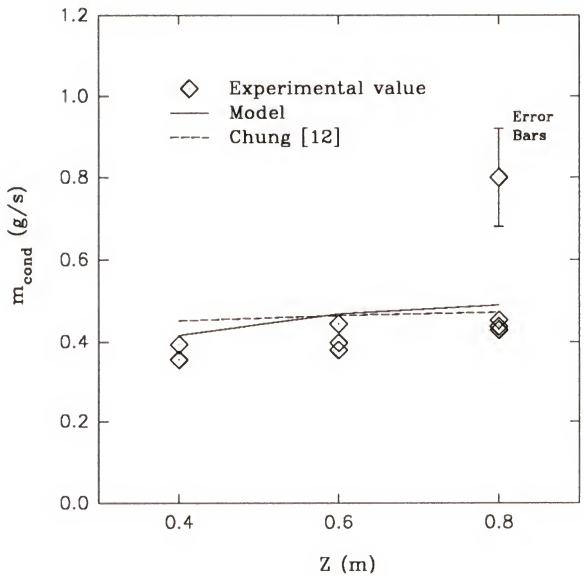

(a)

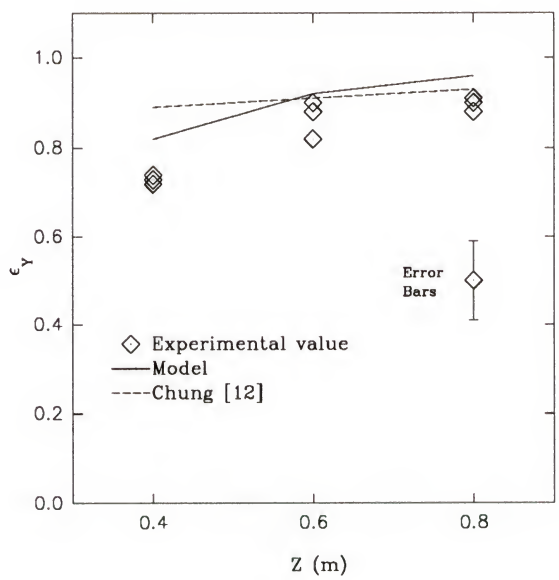

(b)

Figure 3.9: Influence of packed bed height on (a) condensation rate; (b) humidity effectiveness; (c) enthalpy effectiveness.

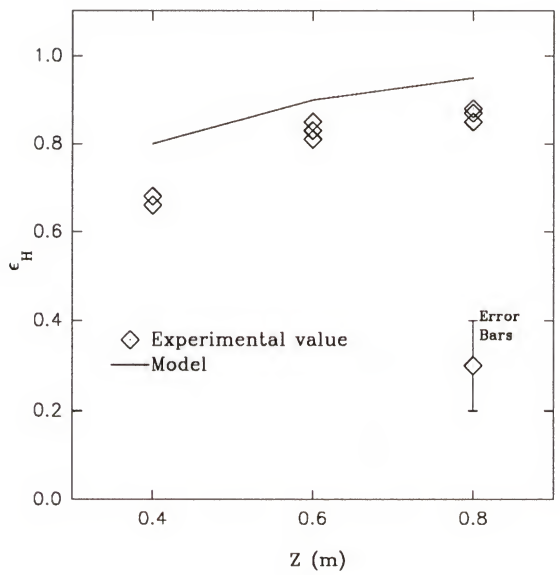

(c)

Figure 3.9 -- continued.

experiments. In cases where a discrepancy is apparent, the finite difference model generally overpredicts the performance of the dehumidifier. This is presumably due to the assumption made in the model that the area available for heat and mass transfer is equal to the total specific surface area of the packing. Even though the liquid flow rates are high as compared to the air flow rate, complete wetting of the packing is difficult to obtain. Therefore, the effective mass transfer area is less than the packing surface area. Also, it should be kept in mind that the correlations used for the transfer coefficients are empirical, and they were obtained for liquid-gas systems and packings other than those used in the present study. Although the correlation by Chung [12] predicted the performance of the dehumidifier within 15 % of the experimental findings of the present study, the finite difference model appears to predict the influence of design variables more accurately; that is, trends shown by the experimental values were also predicted by the finite difference model. More specifically, the decrease in dehumidifier performance with increasing inlet air temperature (Figure 3.5) predicted by the correlation by Chung [12] cannot be seen from the experiments or the finite difference model. Also, the correlation by Chung [12] showed a dependency on the inlet desiccant temperature which was not seen in the results from this experimental study and the finite difference model (Figure 3.6 (b)).

The present study revealed the following variables to have the most significant effect on the dehumidification performance: air flow rate, inlet desiccant temperature, inlet air humidity ratio, inlet desiccant concentration, and the area available for heat and mass transfer (which increases with the height of the packed bed). The condensation rate increased with the air flow rate (Figure 3.3 (a)). However, the change in humidity

ratio through the tower decreased with an increase in the air flow rate due to the reduced residence time for the air in the dehumidifier. Hence, the humidity effectiveness decreased with an increase in the air flow rate (Figure 3.3 (b)). A higher desiccant temperature gives a lower potential for mass transfer in the dehumidifier resulting in a lower condensation rate (Figure 3.6 (a)). However, the humidity effectiveness was not markedly affected by the desiccant temperature (Figure 3.6 (b)). This is because the lowest possible humidity ratio that can be obtained at the air outlet, Y_{equ} , is directly dependent on $T_{L,IN}$, making the effectiveness somewhat normalized with respect to the desiccant temperature. Similarly, the condensation rate increased with the desiccant concentration, but the desiccant concentration did not change the humidity effectiveness significantly (Figure 3.8). An increase in the area available for heat and mass transfer, obtained by increasing the height of the packed bed, increased the condensation rate and the effectiveness (Figure 3.9). A taller bed makes it possible for the air to reach a humidity ratio closer to the equilibrium value, Y_{equ} , at the air outlet.

The enthalpy effectiveness, ϵ_H (Equation (2.4)), is a measure of the effectiveness of the heat and mass transfer processes, combined. As the air and desiccant flows through the tower (counter flow), the air enthalpy approaches the value in equilibrium with the desiccant at the desiccant inlet, $H_{a,equ}$. This enthalpy would be obtained when the outlet air temperature, $T_{a,OUT}$, is equal to the inlet desiccant temperature, $T_{L,IN}$, and the outlet air humidity ratio is that in equilibrium with the desiccant at the desiccant inlet conditions, Y_{equ}. As depicted in figures 3.3 through 3.9, the enthalpy effectiveness is mainly influenced by the air flow rate and the packed bed height. The enthalpy

effectiveness decreases with increasing air flow rate (Figure 3.3 (c)). This is to be expected since for a high flow rate the air has less time to reach the desiccant temperature and equilibrium humidity ratio at the air outlet (desiccant inlet). The enthalpy effectiveness increases with the packed bed height since the area for heat and mass transfer increases with the bed height (Figure 3.9 (c)). A larger contact area between the air and the desiccant makes it possible for the air to leave the tower with an enthalpy closer to the equilibrium value ($H_{a,equ}$).

The influence of design variables is summarized in Table 3.1 along with the experimental findings previously reported in the literature. The table shows the desiccant used, the parameters describing the performance, the independent variables and the ranges examined. Under each independent variable, the influence of the variable on the performance parameter is indicated by up and down arrows. As shown, the present study used liquid flow rates significantly higher than the previous studies with the exception of the work by Chung et al. [13]. In the present study, initial experiments at lower flow rates showed poor performance compared to the predictions from the theoretical model. This was presumably due to inadequate wetting of the packing. Therefore, it was decided to carry out the experiments at higher flow rates. Chung et al. [13] had similar reasons for using high liquid flow rates. Indeed, Patnaik et al. [69] and Chen et al. [11] found the condensation rate to increase with liquid flow rate. They explained this partly by the increased wetting of the packing with increased flow rates. However, in the present study no dependency on the liquid flow rate was found. Hence, it may be concluded that the flow rates used in this study were sufficient to achieve maximum wetting for the present system. Patnaik et al. [69] found that the

Table 3.1: Dehumidifier performance from experimental studies.

Reference	Desiccant	Performance Parameter	Independent Variable						
present study	TEG		L (kg/m^2-s)	X_{IN} (kg/kg)	$T_{L,IN}$ (°C)	G (kg/m^2-s)	$T_{a,IN}$ (°C)	Y_{IN} (g/kg)	Z (m)
			4.5-6.5	0.94-0.96	25-35	0.5-2.0	25-35	11-22	0.4-0.8
		m_{cond}	↑↓	↑	↓	↑	↑↓	↑	↑
		ϵ_Y	↑↓	↑↓	↑↓	↓	↑↓	↑↓	↑
		ϵ_H	↑↓	↑ (slightly)	↑↓	↓	↑ (slightly)	↑↓	↑
Chen et al. [11]	LiCl		L (kg/m^2-s)	X_{IN} (kg/kg)	$T_{L,IN}$ (°C)	G (kg/m^2-s)	$T_{a,IN}$ (°C)	Y_{IN} (g/kg)	Z (m)
			0.1-1.0	0.3-0.4	26-39	0.2-1.2	25-35	17-22	0.1-0.6
		m_{cond}	↑	↑	↓	↑	↑	↑	↑
Chung et al. [13]	TEG		L (kg/m^2-s)		X_{IN} (kg/kg)		G (kg/m^2-s)		
			6-11		0.9-0.95		0.8-1.2		
		ϵ_Y	↑		↑		↓		
		K_Ga	↑		↑		↑		
McDonald et al. [57]	mixture of LiCl and $CaCl_2$		L (kg/m^2-s)		$T_{L,IN}$ (°C)	X_{IN} (kg/kg)	$T_{a,IN}$ (°C)	Y_{IN} (g/kg)	Z (m)
			1.5-3.9		28-43	0.4-0.45	31-36	21-41	0.5-1.4
		$T_{a,OUT}$	↓		↓	↑↓	↑↓	↑	↑↓
		Y_{OUT}	↓		↓	↑↓	↑↓	↑	↑↓
Patnaik et al. [69]	LiBr		L (kg/m^2-s)		$T_{L,IN}$ (°C)	X_{IN} (kg/kg)	G (kg/m^2-s)	$T_{a,IN}$ (°C)	Y_{IN} (g/kg)
			0.6-1.7		24-32	0.45-0.58	1.3-1.9	24-36	9-22
		m_{cond}	↑		↑↓	↑	↑↓	↓	↑

↑ performance parameter increases with increasing variable
↓ performance parameter decreases with increasing variable
↑↓ variable has no significant effect on the performance parameter

condensation rate decreased as the inlet air temperature increased. They explained this dependency on the increase in liquid temperature due to sensible heat transfer from the air to the desiccant. The present study showed no dependency of the condensation rate on the inlet air temperature. The reason for this observation is that the desiccant flow rate was significantly higher than the air flow rate. Therefore, the sensible heat transfer from the air to the desiccant was too small to affect the desiccant temperature significantly. Chen et al. [10] found that the condensation rate increased with the inlet air temperature. This was probably due to the fact that they used relative humidity as a variable instead of humidity ratio. For a constant relative humidity, the warmer the air, the higher the humidity ratio, which gives a higher condensation rate.

From Table 3.1 it is evident that no previous experimental investigation has examined the influence of design variables on the enthalpy effectiveness, ϵ_H. Therefore, the findings from the present study are of great interest. Through theoretical modeling, Khan [42, 43] examined the influence of design variables on ϵ_H for a packed bed dehumidifier using lithium chloride as the desiccant. A summary of these results previously given in Table 2.2 shows that ϵ_H increased with the desiccant to air flow ratio (L/G), and the number of transfer units (NTU). This is consistent with the experimental findings in the present study in that ϵ_H increases with decreasing air flow rate (i.e., with increasing L/G ratio), and increasing packed bed height (i.e., with increasing heat and mass transfer area and NTU).

3.4 Results of Desiccant Regeneration

Experimental and theoretical performance results for a packed bed desiccant regenerator are shown in figures 3.10 to 3.16. These figures show the water evaporation rate, m_{evap}, the humidity effectiveness, ϵ_Y (Equation (2.1)), and the enthalpy effectiveness, ϵ_H (Equation (2.4)), as a function of the air and desiccant flow rates and temperatures, desiccant concentration, air humidity, and the height of the packed bed. Results obtained from the correlation by Chung [12] are also shown. Error bars show the uncertainty of the experimental measurements. A water mass balance across the regenerator gave a ± 5 % deviation between the amount of water entering and leaving the regenerator, while an energy balance gave ± 10 % deviations. The pressure drop across the regenerator was the same as for the dehumidifier; between 30 and 210 Pa/m, depending on the air flow rate.

Predictions from the finite difference model agree well with the experimental findings for the desiccant regenerator (approximately within ± 15 %). As for the dehumidification process, the model slightly overpredicts the regenerator performance. Again this is due to the model assumption that the area for both heat and mass transfer is equal to the total specific surface area of the packing. However, only the wetted part of the packing provides surface area for the mass transfer. Since complete wetting of the packing is difficult to obtain, the area available for mass transfer is lower than the total packing surface area. The correlation by Chung [12] greatly overpredicts the performance of the regenerator, and the influence of design variables is not accurately shown from this correlation. For instance, the humidity effectiveness obtained from the

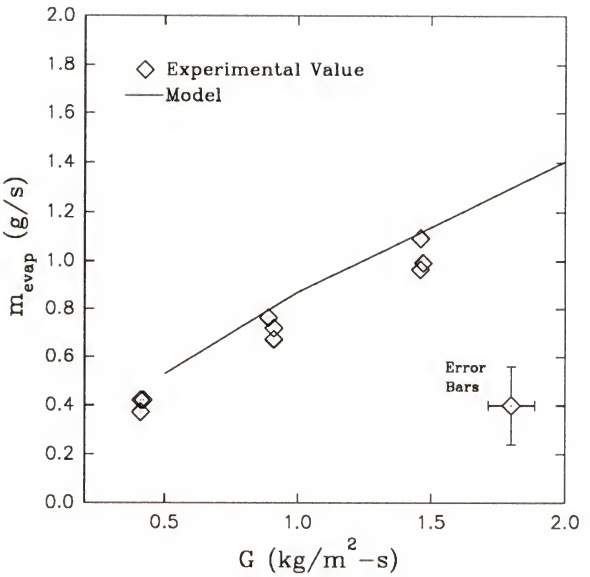

(a)

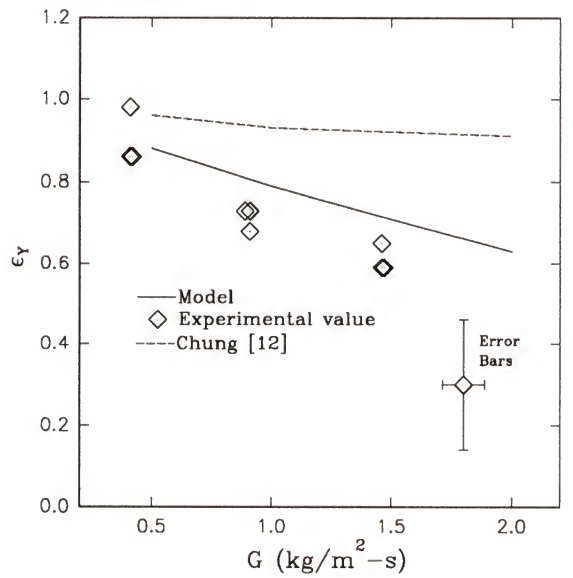

(b)

Figure 3.10: Influence of air flow rate on (a) water evaporation rate; (b) humidity effectiveness; (c) enthalpy effectiveness.

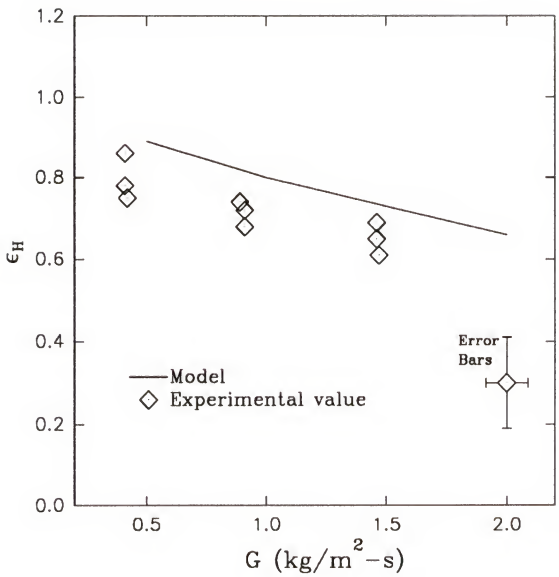

(c)

Figure 3.10 -- continued.

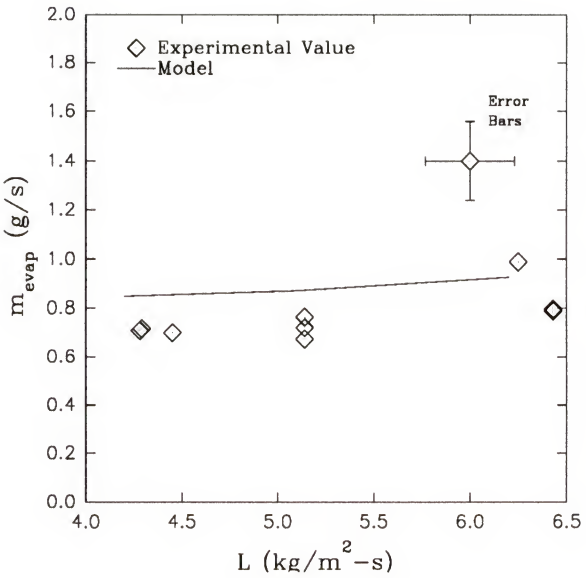

(a)

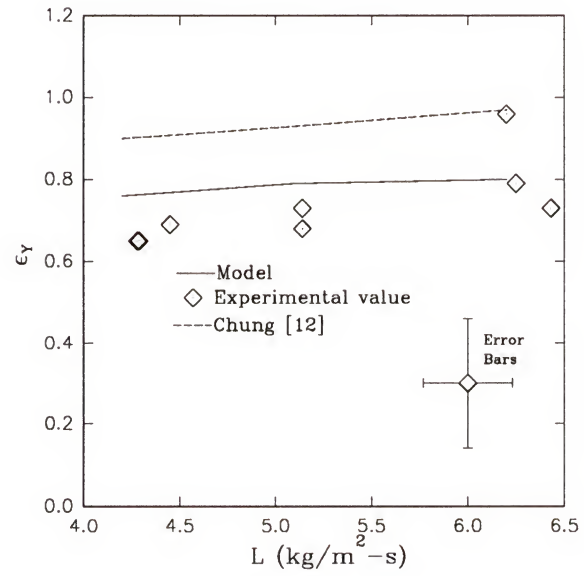

(b)

Figure 3.11: Influence of desiccant flow rate on (a) water evaporation rate; (b) humidity effectiveness; (c) enthalpy effectiveness.

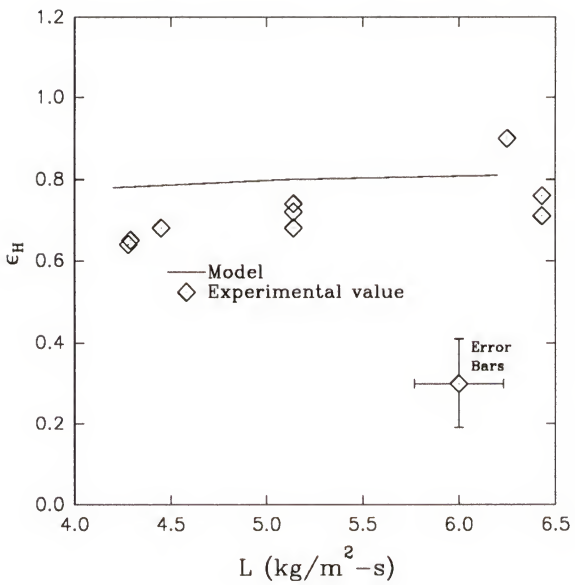

(c)

Figure 3.11 -- continued.

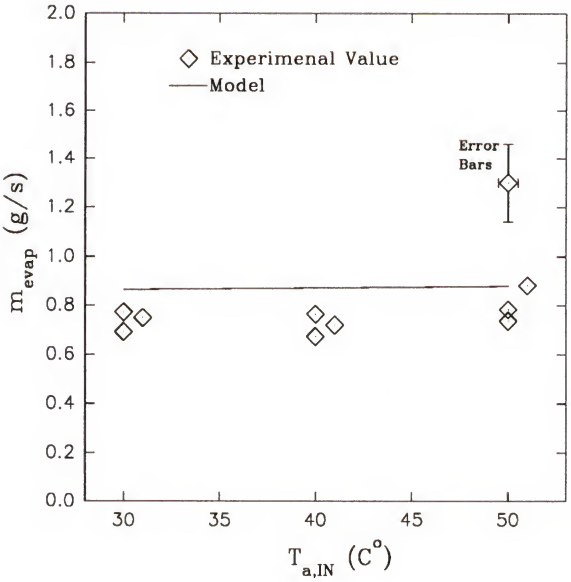

(a)

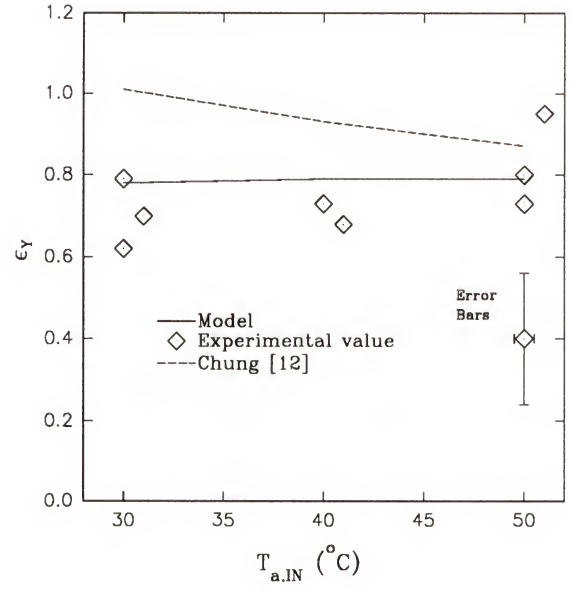

(b)

Figure 3.12: Influence of inlet air temperature on (a) water evaporation rate; (b) humidity effectiveness; (c) enthalpy effectiveness.

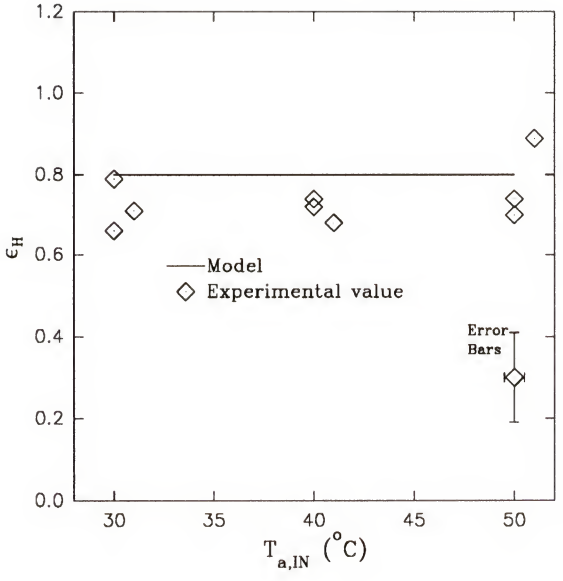

(c)

Figure 3.12 -- continued.

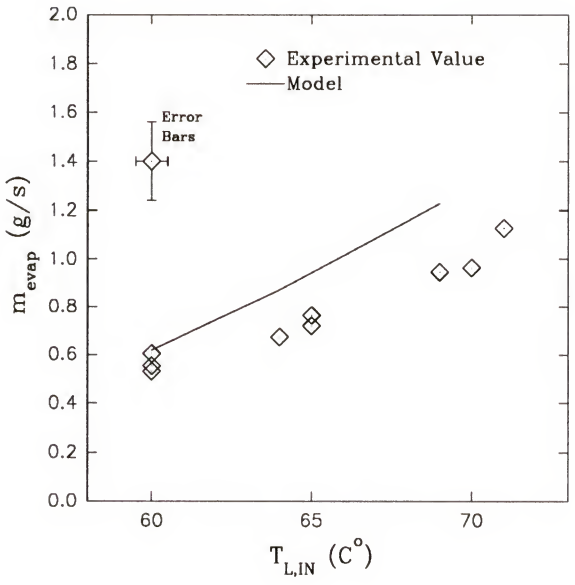

(a)

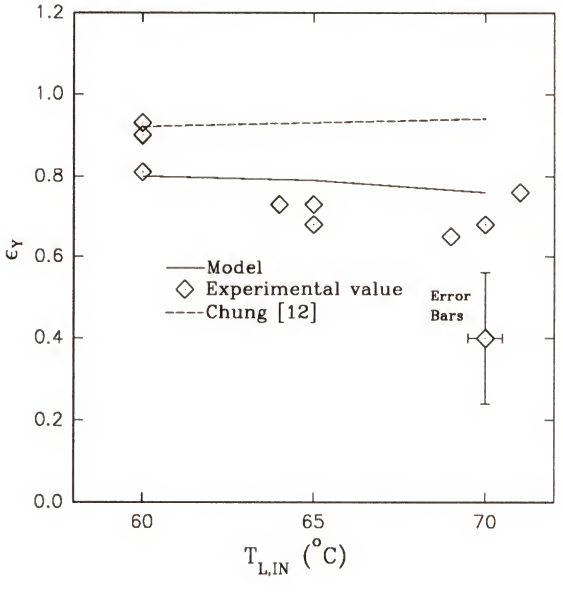

(b)

Figure 3.13: Influence of inlet desiccant temperature on (a) water evaporation rate; (b) humidity effectiveness; (c) enthalpy effectiveness.

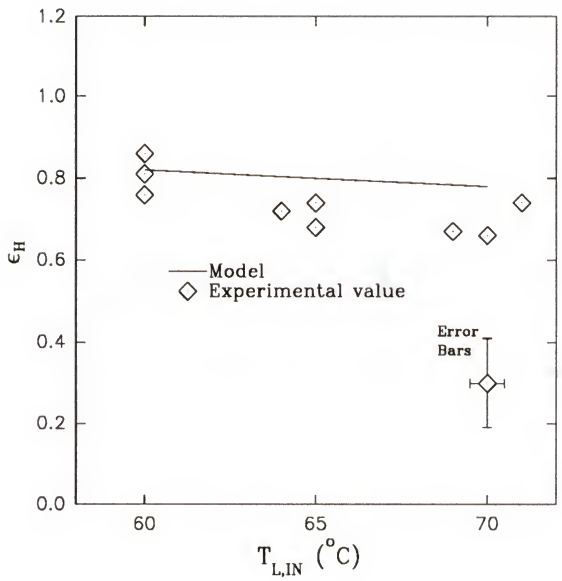

(c)

Figure 3.13 -- continued.

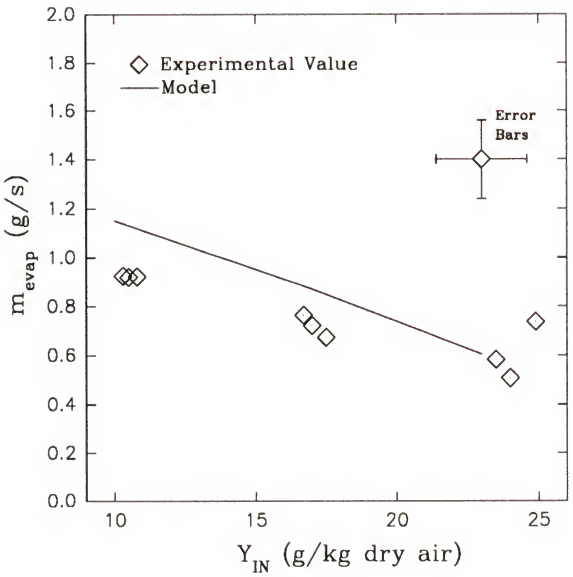

(a)

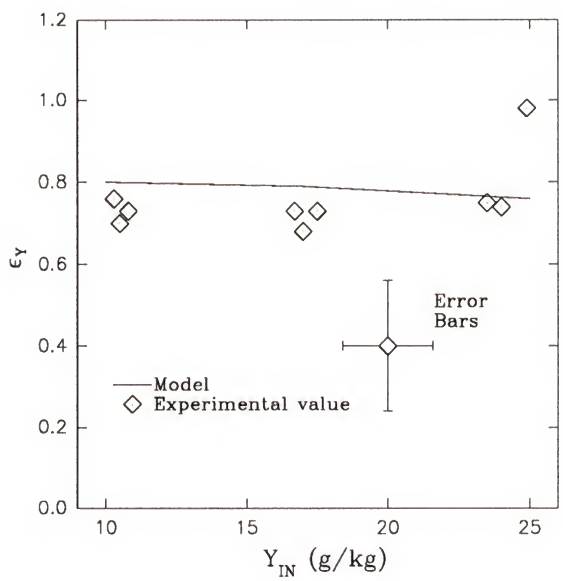

(b)

Figure 3.14: Influence of inlet air humidity ratio on (a) water evaporation rate; (b) humidity effectiveness; (c) enthalpy effectiveness.

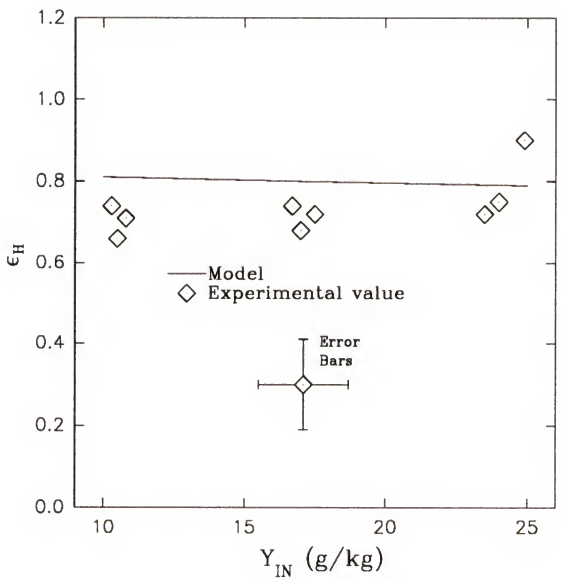

(c)

Figure 3.14 -- continued.

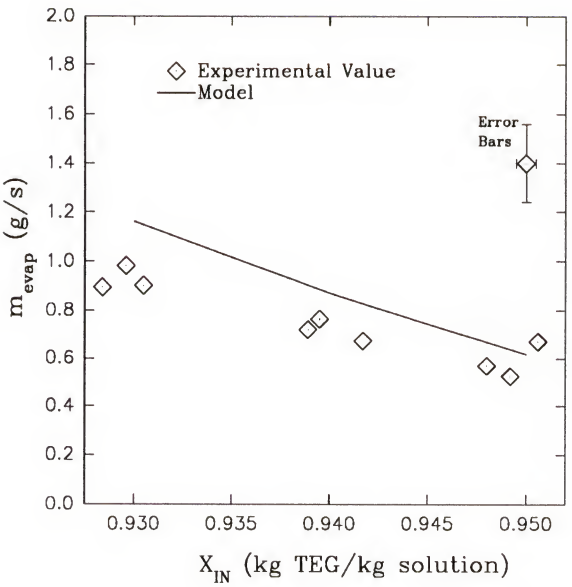

(a)

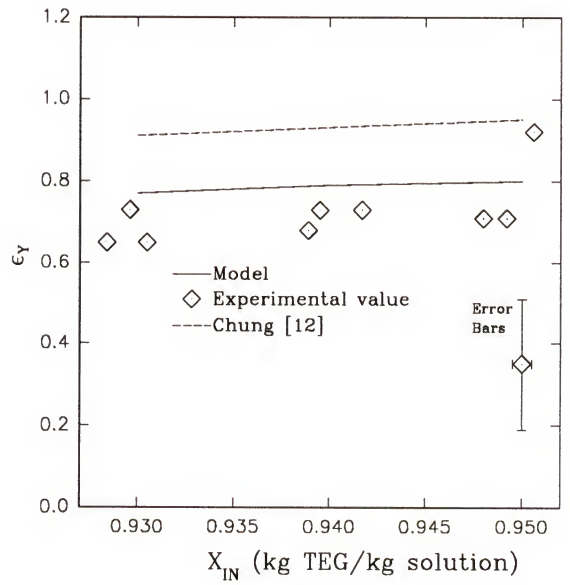

(b)

Figure 3.15: Influence of inlet desiccant concentration on (a) water evaporation rate; (b) humidity effectiveness; (c) enthalpy effectiveness.

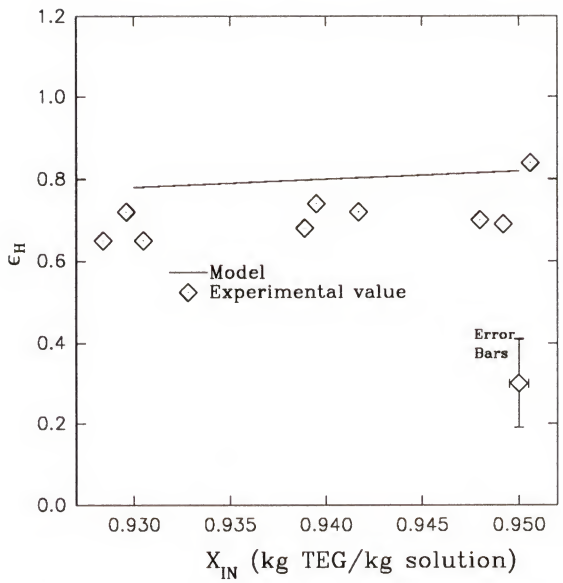

(c)

Figure 3.15 -- continued.

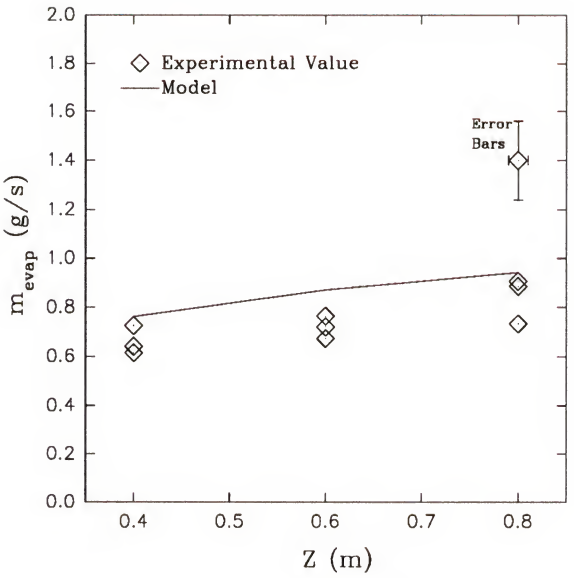

(a)

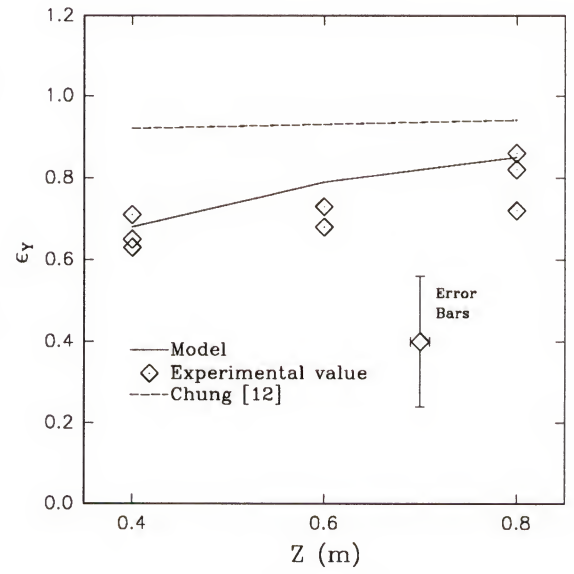

(b)

Figure 3.16: Influence of packed bed height on (a) water evaporation rate; (b) humidity effectiveness; (c) enthalpy effectiveness.

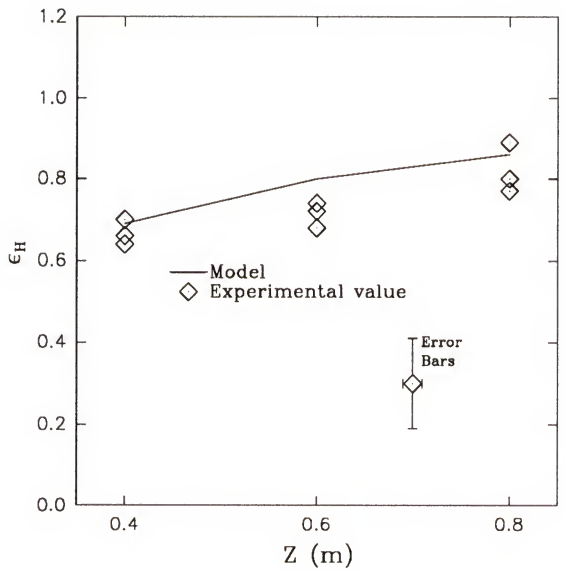

(c)

Figure 3.16 -- continued.

finite difference model and the experiments shows a larger dependency on the air flow rate and packed bed height than what is predicted by Chung's correlation. As was explained in section 2.2.1.1, this correlation was obtained from experimental data on packed bed dehumidifiers. Hence, it is not to be expected that accurate predictions on desiccant regeneration would be possible using this correlation.

The experimental study on the packed bed regeneration tower showed the following variables to significantly influence the regeneration performance: air flow rate, inlet desiccant temperature, inlet air humidity ratio, inlet desiccant concentration, and the packed bed height. The water evaporation rate increased with the air flow rate (Figure 3.10 (a)). However, the humidity effectiveness decreased with the air flow rate (Figure 3.10 (b)) since the change in humidity ratio across the tower decreased as the air flow rate increased. In the regeneration process, the vapor pressure in the liquid is higher than the vapor pressure in the air so that water is evaporated from the desiccant to the air. Therefore, as the liquid vapor pressure increases with the desiccant temperature, the potential for mass transfer increases. Hence, the water evaporation rate increases with the liquid temperature (Figure 3.13 (a)). It was previously explained (section 3.3) that the humidity effectiveness is normalized with respect to the inlet desiccant temperature, $T_{L,IN}$, since the equilibrium humidity ratio, Y_{equ}, is dependent on $T_{L,IN}$. Thus, the effectiveness only shows a slight dependency on the inlet desiccant temperature (Figure 3.13 (b)). By similar reasoning it may be explained why the water evaporation rate decreased with increasing desiccant inlet concentration, while the desiccant concentration did not influence the humidity effectiveness significantly (Figure 3.15). An increase in the inlet humidity ratio increases the vapor pressure in the

air, decreasing the potential for mass transfer between the desiccant and the air. Therefore, the water evaporation rate decreases with increasing inlet air humidity (Figure 3.14 (a)). By definition, the humidity effectiveness is already normalized with respect to the inlet humidity ratio (Equation (2.1)) so that no dependency is shown (Figure 3.14 (b)). Increasing the bed height increased the water evaporation rate, as well as the effectiveness (Figure 3.16). This is because a taller bed increases the area for heat and mass transfer so that a humidity ratio closer to the equilibrium value, Y_{equ}, may be reached at the air outlet.

The enthalpy effectiveness, ϵ_H (Equation (2.4)), for desiccant regeneration is most significantly influenced by the air flow rate (Figure 3.10 (c)) and the packed bed height (Figure 3.16 (c)). The enthalpy effectiveness decreases with increasing air flow rate since the change in humidity ratio across the tower decreases with increasing air flow rate. The enthalpy effectiveness increases with the packed bed height because of the increased area for heat and mass transfer. A larger contact area between the air and the desiccant makes it possible for the air to leave the tower with an enthalpy closer to the equilibrium value ($H_{a,equ}$).

A comparison between the findings in this investigation and experimental findings from studies previously reported in the literature is given in Table 3.2. The table shows the desiccant used, the parameters describing the performance, the independent variables and the ranges examined. Under each variable, the influence of the variable on the performance parameter is indicated by up- and down-arrows. Table 3.2 shows that only a limited amount of experimental data on packed bed regenerators are available in the literature. Thus, the present detailed investigation provides valuable

Table 3.2: Regenerator performance from experimental studies.

Reference	**Desiccant**	**Performance Parameter**	**Independent Variable**						
present study	TEG		L (kg/m^2-s)	X_{IN} (kg/kg)	$T_{L,IN}$ (°C)	G (kg/m^2-s)	$T_{a,IN}$ (°C)	Y_{IN} (g/kg)	Z (m)
			4.2-6.5	0.93-0.95	60-70	0.4-2.0	30-50	10-25	0.4-0.8
		m_{evap}	↑↓	↓	↑	↑	↑↓	↓	↑
		ϵ_Y	↑↓	↑↓	↑↓	↓	↑↓	↑↓	↑
		ϵ_H	↑ (slightly)	↑ (slightly)	↓ (slightly)	↓	↑↓	↑↓	↑
Ertas et al. [19]	mixture of LiCl and $CaCl_2$		L (kg/m^2-s)		X_{IN} (kg/kg)		$T_{L,IN}$ (°C)	Y_{IN} (g/kg)	
			0.8-3.1		0.32-0.46		60-90	18-25	
		X_{OUT}	↓		↑		↑	↓	
		$T_{L,OUT}$	↑		↑		↑	↑	
Löf et al. [51]	LiCl		G (kg/m^2-s)						
			0.7-0.74						
		h_Ga	↑						
Patnaik et al. [69]	LiBr		L (kg/m^2-s)		$T_{L,IN}$ (°C)	X_{IN} (kg/kg)	$T_{a,IN}$ (°C)		Y_{IN} (g/kg)
			1.1-1.5		40-56	0.57-0.60	55-75		5-9
		m_{evap}	↑		↑	↑	↑		↓
Potnis and Lenz [77]	LiBr		L (kg/m^2-s)						
			0.8-2.3						
		m_{evap}	↑						

↑ performance parameter increases with increasing variable
↓ performance parameter decreases with increasing variable
↑↓ variable has no significant effect on the performance parameter

insight into the design of the desiccant regeneration process, especially for the use of triethylene glycol as the desiccant. In general, findings from all the studies agree well. However, Ertas et al. [19], Patnaik et al. [69], and Potnis and Lenz [77] found that the water evaporation rate increased with desiccant flow rate, whereas the present study found only a slight dependency on the desiccant flow rate. Patnaik et al. [69] and Potnis and Lenz [77] explained the large dependency on desiccant flow rate as being due to the large resistance to mass transfer in the liquid phase. This may be the case, as the present investigation utilized triethylene glycol as the desiccant compared to salt solutions in the other investigations. However, the desiccant flow rates used in this study were also higher as compared to those used in the other studies. If the liquid flow rate is low, an increase may provide better wetting of the packing, and therefore increase the performance of the regenerator. At a certain desiccant flow rate, maximum wetting of the packing is obtained and a further increase of the flow rate will not improve the performance. In addition to a large resistance to mass transfer in the liquid phase, it is believed that the performance improvement reported in the previous investigations [19, 69, 77] may also be explained by the increased wetting of the packing with increasing flow rate. Since no significant dependency was obtained in the present investigation, it may be concluded that the flow rates used were sufficient to obtain maximum wetting in the system used.

In the study by Patnaik et al. [69], the evaporation rate increased with air temperature. In the present study, no dependency on the air temperature was obtained. Again, this discrepancy can be explained by the higher desiccant flow rates used in the present study. The performance of the regeneration process will increase with increased

heat addition since this will increase the average temperature in the regenerator, which in turn will increase the driving force for mass transfer. With higher desiccant flow rate, the relative amount of heat added to the regenerator by the air stream becomes lower. Thus, the inlet air temperature is not as important using high desiccant flow rates compared to lower flow rates.

With respect to the enthalpy effectiveness, no previous experimental findings are reported in the literature. Khan [43] examined the influence of design variables on ϵ_H through theoretical modeling of a packed bed regenerator using lithium chloride as the desiccant. As summarized in Table 2.3, the author reported that ϵ_H increased with the number of transfer units, the desiccant to air flow ratio, and the desiccant concentration. Also, ϵ_H was found to decrease with increasing inlet desiccant temperature. Again, Table 3.2 show that the experimental findings in the present study are consistent with those obtained by Khan [43].

3.5 Absorber/Regenerator Performance Correlation

The current investigation has shown that the finite difference model employed gives good predictions of both the effectiveness and the rate of mass transfer as compared to the experimental findings. Thus, for heat and mass transfer studies in the absorber/regenerator this model provides an excellent tool. However, for the integration of the packed bed tower in a model for long term performance simulation of a desiccant cooling system, an algebraic correlation of the humidity and enthalpy effectiveness for the dehumidification and regeneration processes would be more

convenient. In section 2.2.1.1, a correlation for the humidity effectiveness of desiccant dehumidification in a packed bed absorber developed by Chung [12] (Equation (2.3)) was described. This correlation was obtained using experimental data for packed bed dehumidifiers already available in the literature. Thus, a number of packings and two desiccants (lithium chloride and triethylene glycol) were represented. The experimental findings from the present study revealed that this correlation predicted the performance of the dehumidifier within 15 %, but the dependency of the variables was not accurately shown. For the case of desiccant regeneration, this correlation did not give good predictions. Also, no correlation for predicting the enthalpy effectiveness, ϵ_H , is currently available. For these reasons, there is a need for correlations, containing nondimensional groups, that can accurately predict the humidity effectiveness, as well as the enthalpy effectiveness, as a function of the variables. This chapter presents two such correlation obtained through an evaluation of the experimental data from the present study and from the literature.

The variables assumed to influence ϵ_Y and ϵ_H are: the air flow rate (G); the desiccant flow rate (L); the inlet enthalpy of the air ($H_{a,IN}$), and the desiccant ($H_{L,IN}$); the surface area of the packing (a_t); the packed bed height (Z); the wetting characteristics of the desiccant represented by its surface tension (γ_L); and the wettability of the packing represented by the critical surface tension of the packing material (γ_c). Compared to Chung's correlation [12], here the inlet desiccant concentration and temperature are not directly included. This is because these variables are already used when calculating the value of ϵ_Y (Equation (2.1)) and ϵ_H (Equation (2.4)) since Y_{equ} and $H_{a,equ}$ are dependant on $T_{L,IN}$ and X_{IN}. However, $T_{L,IN}$ and X_{IN} are indirectly included in the present

correlations through the inlet desiccant enthalpy ($H_{L,IN}$). In addition, a parameter was used by Chung [12] to represent the type of desiccant used. This parameter considered the ratio of the vapor pressure depression of the desiccant to the vapor pressure of pure water (Equation (2.3)), which gives a nondimensional measure of the equilibrium properties of the desiccant. However, these properties are already used when calculating the effectiveness since Y_{equ} and $H_{a,equ}$ depend on the equilibrium properties of the desiccant used. Hence, it is not necessary to include such a parameter in the correlation. Since the desiccant's equilibrium properties are already included when calculating the effectiveness, it is believed that additionally only the wetting characteristics of the desiccants need to be considered, which are represented by the desiccant surface tension. Chung [12] did not consider the wetting characteristics of the desiccants or the wettability of the packing material. To find the nondimensional groups to be included in the correlations, a dimensional analysis using the Buckingham-Pi Theorem was carried out as described below.

For any physical quantity x, the absolute size x^* is given by

$$x^* = x\, m^a\, l^b\, t^c \tag{3.28}$$

where m, l, and t are the mass, length, and time dimensions, respectively [65]. This is the so called Bridgman's equation. Three primary variables such as m, l, and t are sufficient to express the dimensions of all physical variables. However, m, l, and t are not the only choices of primary variables. For a nondimensional variable, the exponents of the primary variables are all zero.

$$\Pi^* = \Pi\ m^0\ l^0\ t^0 \tag{3.29}$$

Hence, it is completely independent of measuring unit. Given a physical function $x_1 = f(x_2, x_3, ..., x_n)$, where all the variables obey the Bridgman's equation (Equation (3.28)), the function can be expressed in terms of nondimensional variables. This function, $\Pi_1 = f(\Pi_2, \Pi_3, ..., \Pi_m)$, will contain $m = n - r$ variables where r is the rank of the dimensional matrix. For the present case, the physical function is

$$\epsilon_Y\ ,\ \epsilon_H = f\ (\ G,\ L,\ H_{a,IN}\ ,\ H_{L,IN}\ ,\ a_t\ ,\ Z,\ \gamma_L\ ,\ \gamma_c\ ) \tag{3.30}$$

and the dimensional matrix is given in Table 3.3.

Table 3.3: Dimensional matrix for performance correlations.

	ϵ_Y, ϵ_H	G	L	$H_{a,IN}$	$H_{L,IN}$	a_t	Z	γ_L	γ_c
m	0	1	1	0	0	0	0	1	1
l	0	-2	-2	2	2	-1	1	0	0
t	0	-1	-1	-2	-2	0	0	-2	-2

The rank of this matrix is found by checking all the possible square submatrices until a nonzero determinant is found. For instance, a nonzero determinant is given by the submatrix of the G, $H_{a,IN}$, and γ_L columns (Table 3.3). Therefore, the rank of the dimensional matrix is 3 (r = 3), and the function will contain m = 6 variables. Next, since r = 3, three repeating variables that may occur in all the nondimensional groups are chosen as: Z, G, and $H_{L,IN}$. The details of the derivation of the first nondimensional

group are presented below.

$$\Pi^1\ m^0\ l^0\ t^0 = L\ (\ m\ l^{-2}\ t^{-1}\ )\ Z\ (\ l^1\ )^{\alpha}\ G\ (m\ l^{-2}\ t^{-1}\ )^{\beta}\ H_{L,IN}\ (\ l^2\ t^{-2}\ )^{\delta}$$

$$\begin{aligned} m: &\quad 0 = 1 + \beta \\ l: &\quad 0 = -2 + \alpha - 2\beta + 2\delta \\ t: &\quad 0 = -1 - \beta - 2\delta \end{aligned} \tag{3.31}$$

Collecting the values of the exponents of the primary variables yields

This gives $\alpha = 0$, $\beta = -1$, and $\delta = 0$ so that the first Π-group becomes

$$\Pi_1 = \frac{L}{G} \tag{3.32}$$

The remaining nondimensional groups may be found in a similar way, and these groups are listed below.

$$\Pi_2 = \epsilon_Y\ ,\ \epsilon_H \tag{3.33}$$

$$\Pi_3 = \frac{H_{a,IN}}{H_{L,IN}} \tag{3.34}$$

$$\Pi_4 = a_t Z \tag{3.35}$$

$$\Pi_5 = \frac{\gamma_L}{G\ Z\ H_{L,IN}^{\frac{1}{2}}} \tag{3.36}$$

$$\Pi_6 = \frac{\gamma_c}{G\ Z\ H_{L,IN}^{\frac{1}{2}}} \tag{3.37}$$

However, for convenience Π_5 and Π_6 may be combined to form a single nondimensional group Π_7.

$$\Pi_7 = \frac{\gamma_L}{\gamma_c} \tag{3.38}$$

Thus the effectiveness (ϵ_Y and ϵ_H) will be a function of the following nondimensional groups.

$$\epsilon_Y\ ,\ \epsilon_H = f\left(\frac{L}{G},\ \frac{H_{a,IN}}{H_{L,IN}},\ a_t Z,\ \frac{\gamma_L}{\gamma_c} \right) \tag{3.39}$$

To obtain a curve fit, experimental data from the present study, along with data previously reported in the literature [13, 14] were analyzed. Through this data, the different types of packings listed in Table 3.4 were represented. Also, experiments using both TEG (90-95 % by weight) and lithium chloride (30-40 % by weight) as the desiccants were included. Note that the experimental data on the performance of the packed bed regenerator presented in the present investigation were also used so that the

Table 3.4: Packing types represented in the performance correlations.

Packing	**Packing material critical surface tension, $\gamma_c \cdot 10^3$ (N/m)**
13 mm Ceramic Intalox Saddles	61 [73]
16 mm Polypropylene Flexi Rings	29 [55]
25 mm Polypropylene Rauschert Hiflow® Rings	29 [55]

correlations are valid for air dehumidification, as well as desiccant regeneration. A functional form of the correlation was suggested (equations (3.40) to (3.42)).

$$\epsilon_Y \, , \, \epsilon_H = 1 - C_1 \left(\frac{L}{G} \right)^a \left(\frac{H_{a,IN}}{H_{L,IN}} \right)^b (aZ)^c \qquad (3.40)$$

where

$$a = k_1 \frac{\gamma_L}{\gamma_c} + m_1 \qquad (3.41)$$

$$c = k_2 \frac{\gamma_L}{\gamma_c} + m_2 \qquad (3.42)$$

Here, C_1, b, k_1, k_2, m_1, and m_2 are the constants to be found. Thus, it is assumed that the dependency of the effectiveness on the desiccant to air flow ratio (L/G), and the available area for heat and mass transfer (a_tZ) will vary with the wetting characteristics. This assumption was made based on the following reasoning: in order to obtain a certain effectiveness, for a system where the wetting of the packing is facilitated by low

γ_L and/or high γ_c , a lower L/G ratio and area for mass transfer may be used as compared to a system where the wetting is difficult.

Using a computer program with curve-fitting capabilities, a correlation of the form in Equation (3.40) was obtained for the humidity effectiveness, ϵ_Y, as well as for the enthalpy effectiveness, ϵ_H . The constants obtained are shown in Table 3.5.

Table 3.5: Constants for performance correlations.

	C_1	b	k_1	m_1	k_2	m_2
ϵ_Y	48.34456	-0.75103	0.3959	-1.57311	0.03312	-0.90589
ϵ_H	3.76606	-0.52794	0.28937	-1.11609	-0.0044	-0.36498

Figures 3.17 and 3.18 show the curve fits for ϵ_Y and ϵ_H, respectively. As shown, the correlations derived in the present investigation predict the values within 15 %. To show how well the correlation would predict the influence of design variables, figures 3.19 through 3.22 present ϵ_Y and ϵ_H as predicted from the correlation along with the experimental findings from the present investigation. In figures 3.19 and 3.21 the predictions from Chung's correlation [12] are shown as well. For dehumidification, the correlation for ϵ_Y from the present investigation gives better predictions of the dependency of design variables compared to the predictions from the correlation by Chung [12]. Especially, the influences of the inlet air temperature (Figure 3.19 (c)), inlet desiccant temperature (Figure 3.19 (d)), and tower height (Figure 3.19 (g)), are described more accurately by the correlation from the present study. The correlation for the enthalpy effectiveness, ϵ_H, also predicts the influence of design variables well for

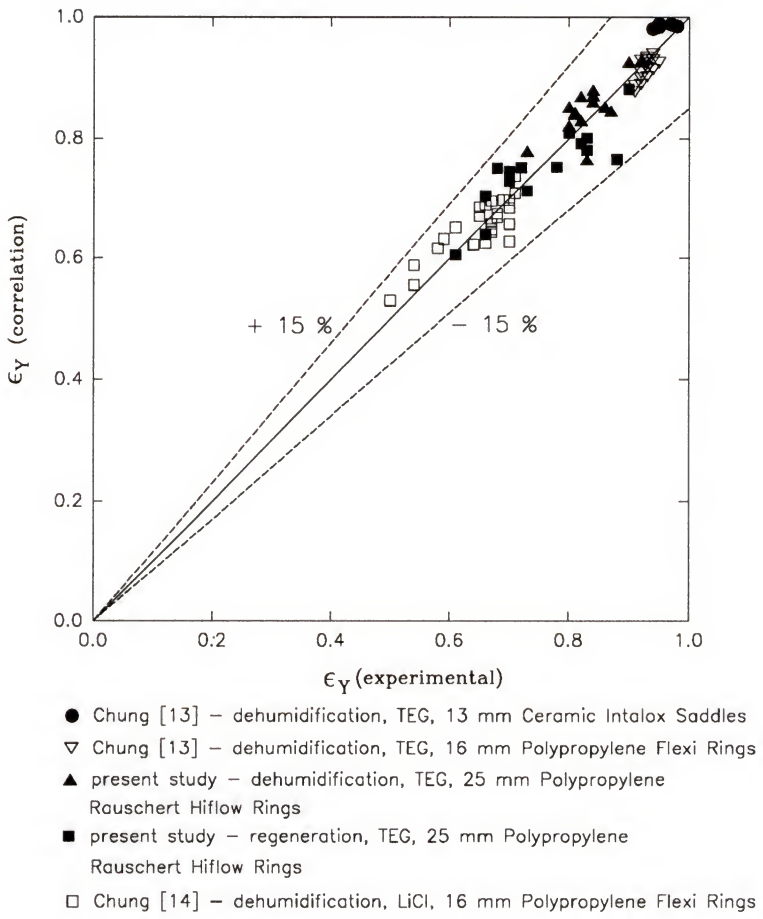

Figure 3.17: Correlation for humidity effectiveness, ϵ_Y for packed bed absorber/regenerator.

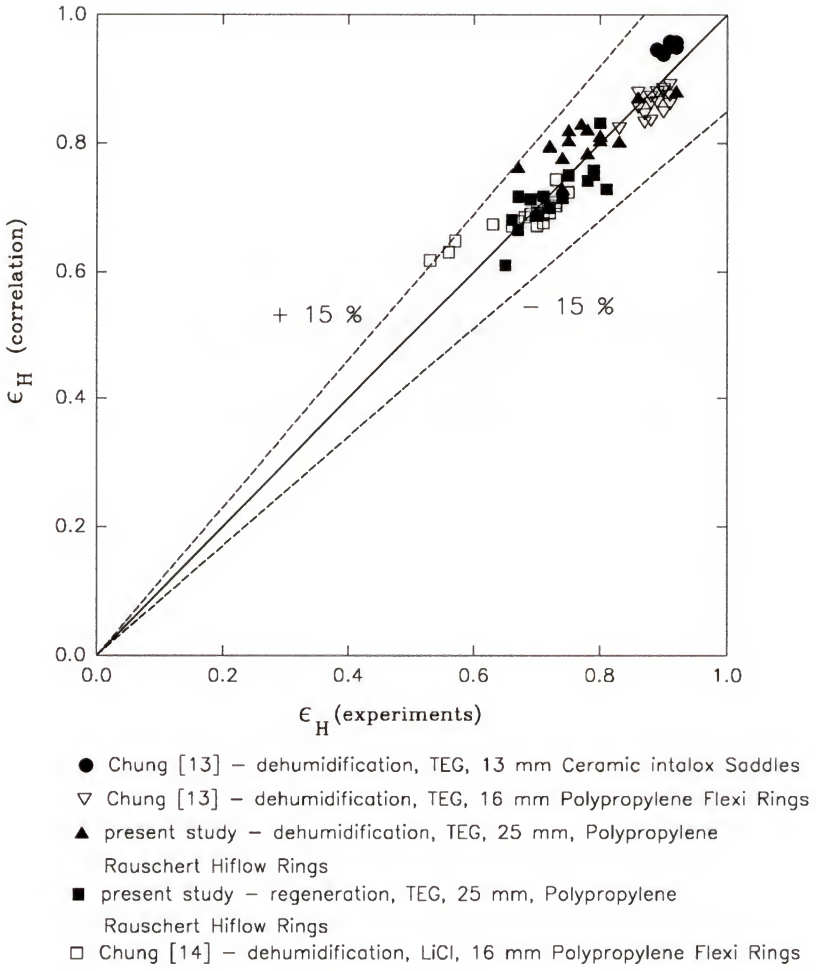

Figure 3.18: Correlation for enthalpy effectiveness, ϵ_H for packed bed absorber/regenerator.

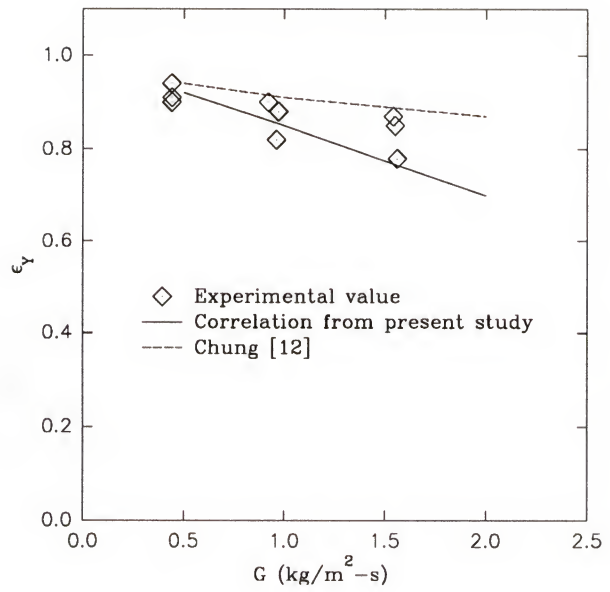

(a)

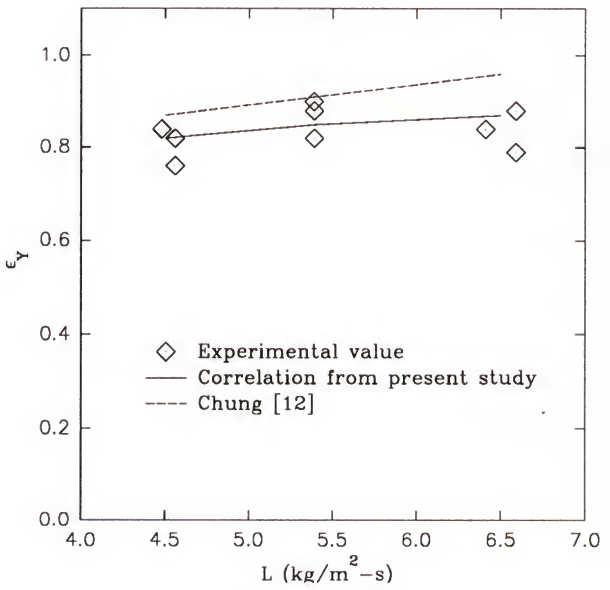

(b)

Figure 3.19: Humidity effectiveness versus design variables for dehumidification: (a) G; (b) L; (c) $T_{a,IN}$; (d) $T_{L,IN}$; (e) Y_{IN} ; (f) X_{IN} ; (g) Z.

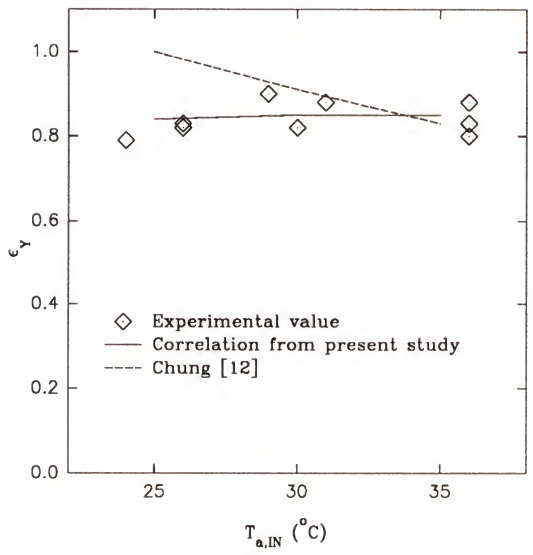

(c)

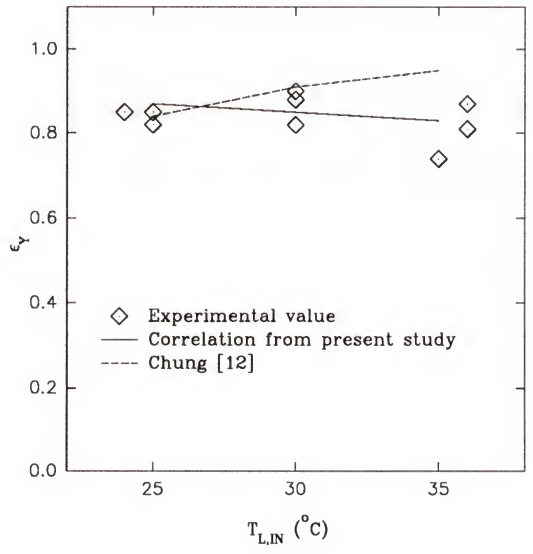

(d)

Figure 3.19--continued.

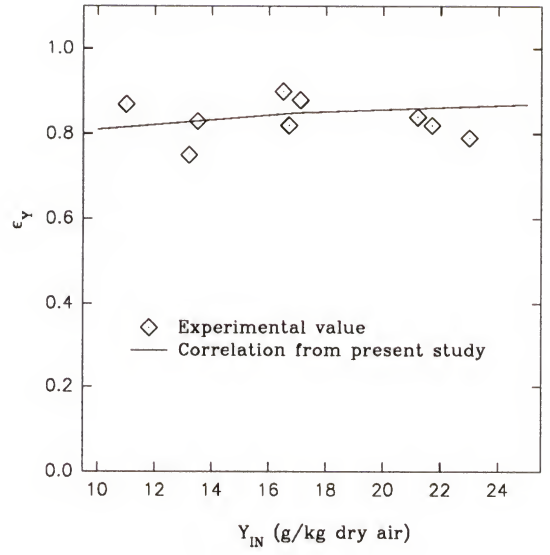

(e)

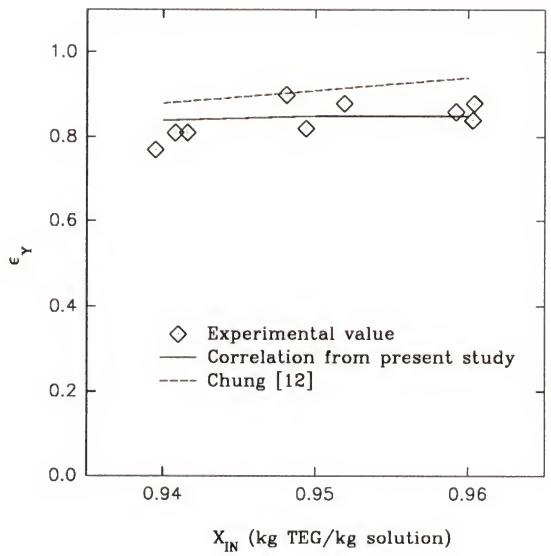

(f)

Figure 3.19--continued.

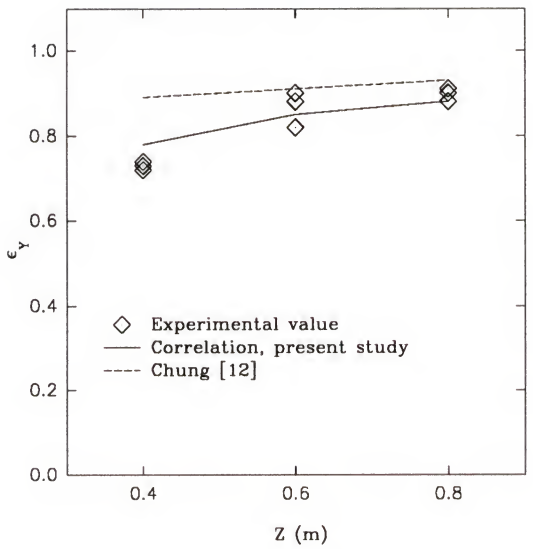

(g)

Figure 3.19--continued.

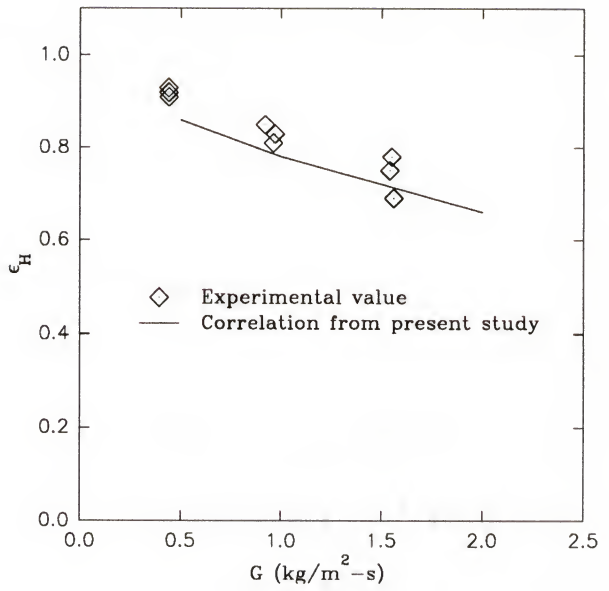

(a)

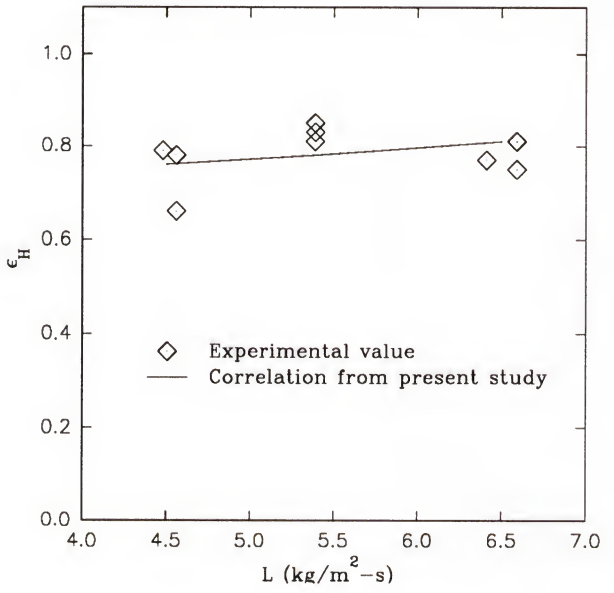

(b)

Figure 3.20: Enthalpy effectiveness versus design variables for dehumidification: (a) G; (b) L; (c) $T_{a,IN}$; (d) $T_{L,IN}$; (e) Y_{IN} ; (f) X_{IN} ; (g) Z.

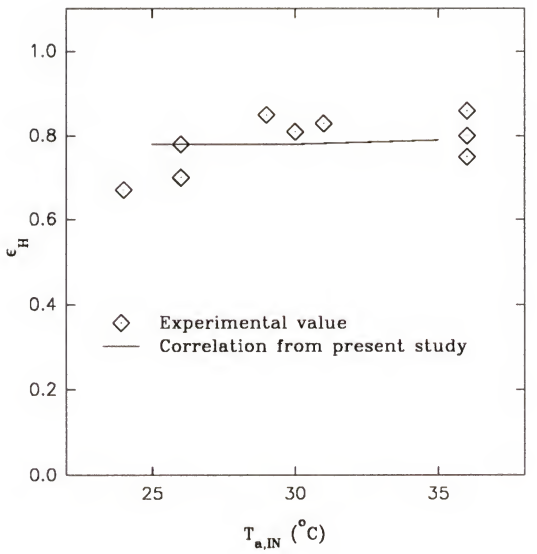

(c)

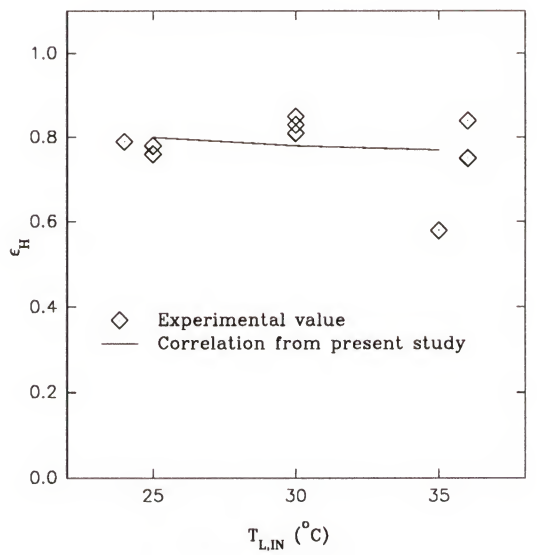

(d)

Figure 3.20--continued.

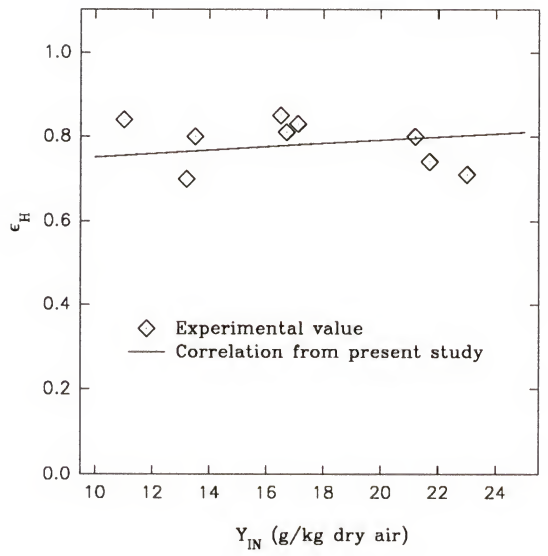

(e)

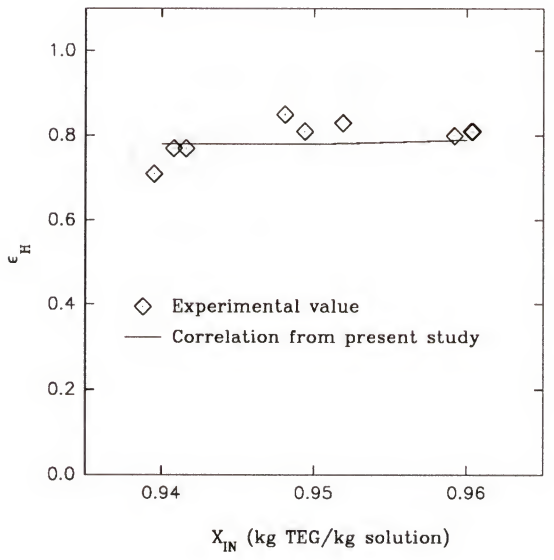

(f)

Figure 3.20--continued.

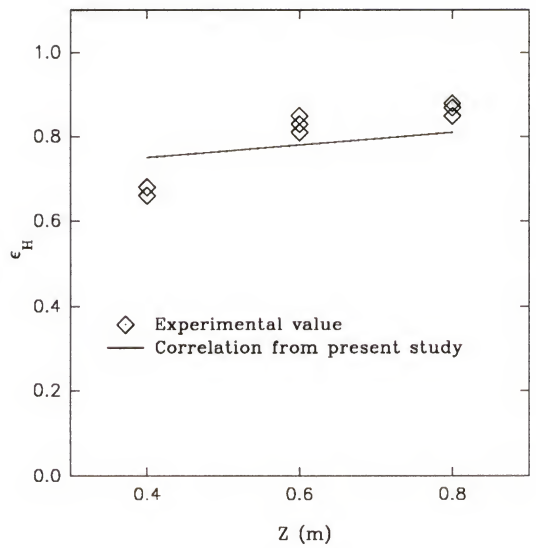

(g)

Figure 3.20--continued.

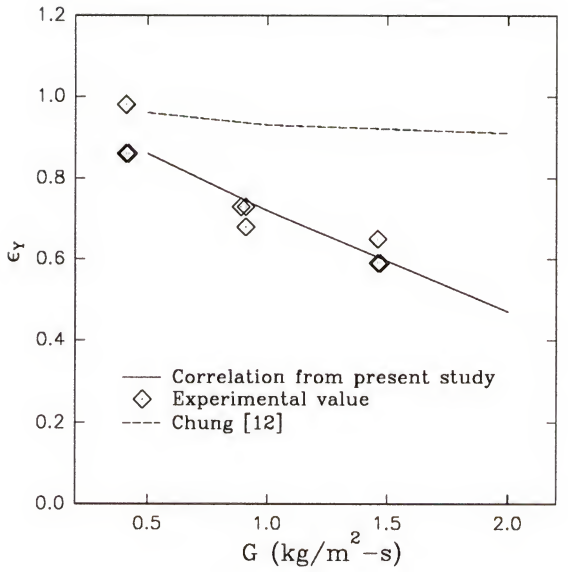

(a)

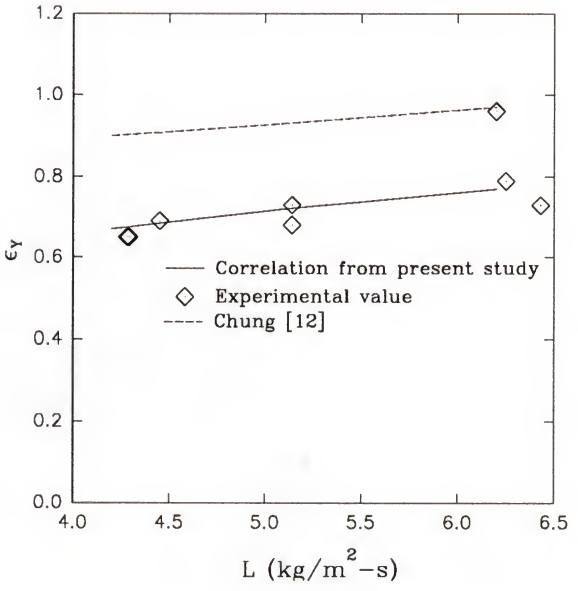

(b)

Figure 3.21: Humidity effectiveness versus design variables for regeneration: (a) G; (b) L; (c) $T_{a,IN}$; (d) $T_{L,IN}$; (e) Y_{IN} ; (f) X_{IN} ; (g) Z.

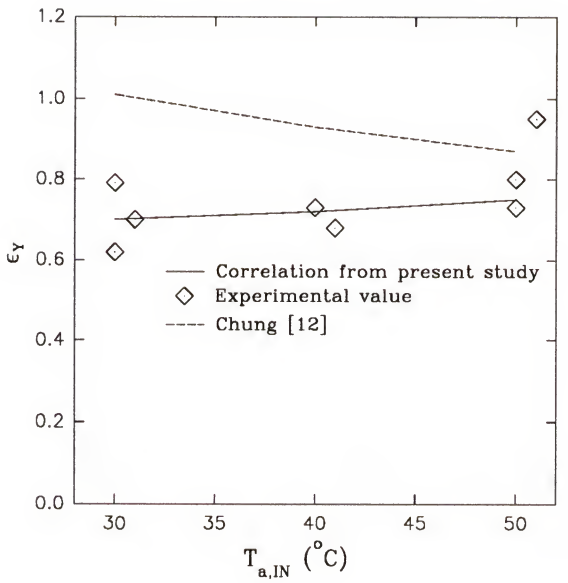

(c)

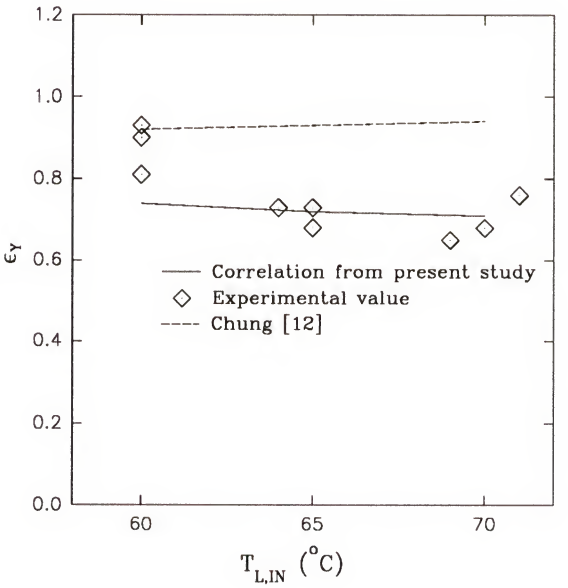

(d)

Figure 3.21--continued.

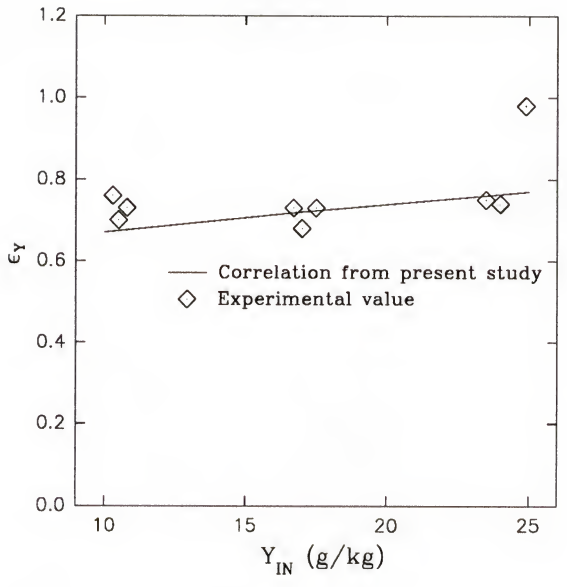

(e)

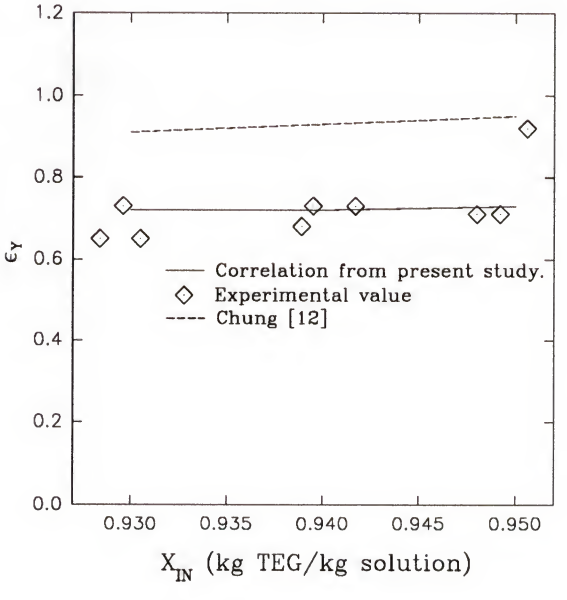

(f)

Figure 3.21-- continued.

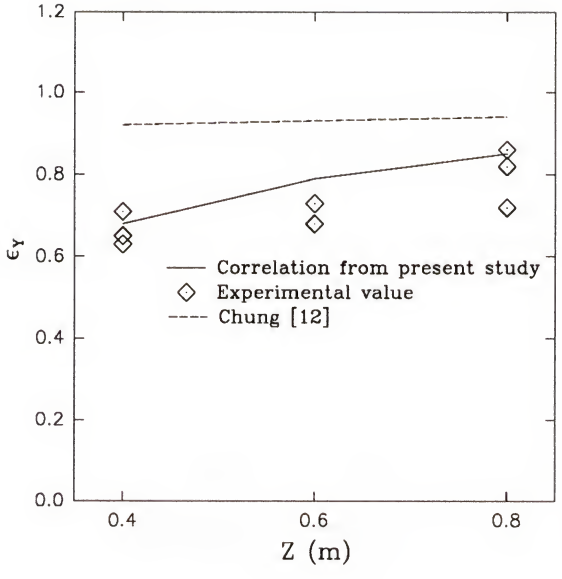

(g)

Figure 3.21--continued.

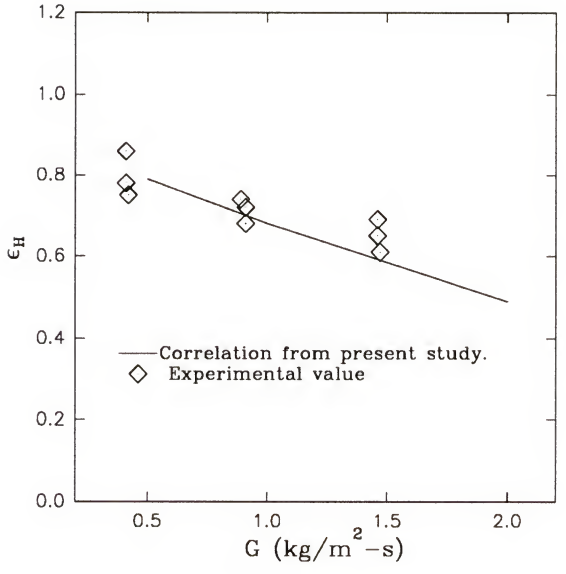

(a)

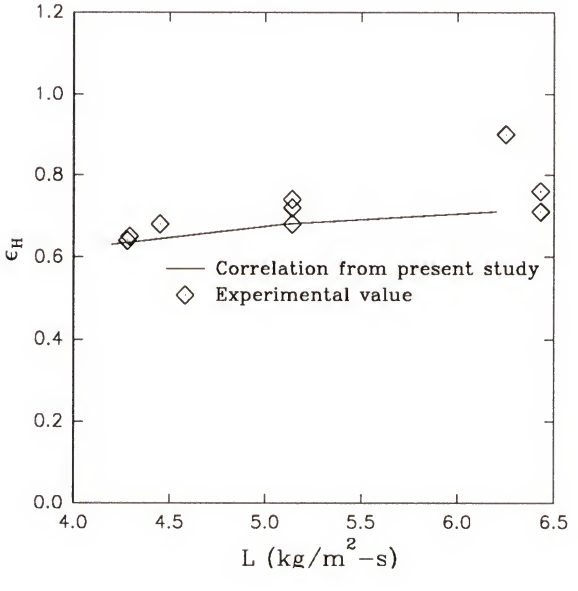

(b)

Figure 3.22: Enthalpy effectiveness versus design variables for regeneration: (a) G; (b) L; (c) $T_{a,IN}$; (d) $T_{L,IN}$; (e) Y_{IN} ; (f) X_{IN} ; (g) Z.

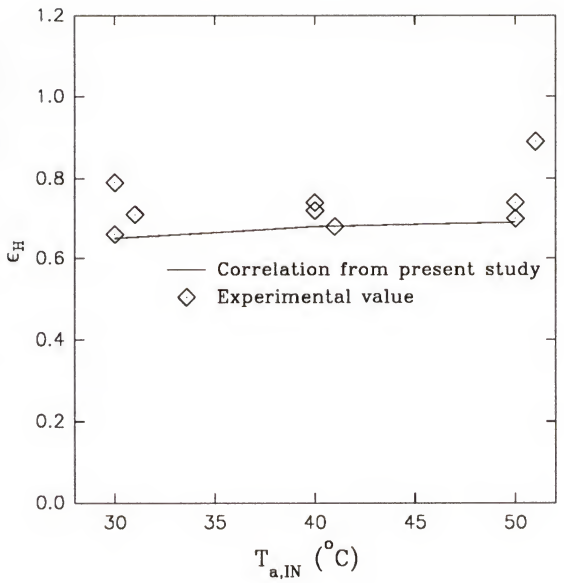

(c)

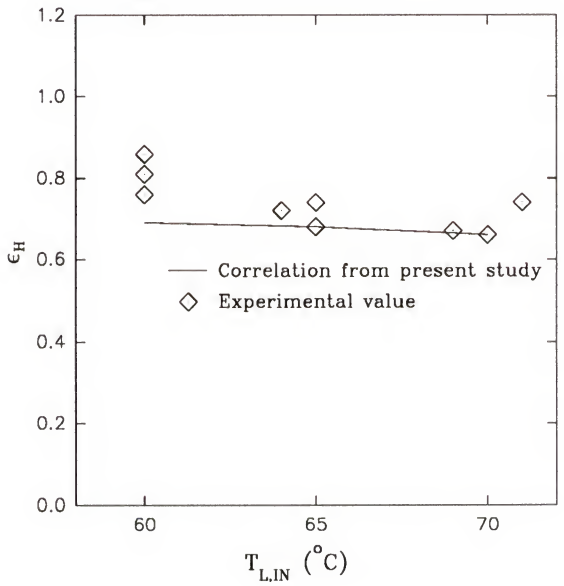

(d)

Figure 3.22--continued.

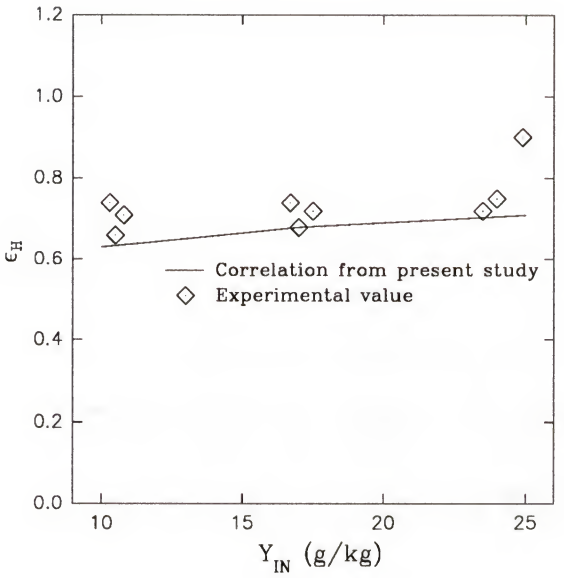

(e)

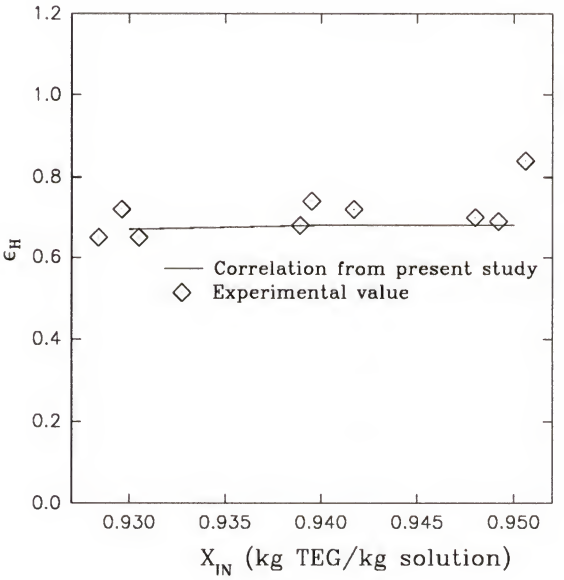

(f)

Figure 3.22--continued.

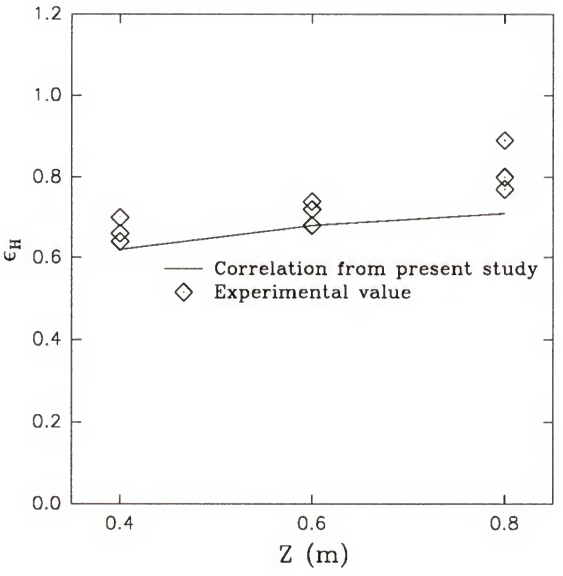

(g)

Figure 3.22--continued.

the case of dehumidification (Figure 3.20), as compared with the experimental findings. The influence of the tower height, Z, on ϵ_H shows the largest discrepancy between the predictions by the correlation and the experimental data (Figure 3.20 (g)), where the experiments suggest a larger dependency on Z than what is predicted by the correlation. Still, the correlation predicts ϵ_H within 10 % of the experimental findings which is excellent when taking into account the wide variety, as well as the uncertainty of the experimental data used to obtain the correlation. For desiccant regeneration, the correlation for ϵ_Y predicts the influence of design variables well as shown in Figure 3.21. As previously discussed in section 3.4, the correlation by Chung [12] does not accurately predict the value of ϵ_Y and the influence of design variables on ϵ_Y for desiccant regeneration, which is clearly shown in Figure 3.21. Figure 3.22 shows that for regeneration the enthalpy effectiveness, ϵ_H, is also predicted well by the correlation from the present study.

3.6 Concluding Remarks

This chapter presents the results from a detailed study of the heat and mass transfer between the desiccant and air in a packed bed absorber/regenerator. The results from this study provide valuable insight into the design of packed bed air dehumidifiers, as well as desiccant regenerators.

A comparison between the experimental and the theoretical results in this study shows that the finite difference model presented in this chapter gives good predictions of the heat and mass transfer between a desiccant and air in a packed bed tower. This

model is applicable to general conditions, for both absorption (air dehumidification) and desorption (regeneration). Thus, for a detailed study of the heat and mass transfer in a packed bed tower, this model provides excellent predictions based on fundamental equations, minimizing the assumptions and use of empirical correlations.

Although the finite difference model describes the performance of the absorber/regenerator well, simpler algebraic equations correlating the performance to design variables would be more convenient in desiccant cooling system simulations. When compared to the experimental findings from the present study, one such correlation by Chung [12] did not predict the performance of the dehumidifier satisfactorily. Furthermore, since no experimental data on desiccant regeneration were included when this correlation was obtained, it was not at all applicable to desiccant regeneration. Also, since the correlation by Chung [12] only considered the change in air humidity across the packed bed, no correlation for the change in air temperature due to the simultaneous heat and mass transfer was available in the literature. For these reasons, two performance correlations were developed by analyzing the experimental data from the present study and the literature: one correlation for the humidity effectiveness, ϵ_Y, and one for the enthalpy effectiveness, ϵ_H. These correlations predicted the performance within 15 % of all the experimental data. In addition, the correlations gave excellent predictions of the influence of design variables, both for air dehumidification and desiccant regeneration.

Only a limited number of experimental studies have been reported in the literature, especially for the use of triethylene glycol as the desiccant. Thus, the findings reported herein are of great interest. Design variables found to have the

greatest impact on the performance of the packed bed dehumidifier and regenerator are: the air flow rate and the humidity; the desiccant temperature and concentration; and the packed bed height. The liquid flow rate and the inlet air temperature did not have a significant effect; however, the liquid flow rate must be high enough to ensure wetting of the packing. In general, the results from the present study compare well with those from other experimental studies.

CHAPTER 4
SOLAR HYBRID LIQUID DESICCANT AIR CONDITIONING

In applications where the ratio of latent to total cooling load is large using desiccant techniques may be especially beneficial; both in terms of the energy efficiency and the quality of the air conditioning. One such application is the conditioning of ventilation air in hot and humid climates. Rengarajan et al. [78] compared a number of strategies for ventilation air conditioning. They found that increased ventilation requirement due to the ASHRAE Standard 62-1989 would increase the annual energy requirement and operating cost by 10-15 % for a large office building in Miami, Florida. Through mathematical modeling the authors found that the conventional vapor compression system was unable to meet the increased latent cooling load, with the result that the indoor relative humidity frequently exceeded 60 %. Pretreating the outside air with a 100 % outside air DX (direct expansion) unit or a gas-fired desiccant unit maintained the indoor relative humidity below 60 % for a larger part of the time (95 %), as compared to pretreatment using a heat pipe assisted water coil (90 % of the time) or an enthalpy recovery wheel (93 to 95 % of the time). Also, the desiccant system was found to reduce the annual electrical energy use significantly. Other researchers have demonstrated the viability of desiccant systems for ventilation air conditioning. For example, Meckler [58] showed that the installed chiller capacity could be reduced by 30 % by using a desiccant preconditioning unit. Thornbloom and

Nimmo [91] compared a solar liquid desiccant dehumidification system to a conventional vapor compression system for treating the ventilation air required in a supermarket in Miami, Florida. In their system, calcium chloride was used as the desiccant and it was regenerated in a trickle solar collector regenerator. A packed bed dehumidifier handled the latent cooling and a vapor compression unit handled the sensible cooling. A cost analysis showed that the annual operating cost of the desiccant system was significantly lower than for a conventional system. In another recent study, Spears and Judge [88] presented results from a one year evaluation of a gas-fired desiccant ventilation air conditioner for a Wal-Mart super center. The control of indoor humidity was significantly better in the store that used the desiccant system as compared to a store using standard air conditioning. Besides the benefit of improved comfort, the store using the desiccant system saved 13 % energy compared to the control store.

In the present study, a system performance simulation of solar hybrid liquid desiccant ventilation air conditioning was carried out for the month of August in Miami, Florida. A desiccant system is proposed where the latent cooling load is handled by a desiccant dehumidifier, while a conventional chiller is used to sensibly cool the air (Figure 4.1). The proposed system uses triethylene glycol as the desiccant and packed bed absorbers as the dehumidifier and regenerator. Solar heat is provided indirectly through a solar collector/storage system. Findings from the experimental and theoretical performance study of the packed bed absorber (CHAPTER 3) were used as the basis for the design of these components. This investigation focuses on the influence of system design parameters such as the desiccant storage volume, the

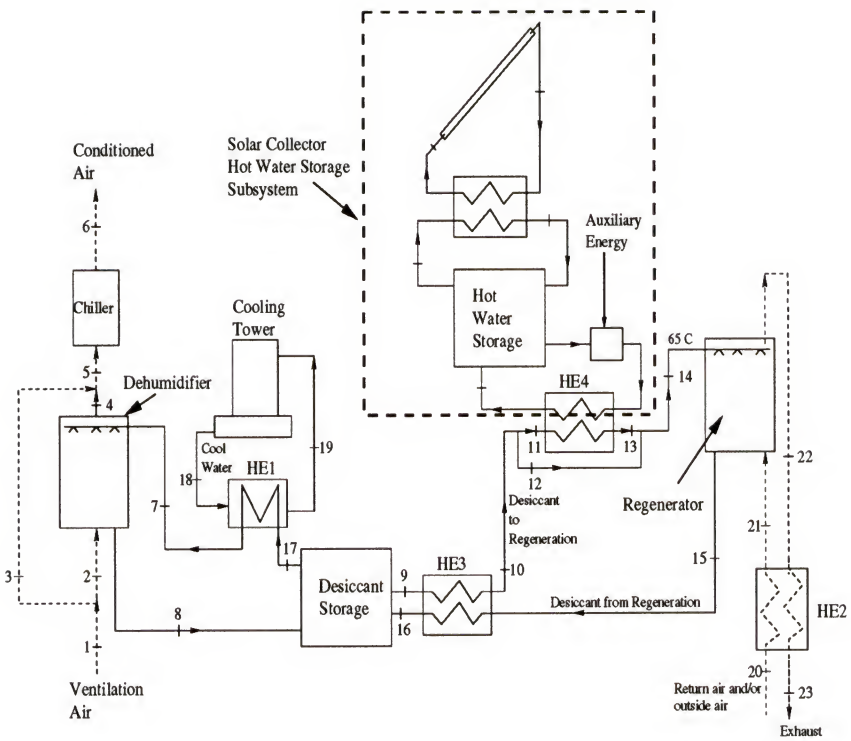

Figure 4.1: Solar hybrid liquid desiccant cooling system for ventilation air preconditioning.

regenerator size, the hot water storage volume, and the solar collector area on the system performance. Insight into the design of solar hybrid desiccant systems is provided from an evaluation of the chiller electrical energy requirement, the regeneration auxiliary energy demand, and the solar fraction for regeneration, as functions of the parameters listed above.

4.1 Simulation Model Description

The use of a solar hybrid liquid desiccant system (Figure 4.1) for preconditioning of 0.5 m^3/s ventilation air is simulated. The electrical energy requirement of this process is compared to that of a conventional system. The air is assumed to be cooled

and dehumidified from the ambient conditions to 24 °C and 50 % relative humidity, which corresponds to a humidity ratio Y=9.5 g/kg. In the desiccant system, air is dried in a packed bed dehumidifier before it is sensibly cooled by the chiller. Before the desiccant (approximately 95 % by weight triethylene glycol) enters the dehumidifier, it is cooled by exchanging heat with water from a cooling tower. Desiccant storage provides a buffer so that the desiccant can be regenerated during the hours of the day when solar energy is available. In this study, it is assumed that the regenerator operates at a constant desiccant flow rate between 10 AM and 7 PM solar time, and that no regeneration takes place during the rest of the day. For regeneration, the desiccant is heated and brought in contact with a moisture scavenging air stream in a packed bed tower. The temperature of the desiccant entering the regenerator is 65 °C, with regeneration heat provided by a flat plate solar collector and hot water storage subsystem, and by an auxiliary source if needed.

The performance simulation was carried out in three steps. Initially, hourly weather data for the month of August in Miami, Florida, was obtained using a weather generating subroutine available in the simulation program TRNSYS [50]. Next, the performance of the system, excluding the solar subsystem, was modeled by carrying out mass and energy balances on each component. Referring to Figure 4.1, the equations and assumption used to model the system performance are summarized in Table 4.1. This analysis was conducted using a FORTRAN computer program. Hourly chiller loads and regeneration energy requirement for the desiccant system were calculated as a function of the desiccant storage volume and the desiccant flow rate to the regenerator. This flow rate influences the size of the regenerator part of the system, including the

size of the solar subsystem. The electrical energy requirements to meet the chiller loads were found by dividing the cooling loads by the coefficient of performance (COP). In the desiccant system, this chiller mostly handles the sensible cooling load. Thus, it should be noted that since the air does not have to be cooled below its dew point to condense moisture, the chiller may be able to operate at a higher evaporator temperature compared to that in a conventional system. Therefore, the COP for the chiller in the desiccant system may be higher than the COP for a conventional chiller. Nevertheless, a constant COP of 2.9 (corresponding to EER=10) was assumed for both chillers in this study.

As shown in Table 4.1 the components in the desiccant system were described using algebraic equations representing the energy and mass balances, with certain simplifying assumptions. The cooling tower was modeled using a linear relationship between the temperature of the water leaving the cooling tower and the ambient wetbulb temperature. This relationship was obtained from a curve fit of cooling tower performance data available in the literature [6]. The performance of the packed bed dehumidifier and regenerator was modeled using the dehumidification and the enthalpy effectiveness previously described (equations (2.1) and (2.4)). Both the dehumidification and the enthalpy effectiveness were assumed to be constant at 0.8. Findings from the experimental investigation of the packed bed absorber/regenerator show this to be a reasonable assumption. The liquid to air mass flow ratios in the dehumidifier and regenerator were set at 4.5 and 3.75, respectively. It should also be noted that only the amount of air necessary to meet the load is passed through the dehumidifier. That is, if the conditions of the air and the desiccant entering are such

Table 4.1: Performance simulation summary.

ITEM	VALUE
m_{a1}	2040 kg/hr (constant)
T_{a1} ($=T_{a2}=T_{a3}$)	from TRNSYS simulation of weather data
Y_1 ($=Y_2=Y_3$)	from TRNSYS simulation of weather data
T_{a6}	24 °C (constant)
Y_6	0.0095 kg/kg (constant)
Temperature in desiccant storage at beginning of simulation: $T_{DS}(t=0)$	30 °C
Concentration in desiccant storage at beginning of simulation: $X_{DS}(t=0)$	0.95 kg TEG/kg solution
$c_{p,L}$	2.4 kJ/kg-°C (dehumidification) [18] 2.5 kJ/kg-°C (regeneration) [18]
ϵ_{HE}	0.8 (liquid-liquid heat exchanger numbers 1, 3, and 4, Figure 4.1) 0.6 (air-air heat exchanger number 2, Figure 4.1)
Cooling Tower Performance: T_{w18}	$T_{w18}=0.68*T_{WB}+11.1$ (based on curve fit of performance data from [6])
T_{L7}	$Q_{HE1}=m_{L7}c_{p,L}(T_{DS}-T_{L7})=m_{w18}c_{p,w}(T_{w19}-T_{w18})=C_{min}\epsilon_{HE}(T_{DS}-T_{w18})$ Assume $C_{min}=m_{L7}c_{p,L}$. $T_{L7}=T_{DS}-\epsilon_{HE}(T_{DS}-T_{w18})$
Dehumidifier/Regenerator Effectiveness: $\epsilon_Y=\epsilon_H$	0.8
Y_4	$Y_4=Y_1-\epsilon_Y(Y_1-Y_{equ,DE})$ (Equation (2.1)) $Y_{equ,DE}=f(T_{L7}, X_7)$; obtained from [18]
H_{a4}	$H_{a4}=H_{a1}-\epsilon_H(H_{a1}-H_{a,equ,DE})$ (Equation (2.4)) $H_{a,equ,DE}=f(T_{L7}, Y_{equ,DE})$
Air Enthalpy, H_a	Equation (3.10)
m_{a2}	• If $Y_4 \le Y_6$: $m_{a2}(Y_1-Y_4)=m_{a1}(Y_1-Y_6)$ $m_{a2}=m_{a1}(Y_1-Y_6)/(Y_1-Y_4)$ • If $Y_4>Y_6$: $m_{a2}=m_{a1}$ and the latent load is not met by the dehumidifier. The remaining latent load is then imposed on the chiller.
m_{L7}/m_{a2}	4.5 (constant)

Table 4.1 -- continued.

ITEM	VALUE
X_8	Water mass balance across the dehumidifier: $m_{a2}(Y_1-Y_4)=m_{L7}([1-X_8]-[1-X_7])$ $X_8=X_7-m_{a2}(Y_1-Y_4)/m_{L7}$
T_{L8}	Energy balance across the dehumidifier: $m_{a2}(H_{a1}-H_{a4})=m_{L7}c_{p,L}(T_{L8}-T_{L7})$ $T_{L8}=T_{L7}+m_{a2}(H_{a1}-H_{a4})/(m_{L7}c_{p,L})$
V_{DS}	2.5-10 m^3 (variable)
m_{L9} ($=m_{L10}=m_{L14}=m_{L15}=m_{L16}$)	7650-12000 kg/hr (variable)
m_{L14}/m_{a20}	3.75 (constant)
T_{L14}	65 °C (constant)
Outside Air Requirement - Regenerator: $m_{OA,R}$	Primarily, return air equal to m_{a1} is used in the regenerator. Outside air is added as needed. $m_{OA,R}=m_{a20}-m_{a1}$
$Y_{20}=Y_{21}$	$Y_{20}=(m_{a1}Y_6+m_{OA,R}Y_1)/m_{a20}$ (analyzing the mixing point) (The humidity ratio in the return air is equal to Y_6.)
H_{a20}	$H_{a20}=(m_{a1}H_{a6}+m_{OA,R}H_{a1})/m_{a20}$ (analyzing the mixing point)
T_{a20}	$T_{a20}=(H_{a20}-Y_{20}\lambda_0)/(c_{p,a}+Y_{20}c_{p,v})$ (rearranging Equation (3.10))
Y_{22}	$Y_{22}=Y_{21}-\epsilon_Y(Y_{21}-Y_{equ,R})$ (Equation (2.1)) $Y_{equ,R}=f(T_{L14}, X_{14})$; obtained from [18]
H_{a22}	$H_{a22}=H_{a21}-\epsilon_H(H_{a21}-H_{a,equ,R})$ (Equation (2.4)) $H_{a,equ,R}=f(T_{L14}, Y_{equ,R})$
T_{a22}	$T_{a22}=(H_{a22}-Y_{22}\lambda_0)/(c_{p,a}+Y_{22}c_{p,v})$
T_{a21}	$Q_{HE2}=m_{a20}c_{p,20}(T_{a21}-T_{a20})=C_{min}\epsilon_{HE}(T_{a22}-T_{a20})$ Assume $C_{min}=m_{a20}c_{p,20}$. $T_{a21}=T_{a20}+\epsilon_{HE}(T_{a22}-T_{a20})$
X_{15}	Water mass balance across the regenerator: $m_{a21}(Y_{22}-Y_{21})=m_{L14}([1-X_{14}]-[1-X_{15}])$ $X_{15}=X_{14}+m_{a21}(Y_{22}-Y_{21})/m_{L14}$
T_{L15}	Energy balance across the dehumidifier: $m_{a21}(H_{a21}-H_{a22})=m_{L14}c_{p,L}(T_{L15}-T_{L14})$ $T_{L15}=T_{L14}+m_{a21}(H_{a21}-H_{a22})/(m_{L14}c_{p,L})$
T_{L16}	$Q_{HE3}=m_{L15}c_{p,L}(T_{L15}-T_{L16})=C_{min}\epsilon_{HE}(T_{L15}-T_{L9})$ Assume $C_{min}=m_{L15}c_{p,L}$ since $m_{L15}\approx m_{L9}$ $T_{L16}=T_{L15}-\epsilon_{HE}(T_{L15}-T_{L9})$

Table 4.1 -- continued.

ITEM	VALUE
T_{L10}	$Q_{HE3}=m_{L9}c_{p,L}(T_{L10}-T_{L9})=C_{min}\epsilon_{HE}(T_{L15}-T_{L9})$ Assume $C_{min}=m_{L9}c_{p,L}$ $T_{10}=T_{L9}+\epsilon_{HE}(T_{L15}-T_{L9})$
Time change in desiccant storage concentration: $$V_{DS}\rho_L\frac{dX_{DS}}{dt} = m_{L16}X_{16} - m_{L9}X_{DS} - m_{L17}X_{DS} + m_{L8}X_8$$ $$X_{DS}(t+\Delta t) = \frac{m_{L8}X_8 + m_{L16}X_{16}}{m_{L17}+m_{L9}} + \left[X_{DS}(t) - \frac{m_{L8}X_8 + m_{L16}X_{16}}{m_{L17}+m_{L9}}\right]\cdot\exp\left[-\frac{m_{L17}+m_{L9}}{V_{DS}\rho_L}\Delta t\right]$$	
Time change in desiccant storage temperature (solving a differential equation similar to the one for the desiccant concentration in the tank): $$T_{DS}(t+\Delta t) = \frac{m_{L8}T_{L,8} + m_{L16}T_{L,16}}{m_{L17}+m_{L9}} + \left[T_{DS}(t) - \frac{m_{L8}T_{L,8} + m_{L16}T_{L,16}}{m_{L7}+m_{L9}}\right]\cdot\exp\left[-\frac{m_{L7}+m_{L9}}{V_{DS}\rho_L}\Delta t\right]$$	
Conventional sensible cooling load: $Q_{conv,s}$	$Q_{conv,s}=m_{a1}c_{p,avg}(T_{a1}-T_{a6})$
Conventional latent cooling load: $Q_{conv,l}$	$Q_{conv,l}=m_{a1}(Y_1-Y_6)\lambda_0$
Sensible cooling load, desiccant system: $Q_{DE,s}$	$Q_{DE,s}=m_{a1}c_{p,avg}(T_{a5}-T_{a6})$
Latent cooling load, desiccant system: $Q_{DE,l}$	$Q_{DE,l}=m_{a1}(Y_5-Y_6)\lambda_0$
COP	$$COP = \frac{Q_{oool,tot}}{W_{oool}} = 2.9$$

that the humidity ratio of the air leaving the dehumidifier would be lower than 9.5 g/kg, some of the air is by-passed so that the humidity ratio at the mixing point (point 5, Figure 4.1) following the dehumidifier is 9.5 g/kg. The desiccant flow rate through the dehumidifier is then adjusted to maintain the same liquid to air mass flow ratio. Furthermore, if the dehumidifier cannot meet 100 % of the latent load, the remaining latent cooling load is imposed on the chiller. The effectiveness of the liquid-to-liquid heat exchangers was assumed to be 0.8, and the effectiveness of the air-to-air heat exchanger in the regenerator section was assumed to be 0.6. In the system simulation, desiccant storage volumes between 2.5 m^3 and 10 m^3 were considered, and the desiccant flow rate to the regenerator was varied between 7650 kg/hr and 12000 kg/hr.

Finally, the performance of the solar hot water subsystem was modeled using output from the system simulation for the case with 5 m^3 desiccant storage and the desiccant flow rate to the regenerator equal to 7650 kg/hr. With this flow rate, and assuming that the amount of air to be exhausted from a building equals the amount of ventilation air so that dry return air may be used in the regenerator, the desired desiccant to air mass flow ratio 3.75 is obtained in the regenerator. The solar hot water storage subsystem was modeled using TRNSYS [50]. Results from this part of the simulation included the monthly solar fraction for regeneration (i.e., the part of the regeneration heat provided by solar energy), and the auxiliary energy requirement as a function of the hot water storage volume and the solar collector area. The solar collector area was varied between 200 m^2 and 600 m^2, and the hot water storage volume was varied between 5 m^3 and 15 m^3. Due to additional system components in the desiccant system compared to the conventional system, some parasitic electrical energy

will be required (e.g., pumping power for the desiccant and water, and additional fan power due to a slightly increased system air pressure drop). For the present investigation, these parasitic energy requirements have been assumed negligible compared to the auxiliary regeneration energy in the desiccant system, and the fan and chiller power requirements of a conventional system.

4.2 Results of System Performance Simulation

Figure 4.2 shows the daily solar radiation incident on the solar collector for the month of August in Miami, Florida. The daily cooling loads necessary to bring 0.5 m^3/s of air from the ambient conditions to 24 °C and 50 % relative humidity are plotted in Figure 4.3. This figure shows that the latent cooling load makes up a large part of the total cooling load. The system performance as a function of design parameters such as storage size and collector area is presented below.

4.2.1 Effect of Desiccant Storage Volume and Desiccant Regenerator Size

In order to meet the dehumidification requirement of the ventilation air conditioning, the desiccant concentration and temperature at the desiccant inlet to the dehumidifier must be such that the required outlet air humidity ratio, Y_{OUT}, can be obtained. During the hours when the regenerator is not operating (7 PM to 10 AM, solar time, in the present investigation), the desiccant concentration in the storage will steadily decrease so that the driving force for air dehumidification is lowered. At some point, the latent cooling requirement may not be satisfied due to the high water content

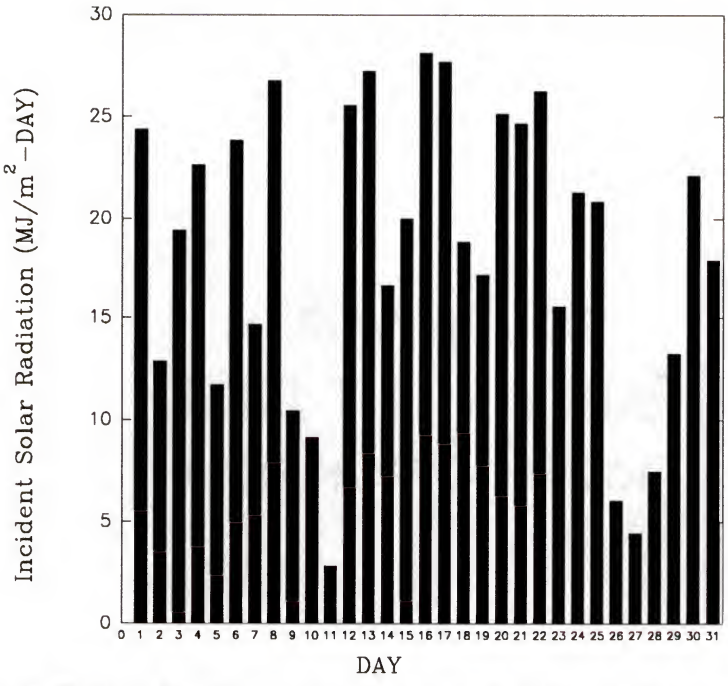

Figure 4.2: Daily solar radiation incident on the tilted collector surface for the month of August in Miami, Florida.

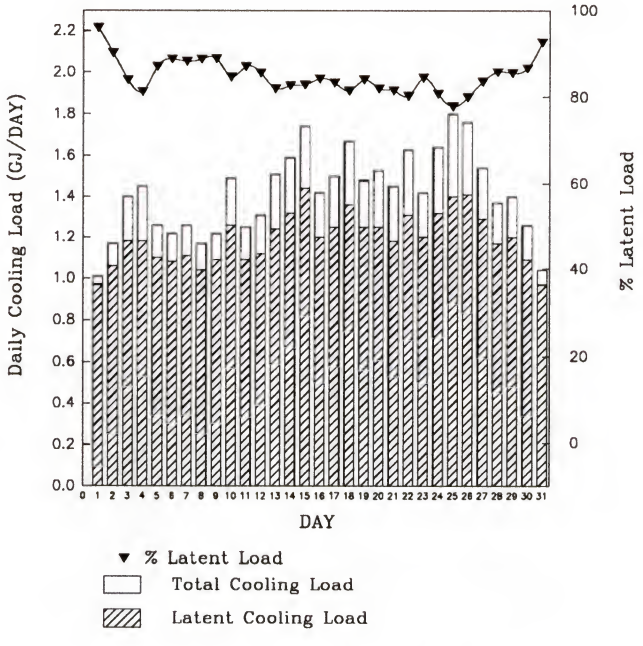

Figure 4.3: Daily total and latent cooling loads for preconditioning of 0.5 m^3/s ventilation air for the month of August in Miami, Florida.

in the desiccant storage. The average concentration in the desiccant storage during a 24 hour period can be maintained at higher levels by increasing the storage volume, by regenerating for longer hours, and/or by increasing the desiccant flow rate to the regenerator during the hours when the regenerator is operating. For a given packed bed height, if the inlet conditions of the air and the desiccant to the regenerator are constant, and the liquid to air mass flow ratio is constant, the change in the desiccant concentration through the regenerator is constant regardless of the desiccant flow rate. Thus, by increasing the desiccant flow rate to the regenerator, more water is removed from the desiccant storage per unit time. However, increasing the desiccant flow rate requires a larger regenerator, making a larger solar subsystem necessary.

Figure 4.4 shows the monthly percent latent load met by the dehumidifier, as a function of the desiccant storage volume and the desiccant flow rate to the regenerator. Over 90 % of the latent load is met by the desiccant system for the entire range of operating conditions. The percent of the latent load met by the dehumidifier slightly increases with increasing desiccant flow rate and/or increasing desiccant storage volume. Figure 4.4 also shows the percent electrical energy saved at the chiller, which is only marginally influenced by the two parameters. In summary, Figure 4.4 illustrates that in order to handle 100 % of the latent load in the dehumidifier, the desiccant storage volume and the desiccant flow rate to the regenerator must be very large. However, the resulting additional electrical energy savings at the chiller may be insignificant, so it is better to size the system at lower percentages.

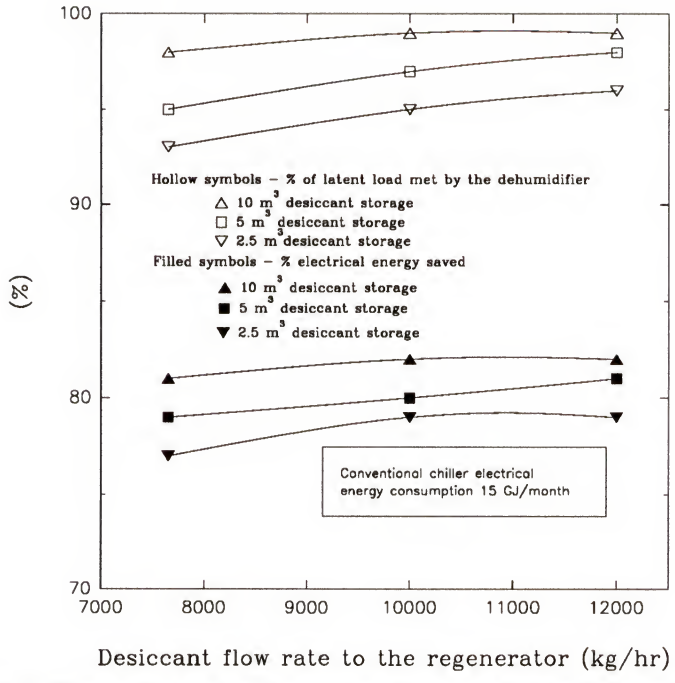

Figure 4.4: The influence of desiccant storage size and the regenerator flow rate on the fraction of the latent load handled by the dehumidifier, and on the percentage electrical energy savings.

4.2.2 Effect of Hot Water Storage Volume and Solar Collector Area

The amount of auxiliary energy required for desiccant regeneration is a function of the amount of solar heat provided by the solar subsystem. Therefore, the monthly auxiliary energy requirement was determined as a function of the hot water storage size as well as the solar collector area, as shown in Figure 4.5 (a). For a given hot water storage volume, the auxiliary energy requirement decreases rapidly with increasing solar collector area until a collector area is reached where the slope of the curve flattens out. Figure 4.5 (b) shows the daily auxiliary energy requirement for three days with varying cloudiness. For a very clear day (August 16) the auxiliary energy requirement is eliminated by using a collector area of 300 m^2, while for a very cloudy day (August 11) increasing the collector area has no effect on the auxiliary energy requirement.

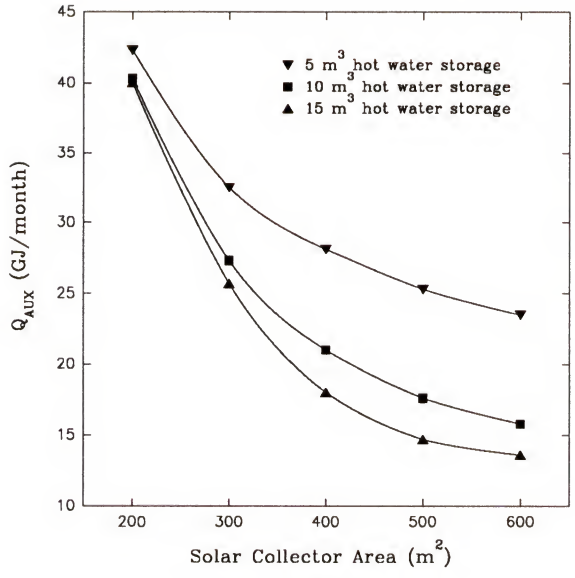

(a)

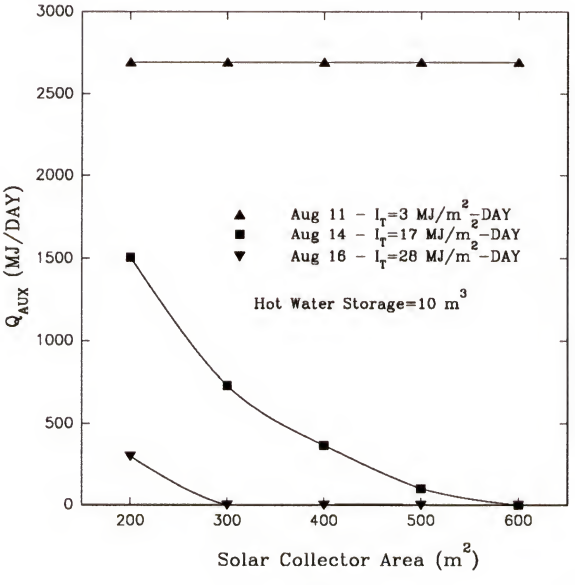

(b)

Figure 4.5: Auxiliary energy requirement versus solar collector area: (a) monthly performance for various hot water storage sizes; (b) daily performance for a range of climatic conditions.

Figure 4.5 (a) displays that a combination of large collector area and large hot water storage volumes gives the largest reduction in auxiliary energy requirement. However, not even 600 m^2 collector area in combination with a 15 m^3 hot water storage eliminates the need for auxiliary energy to precondition 0.5 m^3/s ventilation air.

It is also of interest to know the fraction of the regeneration energy that can be provided by solar energy. Figure 4.6 (a) shows the monthly percent solar energy for regeneration as a function of the hot water storage volume and the solar collector area. For a fixed solar collector area, increasing the hot water storage volume from 5 m^3 to 10 m^3 significantly increases the percent of the regeneration energy provided by solar energy. An additional increase of the storage volume from 10 m^3 to 15 m^3 does not have as large an effect. Also, for a given hot water storage volume, as the solar collector area increases the percent solar energy for regeneration increases. However, as the solar collector area becomes large the slope of this curve levels off. Figure 4.6 (b) shows that for a very clear day, a 300 m^2 collector area makes it possible for the solar subsystem to provide all of the regeneration heat. However, on a very cloudy day the solar system does not provide any heat for regeneration regardless of collector area.

Figures 4.5 and 4.6 indicate that to design a system using 100 % solar energy for regeneration would require a very large solar collector area in combination with a very large hot water storage volume. Thus, it seems more likely that a system would use some auxiliary energy. Figure 4.7 shows that a linear relationship exists between the auxiliary energy requirement and the percent solar energy used for regeneration as obtained from all the simulations performed on the solar subsystem. The monthly electrical energy savings at the chiller as compared to a conventional system is also

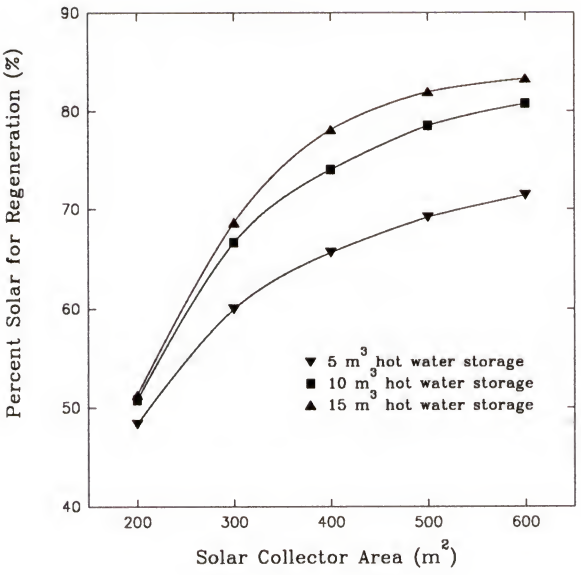

(a)

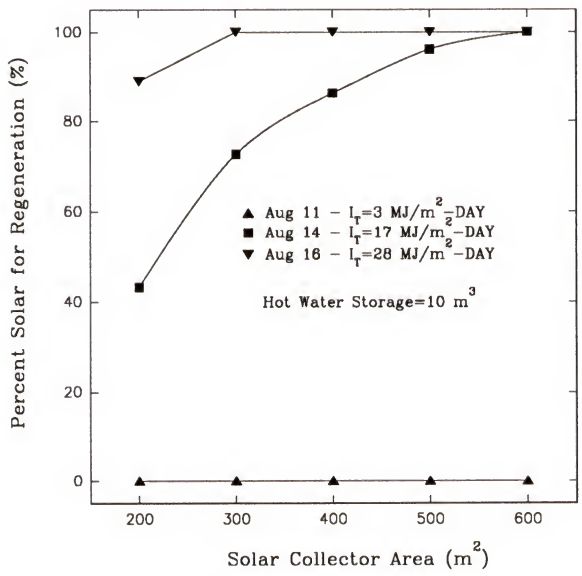

(b)

Figure 4.6: Percent solar for regeneration versus solar collector area: (a) monthly performance for various hot water storage sizes; (b) daily performance for a range of climatic conditions.

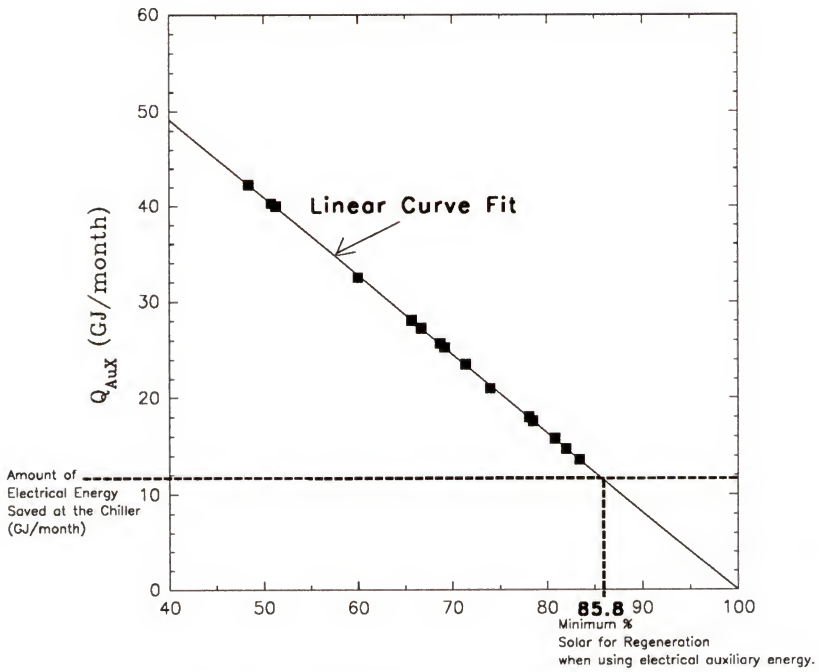

Figure 4.7: Auxiliary energy requirement versus percent solar for regeneration.

indicated in Figure 4.7. If electric heaters are to be used for auxiliary energy, no electrical energy savings will be obtained if the auxiliary energy requirement is larger than the electrical energy savings at the chiller. In this study, with a solar fraction larger than 86 %, the desiccant system will provide electrical energy savings even if electric heaters are used as the auxiliary energy sources. Similar high values (about 88 %) were obtained by Hernández et al. [34] in their performance analysis of a solar-assisted hybrid liquid desiccant system combining a solar absorption chiller with a desiccant dehumidifier.

4.2.3 Low Temperature and Low Concentration Desiccant System

Operating the desiccant system at a temperature below 20 °C has been suggested as an alternative mode of operation. Sick et al. [86] studied a liquid desiccant system in

which the desiccant was cooled in a chiller before entering the dehumidifier. Thus, both latent and sensible cooling of the ventilation air was obtained in the packed bed desiccant conditioner. Because of its simplicity, such a configuration appears attractive. Furthermore, when using triethylene glycol as the desiccant, lower temperatures will minimize the evaporation of glycol in the dehumidifier. Chung et al. [13, 14] carried out experimental studies of dehumidification of air in packed bed absorption towers using desiccant temperatures between 15 °C and 20 °C. In a humid climate, such low desiccant temperatures are not always possible to obtain by using a cooling tower, so cooling using a chiller may be required.

To examine the use of cooler and more dilute desiccant in a solar hybrid desiccant system, a simulation was carried out for an average day in August, in Miami, Florida, using triethylene glycol at 20 °C. Because the desiccant is now cooler, a more dilute desiccant (90 % by weight) can be used while still maintaining the vapor pressure low enough to achieve dehumidification. The system layout was modified as shown in Figure 4.8. By using the cool desiccant, both the dehumidification and the sensible cooling of the air can take place in the dehumidifier. Overall, this layout decreases the number of system components, which may help in reducing the first cost of the system. Another benefit of operating at low desiccant temperature and concentration is that the desiccant can be regenerated at a lower temperature; 45 °C compared to 65 °C when using a higher desiccant concentration. A lower regeneration temperature results in a higher efficiency of the solar collectors.

Results from the simulation of the low temperature desiccant are shown in Figure 4.9. The hourly chiller load of this system is compared to that of a conventional vapor

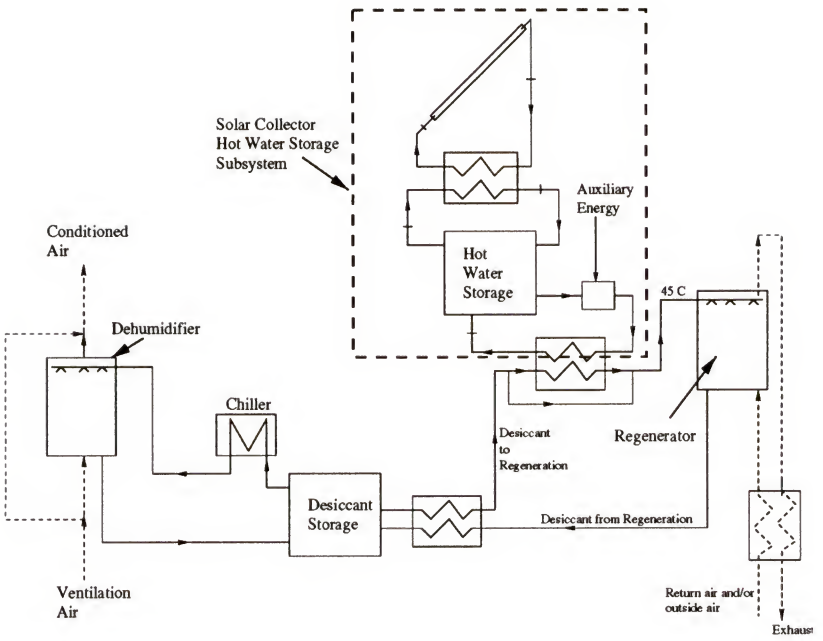

Figure 4.8: Solar hybrid liquid desiccant cooling system for ventilation air preconditioning using a cool, dilute desiccant.

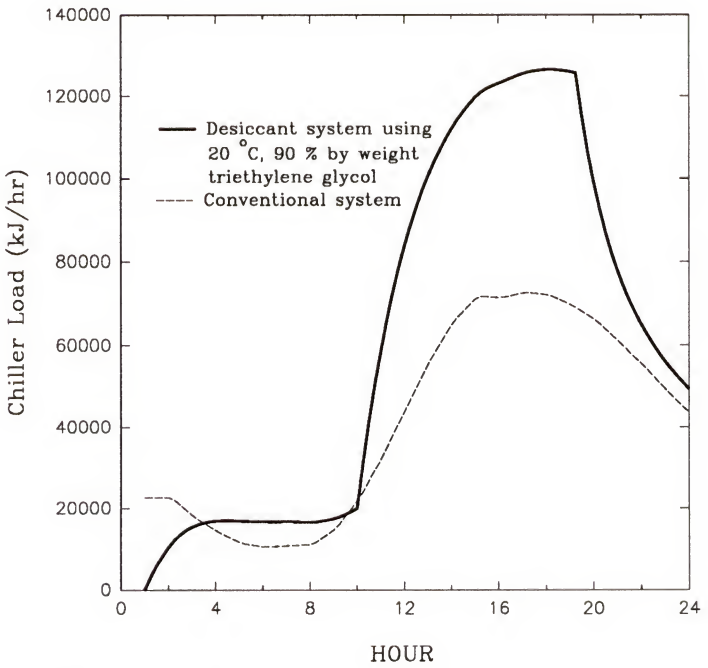

Figure 4.9: Hourly chiller load for a conventional and a low temperature desiccant system.

compression system. As shown, the desiccant system has a much higher chiller load compared to a conventional system. This is due to the parasitic heat added to the desiccant storage, especially during hours of regeneration (10 AM to 7 PM). Configurations where a cooling tower was added between the desiccant storage and the chiller and between the regenerator side and the desiccant storage were also examined. No significant improvement of the desiccant system performance was obtained by these additions, which can be attributed to the high wet bulb temperatures in Miami. Because of high wet bulb temperature the water from the cooling tower cannot cool the desiccant to the required temperature before the desiccant enters the chiller. Therefore, despite the apparent benefits of using a cool dilute desiccant, it is not desirable from an energy point of view. These findings differ from the results presented by Sick et al. [86], who showed a reduction in the chiller load and the operating costs for the solar desiccant system as compared to a conventional system. This may be explained by the lower ratio of desiccant flow rate to air flow rate in the dehumidifier as compared to the ratio used in the present study. For a lower ratio, the amount of desiccant to be cooled per unit mass of air to be conditioned is lower. As previously mentioned, the higher desiccant flow rates employed in the present study were selected based on the experiments conducted on the packed bed absorption tower. With a low flow rate, adequate wetting of the packing was not possible and resulted in low effectiveness of the dehumidification and regeneration processes. Thus, in actual desiccant cooling systems, the need for relatively high desiccant to air flow ratios may severely penalize this particular configuration.

4.3 Concluding Remarks

By using solar hybrid liquid desiccant cooling for ventilation air preconditioning in a hot and humid climate, as much as 80 % electrical energy can be saved compared to a conventional vapor compression system. If electrical energy is to be used as auxiliary energy for the desiccant regeneration , a large solar fraction for regeneration (>0.86) is needed in order to save electrical energy compared to a conventional system. Because of cloudy days where no useful energy is provided by the solar system, very large collector area and hot water storage volume are required in order to obtain such high monthly solar fractions.

Since the simulation was conducted on a per air flow rate basis, the results can be scaled up or down depending on the flow rate needed. Some applications where ventilation air preconditioning may result in large annual electrical energy savings and improved indoor humidity control are laboratories, supermarkets, and health care facilities. Therefore, future studies of desiccant cooling for these applications are warranted.

CHAPTER 5
CONCLUSIONS

Effectiveness of simultaneous heat and mass transfer processes in a liquid desiccant air dehumidifier and a desiccant regenerator greatly influence the overall performance of a desiccant cooling system. It is clear that the effects of the design variables on the performance of the absorber/regenerator are of great interest. Due to the complexity of the absorption/desorption process between the desiccant and the air, theoretical modeling relies heavily upon experimental studies. A review of the literature showed that only a limited number of experimental studies have been reported. Therefore, a detailed study of the influence of design variables on the performance of a randomly packed bed absorber/regenerator has been carried out experimentally, and by theoretical modeling. A finite difference model was employed for the adiabatic absorption process, and it accounted for the resistance to mass transfer in the gas and liquid phases, and the resistance to heat transfer in the gas phase. New performance correlations have been developed which are based on experimental data from the present investigation and from data available in the literature. In addition, a solar hybrid liquid desiccant system has been proposed, since a review of the literature showed hybrid systems to be especially promising for providing efficient control of indoor humidity and temperature, while at the same time reducing the electrical energy requirement for air conditioning. A performance simulation of this system has been

conducted, investigating the influence of design variables such as desiccant storage, regenerator size, hot water storage volume, and solar collector area.

Several conclusions may be drawn from the results presented in this study. The heat and mass transfer study of a packed bed absorber/regenerator showed that the results obtained from the finite difference model compared well with the experimental findings. Such good agreement is seen because fundamental conservation equations were included in the model, minimizing the number of assumptions and the use of empirical correlations. Hence, for a detailed study, this model yields excellent predictions.

Design variables found to have the largest impact on the performance of the packed bed dehumidifier and regenerator are: the air flow rate and humidity; the desiccant temperature and concentration; and the packed bed height. The liquid flow rate and the air temperature did not have a significant effect; however, the liquid flow rate must be high enough to ensure wetting of the packing.

Although the finite difference model describes the performance of the absorber/regenerator well, simpler algebraic performance correlations are more convenient when simulating the performance of a desiccant cooling system. One such correlation available in the literature considered the humidity effectiveness as a function of design variables. However, it did not give good predictions of the performance of the packed bed dehumidifier as compared to the experimental results of the present investigation. This correlation was also not applicable to the conditions in the packed bed desiccant regenerator. In addition, no correlation for the change in air temperature due to the simultaneous heat and mass transfer in the absorber/regenerator was available

in the literature. Thus, two performance correlations have been developed based on experimental data from the present investigation and the literature: one for the humidity effectiveness, and one for the enthalpy effectiveness of the absorption/regeneration. These correlations predicted the performance within 15 % of all the experimental data, and they gave good predictions of the influence of design variables, both for air dehumidification and desiccant regeneration.

From the performance simulation of the proposed solar hybrid liquid desiccant cooling system, it is shown that with the desiccant dehumidifier providing over 90 % of the latent cooling requirement in an application with a large latent cooling load, as much as 80 % electrical energy can be saved as compared to conventional cooling techniques. However, when using electrical energy to provide auxiliary heat to the desiccant regeneration process, a large solar fraction for regeneration is needed in order to save electrical energy. This would require a large solar collector area and large storage capacities to minimize the auxiliary energy requirement during cloudy days.

The present investigation gives valuable insight into the design of liquid desiccant cooling systems. Important design variables for packed bed absorbers/regenerators have been brought forward, and the derived performance correlations can be valuable for future system design. Based on the promising results from the performance simulation of one proposed desiccant cooling system, seasonal performance simulations of the desiccant system for applications with large latent cooling load are warranted at this time. With respect to the system design variables previously mentioned, an optimization based on cost, energy efficiency, and the quality of the air conditioning process would be valuable. Furthermore, as some auxiliary heat for the desiccant

regeneration will always be required, different heat sources should be compared through an analysis of the primary source energy efficiency. Full scale demonstrations of liquid desiccant cooling are also of interest as they will make it necessary to address design issues such as desiccant carry-over into the conditioned air, materials and equipment selection, the compactness of the system, and possible degradation of the desiccant. With further research it should be possible to develop cost-competitive and energy efficient solar alternatives to today's air conditioning techniques. After all, solar cooling has the advantage of having the largest amount of solar energy available when and where the cooling demand is the highest.

APPENDIX
UNCERTAINTY OF EXPERIMENTAL MEASUREMENTS

This appendix gives some details on the uncertainty of the experimental measurements, as well as of quantities calculated using these measurements. Table A-1 shows the uncertainty of the experimental measurements.

Table A-1: Uncertainty of experimental measurements.

Quantity	**Instrument/Method**	**Uncertainty**
Relative Humidity	Mamac Hu-224-2-MA humidity probes	$\xi_{RH} = \pm 1$ %
Temperature	Copper-Constantan Thermocouples	$\xi_T = \pm 0.5$ °C
Liquid Flow Rate	Catch-Bucket Method	$\xi_{VL} = \pm 0.01$ l/s
Air Flow Rate	Vane Anemometer	$\xi_{vG} = \pm$ 5 % of measured air flow rate
Packed Bed Height	Ruler	$\xi_Z = \pm 1$ cm
Desiccant Concentration	Karl Fisher Titration	$\xi_X = \pm 0.0005$ kg TEG/kg solution

The uncertainties of quantities calculated using these measurements were obtained as described below.

If the calculated result, Φ, is a function of the independent variables $x_1, x_2, \ldots, x_n$, then the uncertainty in the results is given by Equation (A-1) [50].

$$\xi_{\Phi} = \left[\left(\frac{\partial \Phi}{\partial x_1} \xi_{x_1} \right)^2 + \left(\frac{\partial \Phi}{\partial x_2} \xi_{x_2} \right)^2 + \ldots + \left(\frac{\partial \Phi}{\partial x_n} \xi_{x_n} \right)^2 \right]^{1/2} \qquad \text{(A-1)}$$

For instance, the density of the desiccant is a function of its temperature, T_L, and concentration, X, and a curve fit of data given in the literature [18] gave the following expression.

$$\rho_L = 1081.9 - 0.755325 \cdot T_L + 57.36364 \cdot X \qquad \text{(A-2)}$$

Hence, the partial derivatives of ρ_L with respect to T_L and X are:

$$\frac{\partial \rho_L}{\partial T_L} = -0.755325 \; ; \quad \frac{\partial \rho_L}{\partial X} = 57.36364 \qquad \text{(A-3)}$$

so that the uncertainty in the values of ρ_L calculated using the measurements of T_L and X is:

$$\xi_{\rho_L} = \left[\left(\frac{\partial \rho_L}{\partial T_L} \xi_{T_L} \right)^2 + \left(\frac{\partial \rho_L}{\partial X} \xi_X \right)^2 \right]^{1/2} \approx 0.4 \; \frac{kg}{m^3} \qquad \text{(A-4)}$$

Additional calculated quantities, the functions of these quantities, and the partial derivatives of these functions with respect to the variables, are listed in Table (A-2). The uncertainties of the quantities shown in figures 3.3 through 3.17 were obtained using the method described above, and the values of these uncertainties are shown in Table (A-3).

Table A-2: Calculated quantities.

Quantity	Function	Partial Derivatives
L	$L = \frac{V_L\left(\frac{l}{s}\right) \cdot \rho_L\left(\frac{kg}{m^3}\right) \cdot \frac{1}{1000}\left(\frac{m^3}{l}\right)}{A_{cs,tower}(m^2)}$	$\frac{\partial L}{\partial V_L} = \frac{\rho_L}{1000 \cdot A_{cs,tower}}$ $\frac{\partial L}{\partial \rho_L} = \frac{V_L}{1000 \cdot A_{cs,tower}}$
p_w	$p_w(kPa) = 0.21888T\ (°C) - 2.17364$ (dehumidifier) $p_w(kPa) = 0.62775T\ (°C) - 1.84014$ (regenerator) (Obtained from curve fits from data given in the literature [5].)	$\frac{\partial p_w}{\partial T} = 0.218875$ (dehumidifier) $\frac{\partial p_w}{\partial T} = 0.62775$ (regenerator)
$p_{v,equ}$	$p_{v,equ}(kPa) = 0.0787068T_{DP,equ}\ (°C) + 0.487373$ (dehumidifier) $p_{v,equ}(kPa) = 0.31375T_{DP,equ}\ (°C) - 5.22882$ (regenerator) (Obtained from curve fits from data given in the literature [5].)	$\frac{\partial p_{v,equ}}{\partial T_{DP,equ}} = 0.0787068$ (dehumidifier) $\frac{\partial p_{v,equ}}{\partial T_{DP,equ}} = 0.31375$ (regenerator)
p_v	$p_v = \frac{RH}{100} \cdot p_w$	$\frac{\partial p_v}{\partial RH} = \frac{p_w}{100}$; $\frac{\partial p_v}{\partial p_w} = \frac{RH}{100}$
Y	$Y = 0.622 \cdot \frac{p_v}{P - p_v}$	$\frac{\partial Y}{\partial p_v} = \frac{1}{P - p_v} - \frac{p_v}{(P - p_v)^2}$

Table A-2--Continued.

Quantity	Function	Partial Derivatives
$T_{DP,equ}$	$T_{DP,equ} = (-179.9X_{IN}^3 + 477.0X_{IN}^2 - 422.0X_{IN} + 125.5)T_{L,IN} + - 726.3X_{IN}^2 + 1207.5X_{IN} - 506.9$ (Obtained from curve fit from data given in the literature [18].)	$\frac{\partial T_{DP,equ}}{\partial T_{L,IN}} = -179.9X_{IN}^3 + 477.0X_{IN}^2 - 422.0X + 125.5$ $\frac{\partial T_{DP,equ}}{\partial X_{IN}} = (-539.8X_{IN}^2 + 953.9X_{IN} - 422.0)T_{L,IN} + -1452.7X_{IN} + 1207.5$
Y_{equ}	The equilibrium humidity ratio is a function of the vapor pressure in air for air at the equilibrium dew point, $T_{DP,equ}$. Thus, the function is the same as for the regular humidity, Y, but p_v is replaced by $p_{v,equ}$.	See the expression for the regular humidity ratio, Y.
ϵ_Y	$\epsilon_Y = \frac{Y_{IN} - Y_{OUT}}{Y_{IN} - Y_{equ}}$	$\frac{\partial \epsilon_Y}{\partial Y_{IN}} = \frac{1}{Y_{IN} - Y_{equ}} + \frac{Y_{IN} - Y_{OUT}}{(Y_{IN} - Y_{equ})^2}$ $\frac{\partial \epsilon_Y}{\partial Y_{OUT}} = -\frac{1}{Y_{IN} - Y_{equ}}$ $\frac{\partial \epsilon_Y}{\partial Y_{equ}} = \frac{Y_{OUT} - Y_{IN}}{(Y_{IN} - Y_{equ})^2}$

Table A-2--Continued.

Quantity	Function	Partial Derivatives
H_a	$H_a = c_{p,a}(T_a - T_0) + Y\left[c_{p,v}(T_a - T_0) + \lambda_0\right]$	$\frac{\partial H_a}{\partial T_a} = c_{p,a} + Yc_{p,v}$ $\frac{\partial H_a}{\partial Y} = c_{p,v}(T_a + T_0) + \lambda_0$
ϵ_H	$\epsilon_H = \frac{H_{a,IN} - H_{a,OUT}}{H_{a,IN} - H_{a,equ}}$	$\frac{\partial \epsilon_H}{\partial H_{a,IN}} = \frac{1}{H_{a,IN} - H_{a,equ}} + \frac{H_{a,IN} - H_{a,OUT}}{(H_{a,IN} - H_{a,equ})^2}$ $\frac{\partial \epsilon_H}{\partial H_{a,OUT}} = -\frac{1}{H_{a,IN} - H_{a,equ}}$ $\frac{\partial \epsilon_H}{\partial H_{a,equ}} = \frac{H_{a,OUT} - H_{a,IN}}{(H_{a,IN} - H_{a,equ})^2}$
ρ_G	$\rho_G = \frac{M_a P}{RT_a(K)[1 + 1.6078Y]}$	$\frac{\partial \rho_G}{\partial T_a} = -\frac{M_a P}{RT_a^2[1 + 1.6078Y]}$ $\frac{\partial \rho_G}{\partial Y} = -\frac{1.6078\, M_a P}{RT_a[1 + 1.6078Y]^2}$

Table A-2--Continued.

Quantity	Function	Partial Derivatives
G	$G = \frac{v_L\left(\frac{m}{s}\right) \cdot \rho_G\left(\frac{kg}{m^3}\right) \cdot A_{os,OUT}(m^2)}{A_{os,tower}(m^2)}$	$\frac{\partial G}{\partial \rho_G} = v_G \cdot \frac{A_{os,OUT}}{A_{os,tower}}$ $\frac{\partial G}{\partial v_G} = \rho_G \cdot \frac{A_{os,OUT}}{A_{os,tower}}$
m_{cond}	Gas side: $m_{cond}\left(\frac{g}{s}\right) = 1000\ G(Y_{IN} - Y_{OUT})A_{os,tower}$ Liquid side: $m_{cond}\left(\frac{g}{s}\right) = 1000\ L(X_{IN} - X_{OUT})A_{os,tower}$	Gas side: $\frac{\partial m_{cond}}{\partial G} = 1000\ (Y_{IN} - Y_{OUT})A_{os,tower}$ $\frac{\partial m_{cond}}{\partial Y_{IN}} = -\frac{\partial m_{cond}}{\partial Y_{OUT}} = 1000\ GA_{os,tower}$ Liquid side: $\frac{\partial m_{cond}}{\partial L} = 1000\ (X_{IN} - X_{OUT})A_{os,tower}$ $\frac{\partial m_{cond}}{\partial X_{IN}} = -\frac{\partial m_{cond}}{\partial X_{OUT}} = 1000\ LA_{os,tower}$

Table A-2--Continued.

Quantity	Function	Partial Derivatives
m_{evap}	Gas side: $m_{evap}\left(\frac{g}{s}\right) = 1000\ G(Y_{OUT} - Y_{IN})A_{os,tower}$ Liquid side: $m_{evap}\left(\frac{g}{s}\right) = 1000\ L(X_{OUT} - X_{IN})A_{os,tower}$	Gas side: $\frac{\partial m_{evap}}{\partial G} = 1000\ (Y_{OUT} - Y_{IN})A_{os,tower}$ $\frac{\partial m_{evap}}{\partial Y_{OUT}} = -\frac{\partial m_{evap}}{\partial Y_{IN}} = 1000\ GA_{os,tower}$ Liquid side: $\frac{\partial m_{evap}}{\partial L} = 1000\ (X_{OUT} - X_{IN})A_{os,tower}$ $\frac{\partial m_{evap}}{\partial X_{OUT}} = -\frac{\partial m_{evap}}{\partial X_{IN}} = 1000\ LA_{os,tower}$

Table A-3: Uncertainty of quantities shown in figures 3.3 through 3.16.

Quantity	Uncertainty
G	$\xi_G = \pm 0.1$ kg/m^2-s (dehumidifier) $\xi_G = \pm 0.09$ kg/m^2-s (regenerator)
L	$\xi_L = \pm 0.24$ kg/m^2-s (dehumidifier) $\xi_L = \pm 0.23$ kg/m^2-s (regenerator)
T	$\xi_T = \pm 0.5$ °C
Y	$\xi_Y = \pm 0.5$ g/kg (dehumidifier) $\xi_Y = \pm 1.6$ g/kg (regenerator)
X	$\xi_X = \pm 0.0005$ kg/kg
Z	$\xi_Z = \pm 0.01$ m
m_{cond}	$\xi_{mcond} = \pm 0.12$ g/s
m_{evap}	$\xi_{mevap} = \pm 0.16$ g/s
ϵ_Y	$\xi_{\epsilon Y} = \pm 0.09$ (dehumidifier) $\xi_{\epsilon Y} = \pm 0.16$ (regenerator)
ϵ_H	$\xi_{\epsilon H} = \pm 0.10$ (dehumidifier) $\xi_{\epsilon H} = \pm 0.11$ (regenerator)

REFERENCES

[1] Agarwal, R. S., Aggarwal, M. K., and Das Gupta, P., 1985, "Solar Powered Space Conditioning System Using LiBr as a Desiccant," INTERSOL 85, Proceedings of the 9th Biennial Congress of the International Solar Energy Society, Montreal, Canada, 1, pp. 674-681.

[2] Albers, W. F., Beckman, J. R., Farmer, R. W., Gee, K. G., 1991, "Ambient Pressure, Liquid Desiccant Air Conditioner," ASHRAE Transactions, 97, pt. 2, pp. 603-608.

[3] Albers, W. F., and Beckman, J. R., 1989, Method and Apparatus for Simultaneous Heat and Mass Transfer, U.S. Patent No. 4,832,115.

[4] Armstrong, P. R., and Brusewitz, G. H., 1984, "Design and Testing of a Liquid Desiccant Dehumidifier," Transaction of the ASAE, 27(1), pp. 169-172.

[5] ASHRAE, 1993, ASHRAE Handbook of Fundamentals, American Society of Heating, Refrigerating, and Air-Conditioning Engineers, Inc., Atlanta, Georgia.

[6] ASHRAE, 1992, ASHRAE Systems and Equipment Handbook, American Society of Heating, Refrigerating, and Air-Conditioning Engineers, Inc., Atlanta, Georgia.

[7] Bogatykh, S. A., Evnovich, I. D., and Sidorov, V. M., 1966, "Investigation of the Surface Tension of LiCl, LiBr, and $CaCl_2$. Aqueous Solutions in Relation to Conditions of Gas Drying," Journal of Applied Chemistry of the USSR, 39 (11), pp. 2432-2433.

[8] Burns, P. R., Mitchell, J. W., and Beckman, W. A., 1985, "Hybrid Desiccant Cooling Systems in Supermarket Applications," ASHRAE Transactions, 91, pt. 1b, pp. 457-468.

[9] Buschulte, T. K., and Klein, S. A., 1985, "Analysis of a Hybrid Liquid Desiccant Cooling System," INTERSOL 85, Proceedings of the 9th biennial congress of the International Solar Energy Society, Montreal, Canada, 2, pp. 694-699.

[10] Chebbah, A., 1987, Analysis and Design of a Solar-Powered Liquid-Desiccant Air Conditioner for use in Hot and Humid Climates, Ph.D. Dissertation, University of Florida, Gainesville, FL.

[11] Chen, L. C., Kuo, C. L., and Shyu, R. J., 1989, "The Performance of a Packed Bed Dehumidifier for Solar Liquid Desiccant Systems," Solar Engineering - 1989, Proceedings of the 11th Annual ASME Solar Energy Conference, San Diego, California, pp. 371-377.

[12] Chung, T.-W., 1994, "Predictions of the Moisture Removal Efficiencies for Packed-Bed Dehumidification Systems," Gas Separation & Purification, 8 (4), pp. 265-268.

[13] Chung, T.-W., Ghosh, T. K., Hines, A. L., and Novosel, D., 1995, "Dehumidification of Moist Air with Simultaneous Removal of Selected Pollutants by Triethylene Glycol Solutions in a Packed-Bed Absorber," Separation Science and Technology, 30(7-9), pp. 1807-1832.

[14] Chung, T.-W., Ghosh, T. K., and Hines, A. L., 1993, "Dehumidification of Air by Aqueous Lithium Chloride in a Packed Column," Separation Science and Technology, 28(1-3), pp. 533-550.

[15] Chung, T.-W., Ghosh, T. K., Hines, A. L., and Novosel, D., 1993, "Removal of Selected Pollutants from Air during Dehumidification by Lithium Chloride and Triethylene Glycol Solutions," ASHRAE Transactions, 99, pp. 834-841.

[16] Cyprus Foote Mineral Company, Technical Data on Lithium Bromide and Lithium Chloride, Bulletins 145 and 151, Cyprus Foote Mineral Company, Kings Mountain, NC.

[17] Dow Chemical Company, 1996, Calcium Chloride Handbook, Dow Chemical Company, Midland, Michigan.

[18] Dow Chemical Company, 1992, A Guide to Glycols, Dow Chemical Company, Midland, Michigan.

[19] Ertas, A., Gandhidasan, P., Kiris, I., and Anderson, E. E., 1994, "Experimental Study on the Performance of a Regeneration Tower for Various Climatic Conditions," Solar Energy, 53(1), pp. 125-130.

[20] Ertas, A., Anderson, E. E., and Kiris, I., 1992, "Properties of a New Liquid Desiccant Solution--Lithium Chloride and Calcium Chloride Mixture," Solar Energy, 49, pp. 205-212.

[21] Ertas, A., Anderson, E. E., and Kavasogullari, 1991, "Comparison of Mass and Heat Transfer Coefficients of Liquid-Desiccant Mixtures in a Packed Column," Journal of Energy Resources Technology, 113, pp. 1-6.

[22] Factor, H. M., and Grossman, G., 1980, "A Packed Bed Dehumidifier/ Regenerator for Solar Air Conditioning with Liquid Desiccants," Solar Energy, 24, pp. 541-550.

[23] Fisher Scientific, 1997, Material Safety Data Sheet for Triethylene Glycol, Fisher Scientific, Pittsburgh.

[24] Gandhidasan, P., 1994, "Performance Analysis of an Open-Cycle Liquid Desiccant Cooling System Using Solar Energy for Regeneration," International Journal of Refrigeration, 17 (7), pp. 475-480.

[25] Gandhidasan, P., 1990, "Analysis of a Solar Space Cooling System using Liquid Desiccants," Proceedings of the 25th Intersociety Energy Conversion Engineering Conference, 5, pp. 162-166.

[26] Gandhidasan, P., 1990, "Reconcentration of Aqueous Solutions in a Packed Bed: A Simple Approach," Journal of Solar Energy Engineering, 112, pp. 268-272.

[27] Gandhidasan, P., and Al-Farayedhi, A. A., 1995, "Thermal Performance Analysis of a Partly Closed-Open Solar Regenerator," Journal of Solar Energy Engineering, 117, pp. 151-153.

[28] Gandhidasan, P., Ullah, M. R., and Kettleborough, C. F., 1987, "Analysis of Heat and Mass Transfer Between a Desiccant-Air System in a Packed Tower," Journal of Solar Energy Engineering, 109, pp. 89-93.

[29] Gifford, E. W., 1957, "III-Dehumidification by Liquid Sorbents," Heating, Piping & Air Conditioning, 29(4), pp. 156-159.

[30] Griffiths, W. C., 1979, Solar Energy Assisted Air-Conditioning Apparatus and Method, U.S. Patent No. 4,164,125.

[31] Grossman, G., and Shwarts, I., 1978, "An Open Absorption System Utilizing Solar Energy for Air Conditioning," Energy Conservation in Heating, Cooling, and Ventilating Buildings, Hoogendorn, C. J., and Afgan, N. H., editors, Hemisphere Publishing Corporation, Washington, DC, pp. 641-647.

[32] Harriman, L. G., 1990, The Dehumidification Handbook, second edition, Munters Cargocaire, Amesbury, MA.

[33] Hernández, H. R., González, J. E., and Khan, A. Y., 1997, "A Parametric Study of Solar-Assisted Air-Conditioning and Dehumidification Systems Operating in the Caribbean Region," Solar Engineering - 1997, Proceedings of the 15th Annual ASME Solar Energy Conference, Washington, DC, pp. 327-334.

[34] Hernández, H. R., González, J. E., and Khan, A. Y., 1996, "Modeling of a Solar-Assisted Absorption/Desiccant System for Applications in Puerto Rico and the Caribbean," SOLAR '96, Proceedings of 1996 Annual Conference of the American Solar Energy Society, Asheville, NC, pp. 124-132.

[35] Hollands, K. G. T., 1963, "The Regeneration of Lithium Chloride Brine in Solar Still," Solar Energy, 7, pp. 39-43.

[36] Howell, J. R., 1987, "A Survey of Active Solar Cooling Methods," Progress in Solar Engineering, Goswami, D. Y., editor, Hemisphere, Washington, DC, pp. 171- 182.

[37] Ji, L. -J., and Wood, B. D., 1993, "Performance Enhancement Study of Solar Collector/Regenerator for Open-Cycle Liquid Desiccant Regeneration," Proceedings of 1993 Annual Conference of the American Solar Energy Society, Washington, DC, pp. 351-356.

[38] Johannsen, A., 1984, "Performance Simulation of a Solar Air-Conditioning System with Liquid Desiccant," International Journal of Ambient Energy, 5(2), pp. 59-89.

[39] Johannsen, A., 1979, "Design and Operation of a Liquid-Desiccant Type Solar Air Conditioning System," SUN II, Proceedings of the International Solar Energy Society Silver Jubilee Congress, Atlanta, Georgia, pp. 681-685.

[40] Kelly, R. M., Rousseau, R. W., and Ferrell, J. K., 1984, "Design of Packed, Adiabatic Absorbers: Physical Absorption of Acid Gases in Methanol," Industrial Engineering Chemistry, Process Design and Development, 23, pp. 102-109.

[41] Kettleborough, C. F., and Waugaman, D. G., 1995, "An Alternative Desiccant Cooling Cycle," Journal of Solar Energy Engineering, 117, pp. 251-255.

[42] Khan, A. Y., 1996, "Parametric Analysis of Heat and Mass Transfer Performance of a Packed Type Liquid Desiccant Absorber at Part-Load Operating Conditions," ASHRAE Transactions, 102, pt. 1, pp. 349-357.

[43] Khan, A. Y., 1994, "Sensitivity Analysis and Component Modeling of a Packed-Type Liquid Desiccant System at Partial Load Operating Conditions," International Journal of Energy Research, 18, pp.643-655.

[44] Khan, A. Y., and Ball, H. D., 1993, "Experimental Performance Verification of a Coil-Type Liquid Desiccant System at Part-Load Operation," Solar Energy, 51 (5), pp. 401-408.

[45] Khan, A. Y., and Ball, H. D., 1992, "Development of a Generalized Model for Performance Evaluation of Packed-Type Liquid Sorbent Dehumidifiers and Regenerators," ASHRAE Transactions, 98, pp. 525-533.

[46] Khan, A. Y., and Ball, H. D., 1992, "Development of a Mathematical Model and Computer Simulation to Predict the Annual Energy Consumption of Coil-Type Liquid Desiccant Systems," ASHRAE Transactions, 98, pp. 534-541.

[47] Khelifa, N., Jung, D., Lävemann, E., and Sizmann, R., 1987, "Air Conditioning by Low Temperature Heat," Advances in Solar Energy Technology. Proceedings of the Biennial Congress of the International Solar Energy Society, Hamburg, Germany, 1, pp. 1008 - 1012.

[48] Kinsara, A. A., Elsayed, M. M., and Al-Rabghi, O. M., 1996, "Proposed Energy-Efficient Air-Conditioning System Using Liquid Desiccant," Applied Thermal Engineering, 16 (10), pp. 791-806.

[49] Klein, S. A., Beckman, W. A., Cooper, P. I., Duffie, N. A., Freeman, T. L., Mitchel, J. C., Beekman, D. M., Oonk, R. L., Hughes, P. J., Eberlein, M. E., Karman, V. D., Pawelski, M. J., Utzinger, D. M., Duffie, J. A., Brandemuehl, M. J., Arny, M. D., Theilacker, J. C., Morrison, G. L., Clark, D. R., Braun, J. E., Evans, B. L., Kummer, J. P., and Urban, R. E., 1990, TRNSYS--A Transient System Simulation Program, Version 13.1, Solar Energy Laboratory, University of Wisconsin - Madison, Madison, Wisconsin.

[50] Kline, S. J., and McClintock, F. A., 1953, "Uncertainties in Single-Sample Experiments," Mechanical Engineering, 75, pp. 3-8.

[51] Löf, G. O. G, Lenz, T. G., and Rao, S., 1984, "Coefficients of Heat and Mass Transfer in a Packed Bed Suitable for Solar Regeneration of Aqueous Lithium Chloride Solutions," Journal of Solar Energy Engineering, 106, pp. 387-392.

[52] Lowenstein, A. I., and Dean, M. H., 1992, "The Effect of Regenerator Performance on a Liquid-Desiccant Air Conditioner," ASHRAE Transactions, 98, pt. 1, pp. 704-711.

[53] Lowenstein, A. I., and Gabruk, R. S., 1992, "The Effect of Absorber Design on the Performance of a Liquid-Desiccant Air Conditioner," ASHRAE Transactions, 98, pt. 1, pp. 712-720.

[54] Mahmoud, K. G., Ball, H. D., 1988, "Liquid Desiccant Systems for Cooling Applications,"Proceedings of the 23rd Intersociety Energy Conversion Engineering Conference, Goswami, D. Y., editor, the American Society of Mechanical Engineers, New York, 4, pp. 149-152.

[55] Mark, J. E., 1996, Physical Properties of Polymers Handbook, AIP Press, Woodbury, New York.

[56] Marsala, J., Lowenstein, A., and Ryan, W.A., 1989, "Liquid Desiccant for Residential Applications,"ASHRAE Transactions, 95, pt. 1, pp. 828-834.

[57] McDonald, B., Waugaman, D. G., and Kettleborough, C. F., 1992, "A Statistical Analysis of a Packed Tower Dehumidifier," Drying Technology, 10(1), pp. 223-237.

[58] Meckler, M., 1995, "Desiccant Outdoor Air Preconditioners Maximize Heat Recovery Ventilation Potentials," ASHRAE Transactions, 101, pt. 2, pp. 992-1000.

[59] Meckler, H., 1994, "Desiccant-Assisted Air Conditioner Improves IAQ and Comfort," Heating, Piping & Air Conditioning, 66(10), pp. 75-84.

[60] Meckler, M., 1988, "Off-Peak Desiccant Cooling and Cogeneration Combine to Maximize Gas Utilization," ASHRAE Transactions, 94, pt. 1, pp. 575-596.

[61] Meckler, M., Parent, Y. O., and Pesaran, A. A., 1993, Evaluation of Dehumidifiers with Polymeric Desiccants, Gas Research Institute Report, Contract No. 5091-246-2247, Gas Research Institute, Chicago, Illinois.

[62] Mullick, S. C., and Gupta, M. C., 1974, "Solar Desorption of Absorbent Solutions," Solar Energy, 16, pp. 19-24.

[63] Niagara Blower Company, 1989, Research Bulletin No. 162 A, Niagara Blower Company, Buffalo, New York.

[64] Onda, K., Takeuchi, H., and Okumoto, Y., 1968, "Mass Transfer Coefficients Between Gas and Liquid Phases in Packed Columns," Journal of Chemical Engineering of Japan, 1 (1), pp. 56-62.

[65] Panton, R. L., 1984, Incompressible Flow, John Wiley & Sons, New York.

[66] Park, M. S., Howell, J. R., Vliet, G. C., and Peterson, J., 1995, "Correlations for Film Regeneration and Air Dehumidification for a Falling Desiccant Film with Air in Cross Flow," Solar Engineering - 1995, Proceedings of the 13th Annual ASME Solar Energy Conference, Hawaii, 2, pp. 1229-1238.

[67] Park, M. S., Howell, J. R., Vliet, G. C., and Peterson, J., 1995, "Correlations for Regeneration of a Falling Desiccant Film by Air in Cross Flow," Solar Engineering - 1995, Proceedings of the 13th Annual ASME Solar Energy Conference, Hawaii, 2, pp. 1239-1247.

[68] Park, M. S., Howell, J. R., Vliet, G. C., and Peterson, J., 1994, "Numerical and Experimental Results for Coupled Heat and Mass Transfer between a Desiccant Film and Air in Cross-Flow," International Journal of Heat and Mass Transfer, 37, pp. 395-402.

[69] Patnaik, S., Lenz, T. G., and Löf, G. O. G., 1990, "Performance Studies for an Experimental Solar Open-Cycle Liquid Desiccant Air Dehumidification System," Solar Energy, 44 (3), pp. 123-135.

[70] Patnaik, S., Lenz, T. G., and Löf, G. O. G., 1988, "Solar Open-Cycle Liquid Desiccant Cooling Studies," Solar Engineering - 1988, Proceedings of the 10th Annual ASME Solar Energy Conference, Denver, CO, pp. 121-125.

[71] Peng, C. S. P., and Howell, J. R., 1984, "The Performance of Various Types of Regenerators for Liquid Desiccants," Journal of Solar Energy Engineering, 106, pp. 133-141.

[72] Peng, C. S. P., and Howell, J. R., 1981, "Analysis and Design of Efficient Absorbers for Low-Temperature Desiccant Air Conditioners," Journal of Solar Energy Engineering, 103, pp. 401-408.

[73] Perry, R. H., and Chilton, C. H., 1973, Chemical Engineer's Handbook, fifth edition, McGraw-Hill, New York.

[74] Pesaran, A. A., Parent, Y. O., Meckler, M., and Novosel, D., 1995, "Evaluation of a Liquid Desiccant-Enhanced Heat Pipe Air Preconditioner," ASHRAE Transactions, 101, pp. 713-724.

[75] Pesaran, A. A., Penney, T. R., and Czanderna, A. W., 1992, Desiccant Cooling: State-of-the-Art Assessment, National Renewable Laboratory, Golden, Colorado, NREL Report No. NREL/TP-254-4147.

[76] Peterson, J. I., and Howell, J. R., 1991, Hybrid Vapor-Compression/Liquid Desiccant Air Conditioner, U.S. Patent No. 4,984,434.

[77] Potnis, S., V., and Lenz, T. G., 1994, "Mass Transfer Studies for a Solar Assisted Liquid Desiccant Cooling System," Solar Engineering - 1994, Proceedings of the 12th Annual ASME Solar Energy Conference, San Francisco, CA, pp. 359-365.

[78] Rengarajan, K., Shirey, D. B. III, and Raustad, R. A., 1996, "Cost-Effective HVAC Technologies to meet ASHRAE Standard 62-1989 in Hot and Humid Climates," ASHRAE Transactions, pt. 1, pp. 166-182.

[79] Robison, H., 1977, "Liquid Sorbent Solar Air Conditioner," Alternative Energy Sources, 2, Veziroğlu, T. N., editor, Hemisphere Publishing Company, Washington, DC, pp. 761-779.

[80] Ryan, W., Marsala, J. and Griffiths, W., 1989, "Laboratory and Field Experiment Results for a Residential Liquid Desiccant Dehumidifier," Solar Engineering - 1989, Proceedings of the 11th Annual ASME Solar Energy Conference, San Diego, CA, pp. 353 - 361.

[81] Sadasivam, M., and Balakrishnan, A. R., 1994, "Experimental Investigations on the Thermal Effects in Packed Bed Liquid Desiccant Dehumidifiers," Industrial and Engineering Chemistry Research, 33, pp. 1636-1640.

[82] Sadasivam, M., and Balakrishnan, A. R., 1992, "Effectiveness-NTU Method for Design of Packed Bed Liquid Desiccant Dehumidifiers," Chemical Engineering Research & Design, 70, pp. 572-577.

[83] Sadasivam, M., and Balakrishnan, A. R., 1991, "Analysis of Thermal Effects in Packed Bed Liquid Desiccant Dehumidifiers," Chemical and Engineering Processes, 30, pp. 79-85.

[84] Saunders, J. H., Wilkinson, W. H., Landstrom, D. K. and Rutz, A. L., 1989, "A Hybrid Space Conditioning System Combining a Gas-Fired Chiller and a Liquid Desiccant Dehumidifier," Solar Engineering - 1989, Proceedings of the 11th Annual ASME Solar Energy Conference, San Diego, California, pp. 207-212.

[85] Scalabrin, G. and Scaltriti, G., 1990, "A Liquid Sorption-Desorption System for Air Conditioning With Heat at Lower Temperature," Journal of Solar Energy Engineering, 112, pp. 70-75.

[86] Sick, F., Buschulte, T. K., Klein, P., Northey, P., and Duffie, J. A., 1988, "Analysis of the Seasonal Performance of Hybrid Liquid Desiccant Cooling Systems," Solar Energy, 40, pp. 211-217.

[87] So'Brien, G. C. and Sactunanathan, S., 1989, "Performance of a Novel Liquid Desiccant Dehumidifier/Regenerator System," Journal of Solar Energy Engineering, 111, pp. 345-352.

[88] Spears, J. W., and Judge, J., 1997, "Gas-Fired Desiccant System for Retail Super Center," ASHRAE Journal, 39, pp. 65-69.

[89] Stevens, D. I., Braun, J. E., and Klein, S. A., 1989, "An Effectiveness Model of Liquid-Desiccant System Heat/Mass Exchangers," Solar Energy, 42, pp. 449-455.

[90] Thornbloom, M., and Nimmo, B., 1996, "Impact of design parameters on Solar Open Cycle Liquid Desiccant Regenerator Performance," SOLAR '96, Proceedings of 1996 Annual Conference of the American Solar Energy Society, Asheville, NC, pp. 107-111.

[91] Thornbloom, M., and Nimmo, B., 1995, "An Economic Analysis of a Solar Open Cycle Desiccant Dehumidification System," Solar Engineering - 1995, Proceedings of the 13th Annual ASME Conference, Hawaii, 1, pp. 705-709.

[92] Treybal, R. E., 1980, Mass Transfer Operations, third edition, McGraw-Hill, New York.

[93] Treybal, R. E., 1969, "Adiabatic Gas Absorption and Stripping in Packed Towers," Industrial and Engineering Chemistry, 61 (7), pp. 36-41.

[94] Ullah, M. R., Kettleborough, C. F., and Gandhidasan, P., 1988, "Effectiveness of Moisture Removal for an Adiabatic Counterflow Packed Tower Absorber Operating with $CaCl_2$-Air Contact System," Journal of Solar Energy Engineering, 110, pp. 98-101.

[95] Waugaman, D. G., Kini, A. and Kettleborough, C. F., 1993, "A Review of Desiccant Cooling Systems," Journal of Energy Resources Technology, 115, pp. 1-8.

[96] Wilkinson, W. H., 1991, "A Simplified, High-Efficiency DUBSLORB System," ASHRAE Transactions, 97, pt. 1, pp. 413-419.

[97] Wilkinson, W. H., 1991, "Evaporative Cooling Trade-Offs in Liquid Desiccant Systems,"ASHRAE Transactions, 97, pt. 1, pp. 642-649.

[98] Wilkinson, W. H., 1990, "Alternative DUBSLORB Concepts," ASHRAE Transactions, 96, pt.1, pp. 1273-1279.

[99] Wilkinson, W. H., Landstrom, D. K., and Novosel, D., 1988, "DUBSLORB - A Universal Desiccant Hybrid Approach," ASHRAE Transaction, 94, pt. 1, pp. 563-573.

[100] Wimby, J. M., and Berntsson, T. S., 1994, "Viscosity and Density of Aqueous Solutions of LiBr, LiCl, $ZnBr_2$, $CaCl_2$, and $LiNO_3$. 1. Single Salt Solutions," Journal of Chemical and Engineering Data, 39(1), pp. 68-72.

[101] Yadav, Y. K., 1995, "Vapour-Compression and Liquid-Desiccant Hybrid Solar Space-Conditioning System for Energy Conservation," Renewable Energy, 6(7), pp. 719-723.

[102] Yadav, Y. K., and Kaushik, S. C., 1991, "Psychrometric Technoeconomic Assessment and Parametric Studies of Vapor-Compression and Solid/Liquid Desiccant Hybrid Solar Space Conditioning Systems," Heat Recovery Syst. CHP, 11(6), pp. 563-572.

[103] Yao, W., Bjurström, H., and Setterwall, F., 1991, "Surface Tension of Lithium Bromide Solutions with Heat Transfer Additives," Journal of Chemical and Engineering Data, 36, pp. 96-98.

[104] Zaytsev, I. O., and Aseyev, G. G., 1992, Properties of Aqueous Solutions of Electrolytes, CRC Press, Boca Raton.

[105] Zografos, A. I., and Petroff, C., 1991, "A Liquid Desiccant Dehumidifier Performance Model," ASHRAE Transactions, 97, pt. 1, pp. 650-656.

BIOGRAPHICAL SKETCH

Viktoria Öberg was born on June 13, 1968, in Luleå, located in the northern part of Sweden, but has lived most of her life in Stockholm. She began her engineering studies at the Royal Institute of Technology in Stockholm in 1988, with the goal of pursuing a Master of Science in chemical engineering. Having a large interest in experiencing the world outside Sweden, Viktoria wished to conduct the research for her master's thesis abroad. These wishes brought her to the University of Florida as an exchange student in 1992. Not only did this give her the opportunity to conduct some fascinating research, but she also met her husband-to-be, Andrew Martin. The two grew close over the years, and married in 1996. In January 1993, Viktoria went back to Sweden, and soon after earned her Master of Science. Since she enjoyed her time in Florida so much, Viktoria decided to enroll at the University of Florida as a graduate student at the Department of Mechanical Engineering. Thus, she started the long journey toward the degree of Doctor of Philosophy in August 1993. Suitably, at her tenth anniversary as a professional student, she received this degree in 1998. After graduation, Viktoria will start as a researcher at the Royal Institute of Technology in Sweden.

I certify that I have read this study and that in my opinion it conforms to acceptable standards of scholarly presentation and is fully adequate, in scope and quality, as a dissertation for the degree of Doctor of Philosophy.

D. Yogi Goswami, Chairman
Professor of Mechanical
Engineering

I certify that I have read this study and that in my opinion it conforms to acceptable standards of scholarly presentation and is fully adequate, in scope and quality, as a dissertation for the degree of Doctor of Philosophy.

Chung K. Hsieh
Professor of Mechanical
Engineering

I certify that I have read this study and that in my opinion it conforms to acceptable standards of scholarly presentation and is fully adequate, in scope and quality, as a dissertation for the degree of Doctor of Philosophy.

Sherif A. Sherif
Associate Professor of
Mechanical Engineering

I certify that I have read this study and that in my opinion it conforms to acceptable standards of scholarly presentation and is fully adequate, in scope and quality, as a dissertation for the degree of Doctor of Philosophy.

James F. Klausner
Associate Professor of
Mechanical Engineering

I certify that I have read this study and that in my opinion it conforms to acceptable standards of scholarly presentation and is fully adequate, in scope and quality, as a dissertation for the degree of Doctor of Philosophy.

Dinesh O. Shah
Charles A. Stokes Professor of
Chemical Engineering

This dissertation was submitted to the Graduate Faculty of the College of Engineering and to the Graduate School and was accepted as partial fulfillment of the requirements for the degree of Doctor of Philosophy.

May 1998

Winfred M. Phillips
Dean, College of Engineering

Karen A. Holbrook
Dean, Graduate School